Non-destructive and Failure Evaluation of Tubing from a Retired Steam Generator
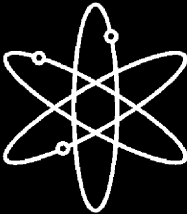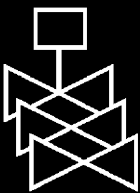
Argonne National Laboratory

U.S. Nuclear Regulatory Commission
Office of Nuclear Regulatory Research
Washington, DC 20555-0001

Non-destructive and Failure Evaluation of Tubing from a Retired Steam Generator

Prepared by
D.S. Kupperman, J.Y. Park, S. Majumdar, S. Bakhtiari
K. Kasza, W.J. Shack

Argonne National Laboratory
9700 South Cass Avenue
Argonne, IL 60439

E. Reichelt, NRC Project Manager

This page is intentionally left blank.

Abstract

Stress corrosion cracks (SCC) in tubes removed from a nuclear reactor retired steam generator (SG) have been examined. Eddy current (EC) nondestructive evaluation (NDE), pressure testing, and metallurgical sectioning or fractography were carried out on six tube support plate SCCs and four tube sheet SCCs. The deposits on the top of the tube sheet in the vicinity of the cracking were analyzed. Failure pressures and leak rates for the tube support plate SCCs were evaluated using finite element analysis and were compared to experimental results. Crack profiles used in the analysis were estimated using eddy current examination and fractography results.

The data obtained from the pressure tests were compared with the industry probability of leakage database and correlation. The results were generally consistent with the probability of leakage values presented by industry, i.e., tubes that would not be expected to leak based on measured eddy current voltages and the industry correlation did not leak.

The best predictions of the SCC profile and crack depth were obtained from the use of a multiparameter algorithm applied to rotating pancake coil data. Very little correlation between +Point amplitude and maximum depth of SCC was found for the tubes that were examined.

Foreword

This report discusses a study performed under the U.S. Nuclear Regulatory Commission (NRC), Office of Nuclear Regulatory Research (RES) Steam Generator Tube Integrity Program, conducted at the Argonne National Laboratory (ANL). This study provides information to help NRC evaluate industry's assessments of steam generator (SG) tube integrity. If flaw indications are discovered during an inservice inspection of SG tubes, significance assessments are performed to predict the burst pressures and leak rates in order to ensure that the NRC's regulatory guidance will be met. These correlations were developed from industry-wide databases. However, these databases contain significant scatter. The experimental testing described in this report provides additional data to evaluate the correlations used for these evaluations. In addition, the experimental results were used to assess failure mechanisms and the effectiveness of the industry's amplitude-based sizing methods.

The experimental tests were conducted on a retired SG, which provided realistic flaws on which burst and leak rate tests could be performed and compared with the industry's correlations. The work began in 1997 with nondestructive examination of tubing from a retired SG. These SG tubes were evaluated with eddy current testing, and the results were used to select the tubes containing indications. Those tubes were then pulled and test samples were cut out of the tube sheet and tube support plate region of the SG. Additional eddy current examinations, as well as pressure and leak rate tests, and destructive examinations of the tubes were performed at ANL.

The experimental results revealed many interesting findings. Comparing the flaw depth profiles from nondestructive examinations against the destructive examinations shows that in general nondestructive results under predict the flaw size. The under prediction of the flaw size by nondestructive examination also leads to an overestimation of the radial ligament rupture pressure and an underestimation in the leak rates. However, it should be noted that only two samples leaked because most of the predicted radial ligament rupture pressures exceeded the maximum pressure capability of the test system. In fact, rupture pressure of the two samples which did leak occurred at values well above the normal operating pressures of a pressurized-water reactor. Additional research is being planned to evaluate the effectiveness of nondestructive examination when applied to a ligamented flaw.

The experimental results from this study were statistically consistent with the industry's data. However, the evaluation of amplitude-based sizing revealed that the industry data showed scatter between maximum crack depth and eddy current signal amplitude, especially for larger flaws. This observation is consistent with the understanding that, in general, the maximum crack depth does not correlate well with eddy current signal amplitude.

Brian W. Sheron, Director
Office of Nuclear Regulatory Research
U.S. Nuclear Regulatory Commission

This page is intentionally left blank.

Contents

List of Figures

List of Tables

This page is intentionally left blank.

Executive Summary

This report presents results of an investigation of field induced stress corrosion cracks (SCCs) found in a retired steam generator. Six of the SCCs evaluated came from tube support plate (TSP) regions while the other four came from the top of the tube sheet (TTS).

The deposits on the TTS near where the cracking occurred were analyzed. Compositional analyses indicate a variety of species exists in the deposit. Detected elements include Fe, Ni, Cr, Al, Si, Mg, Cu, Ti, Mn, Ca, K, and S. The results for Pb were ambiguous because the signal was low and the S and Pb peaks overlap. Iron is the most abundant element. Copper was present in the metallic phase, indicating the potential was at the value where metallic copper and copper oxides exist. The copper deposits were mostly near the bottom area of the deposit above the TTS.

The SCCs were pressure tested at room temperature to 52 MPa (7500 psi). Two of the six TSP SCC leaked at 36 and 49 MPa (5.2 and 7.1 ksi). Two of the four TTS SCCs leaked at 35 and 50 MPa (5.1 and 7.3 ksi). Failure pressures and leak rates were computed for the cracks from the TSP region, based on crack profiles estimated by eddy current examination and fractography, and were compared to the experimental results. Most of the predicted radial ligament rupture pressures exceeded the maximum pressure capability of the test system. This finding is consistent with the observed test specimen behavior (i.e., only four of ten SCCs leaked). For the two axial TSP outer diameter SCCs for which the remaining ligament ruptured and leakage occurred, the failures pressures were overestimated when the eddy current examination results were used to determine the crack geometries. However, when the failure pressures were computed using the post-test fractography profiles, the failure pressure was underestimated in one case and overestimated in the other.

The predicted leak rates based on fractography overestimated the test leak rates and those based on eddy current examination underestimated the test leak rates significantly. Fractography shows that the throughwall ligament did not fail completely and the crack opening was bridged by remaining ligaments of material. The ligaments limit the crack opening area and consequently limit the leak rate. The steep rise in the measured leak rate observed during testing was possibly due to rupture of some of these remaining ligaments. An axial outer diameter SCC which was comprised of four 100% TW cracks separated by three axial ligaments of various widths was analyzed by finite element analysis. The calculated pressures for rupture of the axial ligaments were consistent with the observed rupture pressure and crack length. The importance of identifying ligaments cannot be overemphasized. Ligaments are very effective in preventing unstable burst and reducing the crack opening area and the leak rate.

None of the tubes tested at ANL leaked at pressures under 16.7 MPa (2.56 ksi). The data obtained on these tubes were compared with the industry probability of leakage database and correlation. The results were generally consistent with the probability of leakage values presented by industry, i.e., tubes that would not be expected to leak based on measured eddy current voltages and the industry correlation did not leak. One crack with a relatively high eddy current voltage would have been expected to leak based on the correlation, but did not. However, even in the industry database there are cracks with similar voltages that did not leak.

The best predictions of the SCC profile and crack depth were obtained by the analysis of rotating pancake coil data with a multiparameter algorithm developed at ANL. Very little correlation between +Point amplitude and maximum depth of SCCs was found for the tubes that

were examined. The best chance for a good correlation between +Point signal amplitude and maximum depth occurs when all the cracks used to establish the regression curve and all cracks subsequently detected have the same morphology (crack opening with depth) and have the same extent of deposits and ligaments.

Changes in EC signals over time were observed for the SCCs while in storage. These changes are attributed to changes in corrosion products across the crack faces.

Acknowledgments

Acronyms and Abbreviations

BC	Bobbin coil
CODSCC	Circumferential outer diameter stress corrosion crack
EC	Eddy current
EDM	Electro-discharge machine
EDS	Energy dispersive x-ray spectroscopy
EM	Electromagnetic
EOC	End of cycle
ETSS	Examination Technique Specification Sheet
ID	Inner diameter
IDI	Inner diameter indication
IDSCC	Inner diameter stress corrosion crack
IGA	Intergranular attack
ISI	In-service inspection
LODSCC	Longitudinal outer diameter stress corrosion crack
MAI	Multiple axial indications
MBM	Manufacturer burnish mark
MCI	Multiple circumferential indications
MRPC	Motorized rotating pancake coil
NDE	Nondestructive evaluation
NQI	Nonquantified indication
OD	Outer diameter
ODI	Outer diameter indication
ODSCC	Outer diameter stress corrosion crack
POD	Probability of detection
RPC	Rotating pancake coil
RTZ	Roll transition zone
SAI	Single axial indication
SCC	Stress corrosion crack
SCI	Single circumferential indication
SEM	Scanning electron microscope
SGB	Steam generator B
SGD	Steam generator D
TS	Tube sheet
TSP	Tube support plate
TTS	Top of tube sheet
TW	Throughwall
VOL	Volumetric indication

1   Introduction

Objective

The objective of this report is to present the results of stress corrosion crack (SCC) studies involving tubes removed from a retired steam generator (SG) of a nuclear reactor. The SCCs investigated came from the tube support plate (TSP) regions and from the top of the tube sheet (TTS). Specific tasks involved in this effort include: (a) nondestructive evaluation (NDE) of selected tube support locations from tubes removed from a retired steam generator including operating history, (b) comparison of predicted burst pressure and leak rates from NDE to actual results, (c) destructive examinations (DE) to characterize the degradation morphology of field-induced SCC, and (d) assessment of the industry's amplitude-based sizing method.

This effort included a complete evaluation of six SCCs at TSP locations in the retired steam generator. The six TSP SCCs were pressure tested at room temperature to 52 MPa (7.5 ksi). The failure pressure and leak rate predictions, based on EC crack profiles and fractography, were compared to experimental results. In addition, four tube sheet (TS) SCCs were thoroughly evaluated. NDE and metallographic sectioning results of the four TS SCCs were compared with results of pressure testing.

Sequence of Events

In 1997 in-service inspection (ISI) reports involving bobbin coils (BCs) and rotating pancake coils (RPCs) were reviewed to identify locations of SCCs in two retired steam generators, designated SGD and SGB. The suspected SCCs were in tubes that were previously plugged because of possible degradation. Nineteen tubes in SGD were selected for the study and successfully unplugged. Eddy current (EC) measurements were obtained from 18 of the unplugged tubes and compared to EC data obtained during ISIs in 1994 and 1995. Growth of EC signals could be observed in some cases. These data were used to select the tubes to be removed from the steam generator and delivered to Argonne for further study. The tubes having SCCs at the TSP were pulled, leaving the TSP material behind. Many of the tubes of interest were in two TS sections cut out of SGD. The TS sections also contained tubes that were never plugged. Those tubes were also inspected.

Two large sections of TSP regions in retired SGB were removed and brought to Argonne, but these tubes have not been evaluated. The selection of the two sections of SGB were based on ISI calls indicating possible flaws in areas that were relatively easy to cut out.

Several SCCs from the retired SGD tubing were examined at Argonne in 2002 in a modified glove box using commercial instrumentation and industry-qualified procedures. Pulled tubes and sections of the TS were cut to a size that allowed entry to the glove box. Data obtained with BCs and RPCs in 1997 and 2002 were compared. Differences not necessarily attributed to crack growth were observed. The EC and RPC data from six TSP axial SCCs were studied, as were eight TS tubes, all which had SCC-like indications. Pressure testing and fractography were carried out on the six axial SCCs from the TSP regions and compared with EC crack profiles and predictions of burst and leak pressures. Results from NDE, pressure tests, and DE were compared for four of the TS SCCs. Profiling using the multiparameter algorithm with motorized RPC (MRPC) data compared favorably to DE results in most cases.

Amplitude-based sizing using laboratory and field data from a +Point Probe was evaluated because of industry's interest in estimating crack depth from signal amplitude alone. In this evaluation no significant correlation between +Point amplitude and maximum SCC depth was observed.

Table 1 shows the 20 tubes from retired SGD that were evaluated at Argonne. An X indicates if the tube was inspected with a BC and/or MRPC, a profile was created using Argonne's multiparameter algorithm (MP), the tube was pressure tested, a leak was observed (and at what pressure), a burst and leak pressure was predicted, there is a fractograph for the crack, and metallurgical sectioning was carried out. The type of degradation is also indicated: LOD for axial ODSCC, COD for circumferential ODSCC, and IGA for intergranular attack.

Table 1.   Row and column of tubes from retired SGD with indication of data collected from them.

	EC NDE (BC)	EC NDE MRPC	SCC Type	SCC MP Profile	Press. Test	Leak Obs. (Pres.)	Burst and Leak Prediction	Frac-tograph	Metallur-gical Section
TSP									
R4 C43	X	X	LOD	X	X	X (49 MPa)	X	X	
R5 C17	X	X	LOD						
R5 C51	X	X	LOD	X	X		X	X	
R7 C24	X	X	LOD	X	X		X	X	
R14 C55 Piece#3	X	X	LOD	X	X		X	X	
R14 C55 Piece#5	X	X	LOD	X	X		X	X	
R19 C20	X	X	LOD						
R39 C57	X	X	LOD	X	X	X (36 MPa)	X	X	
R45 C40	X	X	LOD						
Tube Sheet									
R5 C44	X	X	COD						
R11 C96	X	X	COD						
R13 C89	X	X	COD						
R17 C90	X	X	COD						
R33 C33	X	X	COD						
R37 C46 (#1)		X	COD						
R39 C 43 (#6)		X	COD		X	X (35 MPa)			X
R39 C44 (#7)		X	COD		X	X (50 MPa)			X
R39 C45 (#8)		X	IGA		X				X (SEM AND EDS)
R39 C46 (#9)		X	COD		X				X
R38 C46 (#10)		X	COD						
R38 C45 (#11)		X	COD						
R38 C44 (#12)		X	COD						

2   Results of 1997 Field Inspection

The NDE study of tubes from the retired SG began in 1997 with a visit to an SG storage facility. Clearance was adequate for pulling tubes from SGB and SGD. The SGs were stored with the hot leg up and slightly tilted so that water introduced during the water jet cutting operation drained toward the tube sheet. Counting equipment and inventories of radiation protection were housed in a radiation protection trailer, which also served as a change room. The tube removal work was carried out by Westinghouse-PCI.

Argonne specified the tubes that were candidates for pulling and those that needed to be unplugged. Tube pulls were not carried out above TSP level 4 because of the limited success in pulling tubes above that level. Two full-depth TS sections with SCC calls were cut from SGD. The utility packaged and shipped the samples.

Tube selection for pulling from SGD was based on previous ISI results and review of EC data after unplugging selected tubes. Steam-generator EC inspection data from the utility's plant were evaluated in an effort to optimize the selection of tubes for the tube removal effort. Tubes with single and multiple axial and circumferential indications in the TS and the first TSP were the main priority. Several tubes were selected as candidates for removal. Areas where defects were somewhat clustered were also identified. Those areas were the most interesting because selecting tubes in a relatively small area would minimize the total cost of providing tube samples. In-service EC inspection data on a magneto-optical disk were examined with Zetec Eddynet95 software to support the tube selection process. These data are the same as that used to decide which tubes to plug. Individual tubes (SGD), TS sections (SGD), and TSP sections (SGB) were removed and delivered to Argonne.

Twenty tubes from SGD were selected for plug removal. Nineteen of these 20 tubes were successfully unplugged in June 1997 (see Table 1). Eighteen of these 19 tubes were subsequently examined by NDE techniques, and the results were used to select tubes for pulling. Table 1 shows for 1994, 1995, and 1997, the location (row and column) of the 19 tubes, the BC and RPC calls, the location of the suspected flaw relative to TSP or TTS, type of call suspected, and a comparison of previous calls from 1994 and 1995 with those of 1997 after the tubes were unplugged.

Eddy current NDE was carried out in the field on tubes after they were unplugged and on some tubes (part of the TS sections) that were never plugged. Data were taken with a BC and RPCs, including the +Point. The procedure specified in the "Eddy Current Analysis Guidelines, Nuclear Station Unit 1" was followed. This and the subsequent analysis were a collaborative effort carried out with staff from ANL, the utility, and the Electric Power Research Institute (EPRI) NDE Center. An American Society of Mechanical Engineers (ASME) standard and a standard with 19 axial and circumferential OD and ID electro-discharge machined (EDM) notches were used for calibration before data collection.

Indication calls from 1997 are compared with calls from previous inspections in Table 2 for plugged tubes and Table 3 for unplugged tubes. In these tables, if a July 1997 indication is called MAI or MCI and a previous call of SAI or SCI was made at that location, an "x" is placed in the "previous call" column as well as in the "new call" column to reflect the assumption that the new multiple indication includes the previous single indication. When a call is made with two coils [e.g., MCI (+Point, RPC)] the locations following are in the same order as the coils used to locate the indication (e.g., 0.41, 0.01). There were numerous new calls in 1997.

Table 2. NDE Summary for Hot Leg Side from Retired Steam Generator D.
(The notation and acronyms below apply to Tables 1 and 2. All units for location in Tables 2 and 3 are in inches.)

Bold indicates tube-sheet removal samples	VOL = volumetric indication
MAI = multiple axial indication	TTS = top of the tube sheet TE = tube end
SAI = single axial indication	TSP = tube support plate
SCI = single circumferential indication	R-C = row and column
MCI = multiple circumferential indication MBM = manufacturing burnish mark	BC = bobbin coil
ODI = outer diameter indication IDI = inner diameter indication	+Point = Plus Point rotating pancake coil
NQI = non-quantifiable indication	RPC = 3-coil motorized rotating pancake coil

R-C	PREVIOUS ISI OF SELECTED PLUGGED TUBES			JULY 97 NDE AFTER UNPLUGGING TUBES			New Call	Prev. Call
	Indication Call	*Location*	*Date*	*Indication Call*	*Location*	*Date*	*New Call*	*Prev. Call*
04-43			12/95	SAI (+Point) MAI (RPC)	TTS -1.91 TTS -1.25	7/97	x x	
	NQI (BC) SAI (RPC)	1st TSP -0.04 1st TSP +0.04		NQI (BC) MAI (+Point,RPC)	1st TSP 1st TSP -0.09		 x	x x
05-17			12/95	MCI (+Point) MCI (RPC)	TTS -0.16 TTS +0.01	7/97	x x	
	NQI (BC) SAI (RPC)	2nd TSP -0.06 2nd TSP +0.02		NQI (BC) MAI (RPC)	2nd TSP 2nd TSP 0.00		 x	x x
05-44	NQI (BC) SCI (RPC)	TE +5.98 TTS -0.06	12/95	MCI (+Point,RPC) NQI (BC) MBM	TTS -0.07 2nd TSP 3rd TSP +37.7	7/97	x x x	x
05-51	NQI (BC) SAI (RPC)	1st TSP +0.10 1st TSP +0.14	12/95	NQI (BC) SAI (+Point) MAI (RPC) MAI (+Point) MAI (+Point) MAI (+Point) NQI (BC)	1st TSP +0.08 1st TSP +0.06 1st TSP +0.13 2nd TSP -0.09 3rd TSP +0.11 4th TSP +0.35 5th TSP +5.4	7/97	 x x x x x x	x x x
07-24			08/94	SCI (RPC) SAI (+Point) NQI (BC) MAI (+Point) MAI (+Point)	TTS +0.25 1st TSP (+0.47) 2nd TSP 2nd TSP (-0.01) 4th TSP (+0.27)	7/97	x x x x	
	NQI (BC) SAI (RPC)	2nd TSP +0.12 2nd TSP +0.09						x x
11-96	NQI (BC) MAI (RPC) MAI (RPC)	TE +17.41 TTS -4.12 TTS -3.92	12/95	NQI (BC) SCI (+Point)	TTS -4.0 TTS -5.0	7/97	 x	x
13-89	NQI (BC) MAI (RPC) SCI (RPC)	TE +14.59 TTS -4.24 TTS -0.14	12/95	 SCI (RPC,+Point)	TTS -0.03	7/97		 x
14-55	NQI (BC)	2nd TSP +0.04	12/95	MAI (+Point) NQI (BC)	1st TSP 2nd TSP	7/97	x	x

4

	PREVIOUS ISI OF SELECTED PLUGGED TUBES			JULY 97 NDE AFTER UNPLUGGING TUBES				
R-C	*Indication Call*	*Location*	*Date*	*Indication Call*	*Location*	*Date*	*New Call*	*Prev. Call*
	SAI (RPC)	2nd TSP -0.07		MAI (+Point) SAI (+Point)	2nd TSP 3rd TSP		x x	x
17-90	NQI (BC) SAI (RPC) SCI (RPC)	TE +15.50 TTS -1.75 TTS 0.00	12/95	MAI (RPC,+Point) MCI (RPC,+Point)	TTS +0.01 TTS +0.08	7/97	x x	x
19-20	ODI (BC) VOL (RPC)	5thTSP+24.63 5thTSP+25.16	12/95	VOL (+Point) VOL (RPC) MBM (BC)	5th TSP +44.74 5th TSP +30.12 5th TSP +25.2	7/97	x	x x
33-33	NQI (BC) MAI (RPC) MAI (RPC)	TE +17.57 TTS -4.07 TTS -3.87	12/95	NQI (BC) MAI (RPC,+Point) MCI (RPC,+Point)	TTS -4.0 TTS -0.66,0.01 TTS -0.01	7/97	x x	x x
36-33	SCI (RPC)	TTS -0.02	12/95	MCI (+Point,RPC) MAI (+Point)	TTS -0.41,0.00 TTS -0.41	7/97	x x	x
37-30	MCI (RPC)	TTS -0.08	08/94	MCI (+Point,RPC) MAI (+Point,RPC)	TTS -0.15,0.10 TTS +0.10	7/97	x x	x
37-46	SCI	TTS -0.05	04/93	MCI /MAI (+Point,RPC)	TTS (-0.01,0.03)	7/97	x	x
38-46	IDI (BC) MAI (RPC) MCI (RPC)	TE +16.65 TTS -3.92 TTS +0.01	08/94	Broken Reamer, thus no access				
39-43	SCI (RPC)	TTS 0.00	08/94	NQI (BC) MCI (+Point) MAI (+Point/RPC)	TTS +0.87 TTS -0.26 TTS -0.28	7/97	x x	x
39-46	SCI (RPC)	TTS -0.07	08/94	SCI (RPC)	TTS -0.07	7/97		
39-57			08/94	MCI /SAI (+Point) SCI (RPC)	TTS -0.17 TTS -0.05	7/97	x x	
	NQI (BC) SAI (RPC)	1st TSP -0.07 1st TSP -0.01		NQI (BC) SAI (+Point,RPC)	1st TSP +0.03 1st TSP -0.10			x x
45-40			12/95	MAI/MCI (+Point, RPC)	TTS +0.05/06	7/97	x	
	NQI (BC) SAI (RPC)	1st TSP +0.08 1st TSP +0.01		NQI (BC) NQI (BC) SAI (+Point)/ MAI (RPC) MAI (+Point,RPC)	1st TSP +0.03 1st TSP +4.0 1st TSP +0.17 2nd TSP -0.04		x x x	x x

Table 3.   NDE Summary for Hot Leg Side (never plugged) from Retired Steam Generator D.

| R-C | PREVIOUS ISI OF SELECTED TUBES NEVER PLUGGED (In tube sheet removal sections) | | | JULY 97 NDE | | | New Call | Prev. Call |
	Indication Call	Location	Date	Indication Call	Location	Date		
36-32	-			MAI (+Point) MAI (RPC)	TTS +28.00 TTS +0.24	7/97	x	
37-31	NQI	19th TSP	12/95		-	7/97		
37-32	-			NQI (BC) SCI (+Point, RPC)	TTS +0.66 TTS -0.05	7/97	x x	
37-44	-			VOL (RPC)	TTS +0.08	7/97	x	
37-45	-			-	-	7/97		
38-43	-			NQI (BC) SCI (+Point) VOL(+Point)	TTS +0.52 TTS -0.09 TTS +0.38	7/97	x x x	
38-44	-			NQI (BC) MCI (+Point)	TTS 0.9 TTS 0.00	7/97	x x	
38-45	-			NQI (BC) MCI (+Point)	TTS +0.88 TTS -0.09	7/97	x x	
39-44	-			NQI (BC) MAI/MCI (+Point, RPC)	TTS +0.85 TTS +0.04	7/97	x x	

6

2.1 Characterization of Unplugged Tubes in the Field

To determine any changes in EC voltages between current and previous inspections of unplugged tubes, the procedure specified in the "Eddy Current Analysis Guidelines Nuclear Station Unit 1" was followed for the unplugged tubes listed in Tables 4 and 5. Unprocessed BC data taken in previous ISIs were used to reproduce, for the tubes selected, the amplitude and phase results reported in the utility EOC10 (12/95) and EOC9 (8/94) summary sheets. The same procedure used in 1994 and 1995 was applied to data taken in July 1997. The same reference standards and normalizations used in 1994 and 1995 were used in 1997.

The BC voltages for stress corrosion cracking (SCC) at TSP are presented in Table 4; in all cases, the voltage increased after unplugging. Factors that could result in voltage increases include crack growth, cracks opening wider, or a change in deposits. Note that the voltage increase for the one tube plugged in August 1994 (R7 C24) was the most dramatic.

A similar comparison of voltages for a standard 2.9-mm (0.115-in) diameter pancake coil is presented in Table 4. Reproducing the results in the utility summary sheets from EC data of previous ISIs was more difficult for the RPC than the BC data because the analysis is somewhat more subjective. When current RPC data are compared with earlier RPC ISI data, the voltages, except for R33 C33 and R5 C17, were about the same or increased with time. Again, for the tubes plugged in 1994 (R7 C24), the voltage increase was most dramatic.

In addition, several new indications from relatively weak EC signals were identified. These new indications were identified with coils used in prior ISI or from the +Point coil (not used during previous ISI). A review of some earlier EC data indicated that these new calls would not have been made with the data available during previous inspections because either (1) the EC signals initiated after the December 1995 ISI or (2) the EC signals were too weak to be called flaw indications with probes used at that time but had grown enough to be detectable now. Examples are shown in Figs. 2.1 and 2.2, which show a comparison of standard pancake data in the form of an isometric plot (c-scan) around the top of the tube sheet. In 1995, there was no clear evidence of a crack (Figure 2.1). In 1997, the EC signal pattern had changed (Figure 2.2), and multiple axial and multiple circumferential crack calls were made. This example suggests growth of EC signals in plugged tubes.

Table 4.   Bobbin coil voltages before plugging and EC voltages after deplugging for selected tubes from hot-leg side of retired steam generator D.

Tube Position	Bobbin Coil (volts)		Call[b]/ Location[c]	Difference	
	Before Plugging[a]	After Unplugging[a]		Volts	Percent
R4 C43	0.56	1.56	MAI/1st TSP	1.00	179
R5 C17	0.32	0.70	MAI/2nd TSP	0.38	119
R5 C44	8.0	14.00	MCI/TTS	6.00	75
R5 C51	0.45	1.30	MAI/1st TSP	0.85	189
R7 C24	0.56	6.66	MAI/2nd TSP	6.10	1089
R11 C96	10.54	12.50	SCI/TTS[d]	1.96	19
R13 C89	3.88	5.22	SCI/TTS	1.34	35
R14 C55	0.35	0.91	MAI/2nd TSP	0.56	160
R17 C90	4.07	4.90	MAI-MCI/TTS	0.83	20
R19 C20	0.52	0.54	Vol/5th TSP+	0.02	4
R33 C33	6.61	10.00	MCI-MAI/TTS	3.39	51
R39 C57	1.14	1.80	SAI/1st TSP[d]	0.66	58
R45 C40	0.27	0.57	MAI/1st TSP[d]	0.30	111

[a]Tubes plugged 12/95, except R7 C24 plugged 8/94; all tubes unplugged 7/97.
[b]MAI = multiple axial indication, MCI = multiple circumferential indication, SAI = single axial indication, SCI = single circumferential indication, Vol = volumetric indication.
[c]TSP = tube support plate; TTS = top of tubesheet
[d]Nearly through-wall indication from ISI before plugging.

Table 5. RPC coil voltages before plugging and EC voltages after unplugging for selected tubes from hot-leg side of retired steam generator D.

| Tube Position | RPC (volts) | | Call[b]/ Location[c] | Difference | |
	Before Plugging[a]	After Unplugging[a]		Volts	Percent
R4 C43	0.47	1.20	MAI/1st TSP	0.73	155
R5 C17	0.48	0.37	MAI/2nd TSP	-0.11	-23
R5 C44	0.59	0.90	MCI/TTS	0.31	53
R5 C51	0.22	0.93	MAI/1st TSP	0.71	323
R7 C24	0.35	2.75	MAI/2nd TSP	2.40	686
R11 C96	7.64	-	SCI/TTS[c]	-	-
R13 C89	0.34	0.66	SCI/TTS	0.32	94
R14 C55	0.34	0.69	MAI/2nd TSP	0.35	103
R17 C90	0.52	2.40	MAI-MCI/TTS	1.88	362
R19 C20	0.93	1.04	Vol/5th TSP+	0.11	12
R33 C33	2.74	1.02	MCI-MAI/TTS	-1.72	-63
R39 C46	0.7	2.80	MAI-SCI/TTS	2.10	300
R39 C57	0.57	1.17	SAI/1st TSP[d]	0.60	105
R45 C40	0.27	0.39	MAI/1st TSP[d]	0.12	44

[a]Tubes plugged 12/95, except R7 C24 plugged 8/94; all tubes unplugged 7/97.
[b]MAI = multiple axial indication, MCI = multiple circumferential indication, SAI = single axial indication, SCI = single circumferential indication, Vol = volumetric indication.
[c]TSP = tube support plate; TTS = top of tubesheet
[d]Nearly through-wall indication from ISI before plugging.
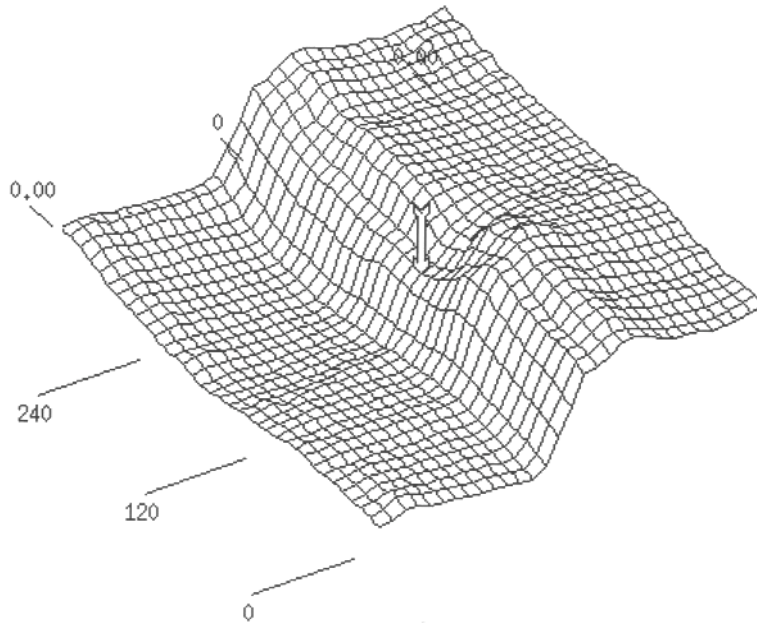
Figure 2.1   C-scan plot of tube R45 C40 using a 2.9-mm (0.115-in.)-diameter MRPC showing the top of tube sheet in December 1995. No crack call was made at that time. The tube axis is from lower left to upper right, with 360° of the tube shown. The roll transition in indicated by the arrow.
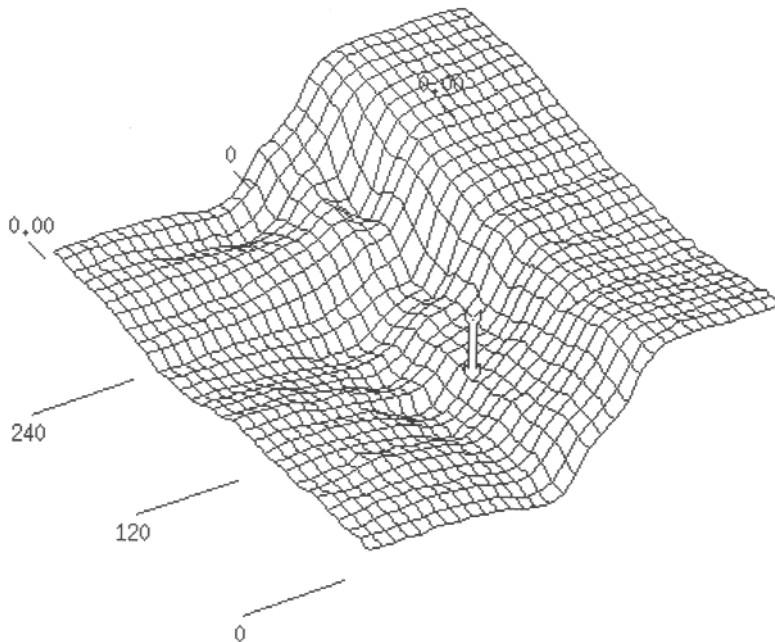
Figure 2.2   C-scan plot of tube R45 C40 using a 2.9-mm (0.115-in.)-diameter MRPC showing the top of tube sheet in July 1997. Multiple axial and circumferential cracks were called at that time. The tube axis is from lower left to upper right, with 360° of the tube shown. The roll transition in indicated by the arrow. The variation in EC signal between 1995 and 1997, from the same type of pancake coil, can easily be seen.

2.2 EC Signal Growth

Growth of an EC signal attributed to an SCC can be seen by comparison of Figs. 2.3 and 2.4. In Figure 2.3, which shows data from 1994, the arrow on the c-scan plot points to an EC signal at the TTS in tube R39 C46 generated by a 2.92-mm (0.115-in.)-diameter MRPC. This indication (SCI) was called an SCC in August 1994 and plugged. Figure 2.4 shows a c-scan of the TTS in July 1997 after the tube was unplugged. These data were also taken with a 2.92-mm (0.115-in.)-diameter MRPC. The signal has grown considerably in amplitude (0.7 to 2.8 V) and the apparent circumferential extent of the indication has increased as shown in Figure 2.5. Potential reasons for these changes are discussed in Sec. 2.1.
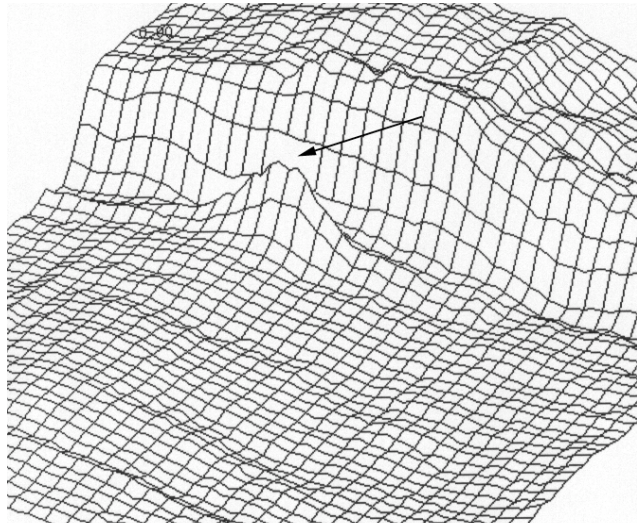
Figure 2.3   C-scan plot from 2.92-mm (0.115-in.) diameter MRPC. Arrow points to indication at top of tube sheet (TTS) in tube R39 C46. This indication was called an SCI in August 1994. Tube axis is from lower left to upper right, with 360° of tube shown.
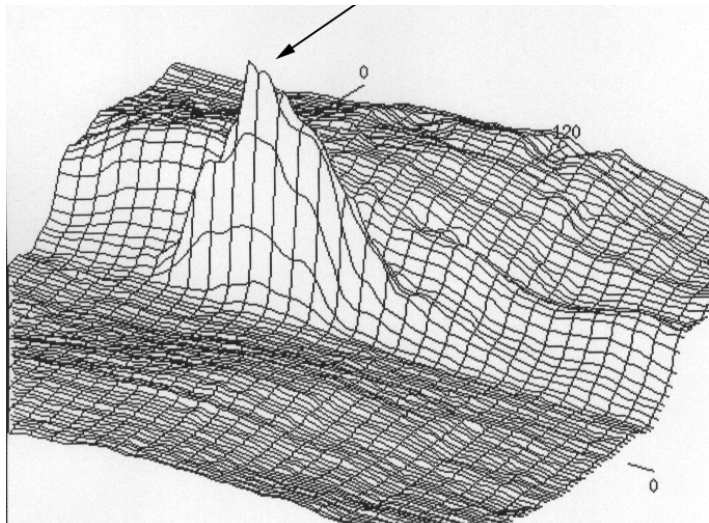
Figure 2.4   C-scan plot of same region shown in Figure 2.3 taken with a 2.92-mm (0.115-in.)-diameter MRPC in July 1997 after tube was unplugged. Signal (arrow) has grown considerably relative to roll transition. Tube axis is from lower left to upper right, with 360° of tube shown.

Upper and lower limits for estimated length
of CODSCC at RT in 1994 and 1997
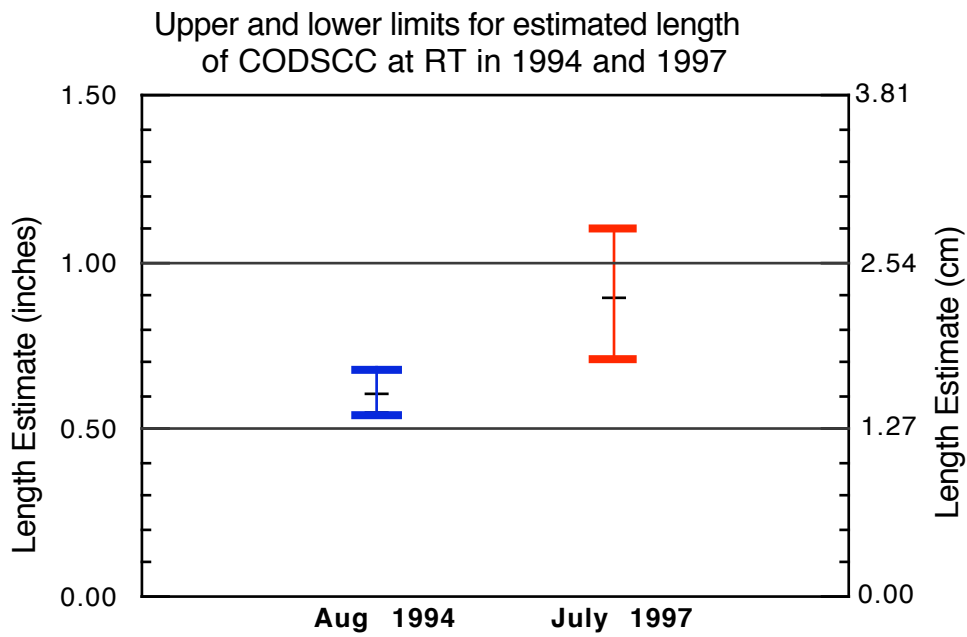
Figure 2.5   Graph showing estimated length with range of uncertainty for circumferential outer diameter stress corrosion crack (CODSCC) at top of tube sheet in tube R39-C46 of retired steam generator before (August 1994) and after (July 1997) unplugging. The data suggest growth of the SCC during the time tube 39-46 was plugged.

3   Examination and Testing of SG Tubes in Argonne Glove Box

Several SCCs from the retired SG tubing have been examined at Argonne using a modified glove box, a 4D Pusher Puller, a MIZ30, and Eddynet 98 software. Figure 3.1 shows a schematic of this sealed facility, which allows for manipulation and examination of SCCs in the glove box. Figure 3.2 shows a sample inside the glove box. Pulled tubes and sections of the TS are cut to a size that allows entry to the glove box. Details of the cutting procedure are presented in Appendix A. Care was taken with the TS sections to not disturb the deposits. Pulled tubes were cleaned with mild soap and water only. Cutting and cleaning reduced the radiation levels to manageable levels. Procedures were developed for sample preparation, NDE, pressure testing, and destructive evaluation of TSP and TS tubes with SCCs from the retired SG. Appendix B gives the decontamination procedures adopted for the TS tubes.
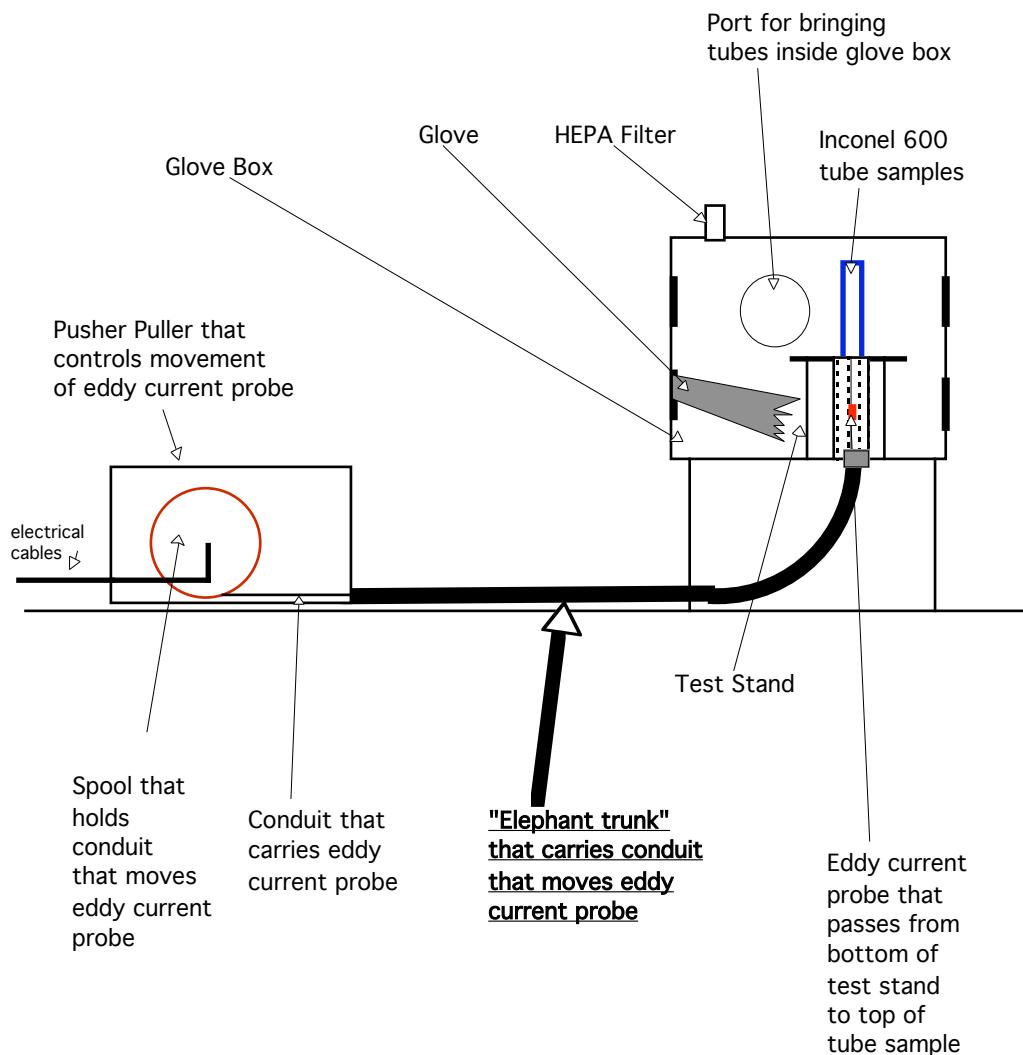
Figure 3.1   Schematic of sealed NDE glove box facility, which allows for manipulation and examination of SCC in the glove box.

13
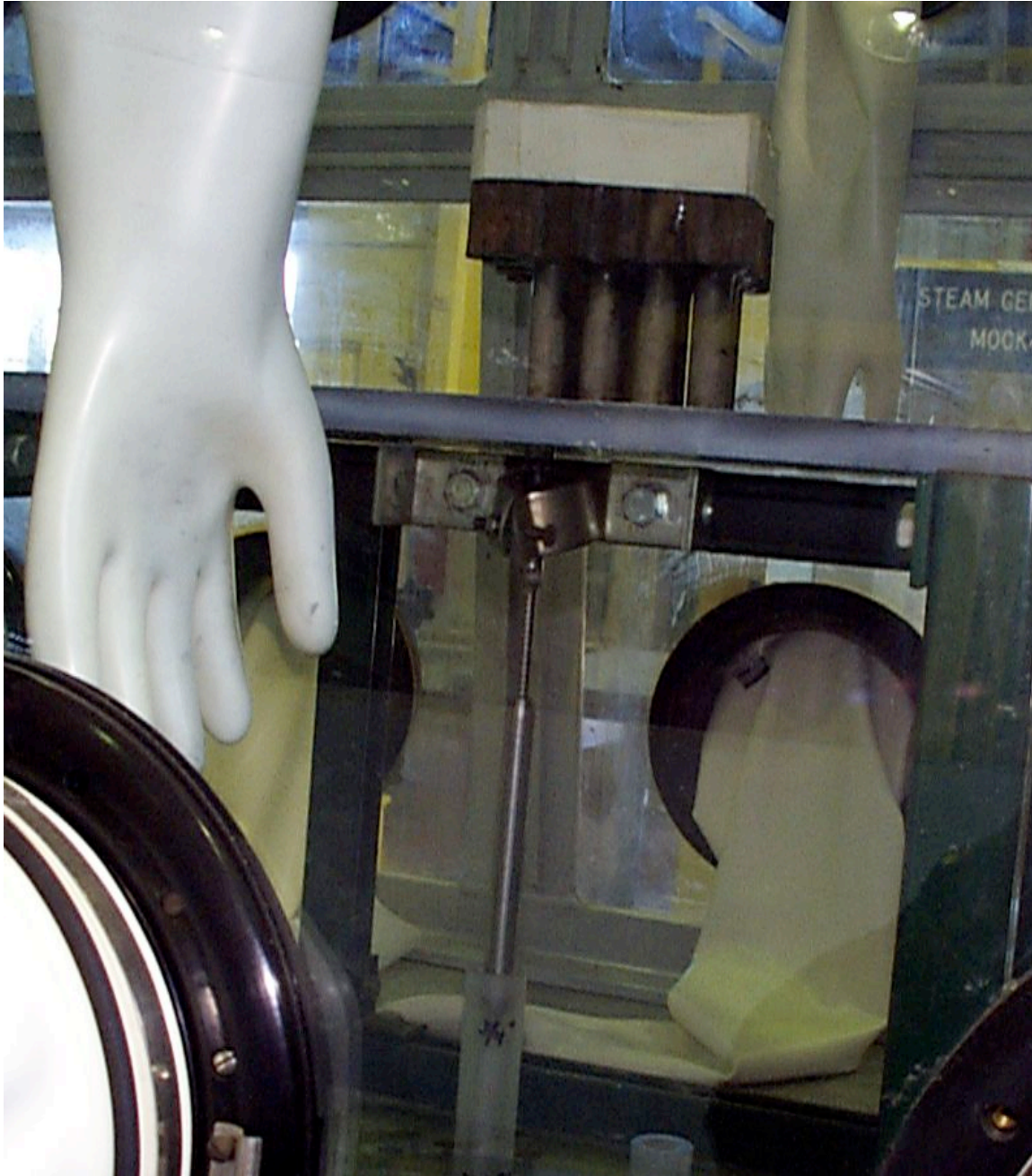
Figure 3.2   Photograph of section of the retired SG tube sheet placed in the Argonne NDE Glove Box. The tube sheet section (seen at top center of photo) contains 12 tubes and is ready for eddy current examination. Each tube extends 7.5 cm above and below the roll transition. The eddy current probe enters the tube from below.

3.1 Comparison of Argonne and Utility SCC TSP data

A comparison has been made between pre-pull 1997 and 2002 Argonne EC data. This comparison using BC and +Point data provides some insight into the effects of the tube pulling on the EC signal. Table 6 shows the unplugged pre-pull BC voltage and phase in 1997 compared with the pulled tube BC voltage and phase measured at Argonne in 2002 for SCC at TSP locations.

The Argonne results are with and without a ring over the crack to simulate the TSP. In general, the voltages measured at Argonne are slightly lower, with the phase essentially unchanged except for SCC noted as "A." Measurements were made at Argonne following the same procedure as that used for measurements at the utility. An ASME standard was used by setting the 550-130 kHz mix channel for the four 20% through-wall (TW) holes to 2.75 V and the phase of the 100% TW hole to 40 degrees. Differences could result from variations in the mix and changes in conduction paths across the crack faces due to the tube pulling procedure (i.e., crack faces now touching). All five test sections were pressurized at room temperature to a maximum pressure of 7500 psi (52 MPa). Tube B failed (first observed leak) at 7100 psi (49 MPa) and leaked at a rate of 8.5 gal/min (0.54 kg/s). Tube E failed at 5100 psi (35 MPa). The others did not fail at the maximum system pressure of 7500 psi (52 MPa). A detailed discussion of pressure testing is provided in Section 6 and in Ref. 2.

While some variation in BC voltages between 1997 and 2002 data is observed (Table 6), there is much less change than for the +Point volts (Table 7). The bobbin coil is a measure of the volume of the degradation while a +Point signal is more a measure of how the eddy currents are interrupted locally. Figure 3.3 shows +Point maximum volts obtained by EC analysis of six axial SCCs at TSP intersections of the retired steam generator. Voltages are compared to maximum depth established by fractography. Also, pre-pull EC data (BC and +Point) analyzed at Argonne using standard industry practices were compared with pre-pull data provided by the utility. The voltages are virtually identical. While BC data may be affected by tube pulling and change in corrosion products, the +Point signal for the TSP SCC are much less affected. TS +Point data is affected by change in deposits between the crack faces and not by geometry changes as the TS tubes were cut out of the steam generator, not pulled.

Table 6.   Comparison of BC data (550-130 kHz mix channel) before and after tube pull

Flaw Type and Location	Bobbin Coil Voltage and Phase Measured at the Utility (550-130 kHz Mix) before the Tube was Pulled (1997)	Bobbin Coil Voltage and Phase Measured at Argonne (550-130 kHz Mix) with and without TSP Simulation (2002)
A.(R5C51) 1st TSP, LODSCC	1.3 volts/83 deg	1.1 volts/130 deg -with TSP 1.2 volts/123 deg -no TSP
B.(R4C43) 1st TSP, LODSCC	1.6 volts/87 deg	1.3 volts/ 87 deg -with TSP 1.0 volts/ 69 deg -no TSP
C.(R7C24) 2nd TSP, LODSCC	6.7 volts/81 deg	3.9 volts/ 79 deg -with TSP 4.3 volts/ 82 deg -no TSP
D.(R14C55)2nd TSP, LODSCC	0.9 volts/120 deg	0.8 volts/133 deg -with TSP 0.9 volts/137 deg -no TSP
E.(R39C57 1st TSP, LODSCC	1.8 volts/ 46 deg	1.8 volts/ 40 deg –with TSP 1.8 volts/ 40 deg. –no TSP

LODSCC = longitudinal outside diameter stress corrosion crack.
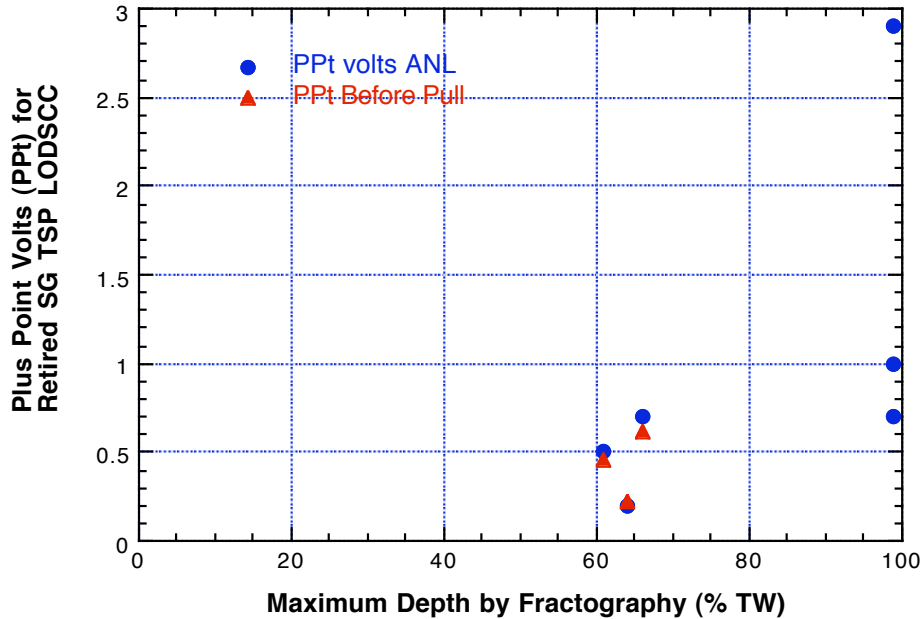
Figure 3.3   Graph of EC Plus Point (PPt) volts vs. maximum depth determined at Argonne by fractography for axial ODSCC at TSP intersection in retired steam generator. The two ODSCC at 100% TW at 1.0 and 0.7 V leaked at 5.2 ksi (36 MPa) and 7.1 ksi (49 MPa), respectively (+Point data before pulling is not available).

No correlation between +Point volts and maximum depth is observed for the set of TSP field induced SCC of Fig. 3.3. In contrast, industry has presented a better correlation between +Point volts and maximum depth specifically for circumferential ODSCC at a roll transition. Those data can be found in Figure G-14b of Appendix G of the December 1997 EPRI Report TR-107 197-P2 [1]. A similar lack of correlation between +Point volts and depth has been observed for Argonne–laboratory–grown circumferential and axial SCC. In contrast, in a benchmarking exercise at Argonne using laboratory-grown SCC, the multiparameter algorithm with pancake coil data was reasonably successful in profiling both axial and circumferential cracks [2].

3.2   Pressure tests on SG tubes from the Tube Sheet

Tests with the retired SGD TS sections were also carried out at ANL. Eddy current testing of tubes from the tube sheet is different from that of pulled tubes with SCC at the TSP levels. The TS tubes are not pulled, so distortion of the EC signals from SCC is not a factor in any change of signal over time. The roll transition, however, does complicate the signal analysis. In addition, although some metallographic sectioning was carried out, no crack profiles were obtained to compare with NDE profiles.

The cleaning of a 12-tube TS section from SGD (Figure 3.4) was carried out with a special thin epoxy spread around the top of the tube sheet to protect the corrosion products. The bottom of the TS and the excess portion of the tubes were cut off. The remaining piece was 6-in. (15-cm) high with most of the piece below the top of the TS and small enough to be brought into the NDE glove box for examination. Three tubes were unplugged before the TS section was delivered to Argonne. Blockages in two tubes (one a plug and the other a part broken off during unplugging) were removed when the section was reduced in size. Six tubes were never plugged, though before

shipping to Argonne, MRPC data suggested small circumferential indications in most of those tubes.

In Figure 3.4, calls from the 1997 EC examination are shown for tubes inspected. Results from examination at Argonne were compared to data acquired before the TS section was cut from the retired SG. Following EC examination of the tubes, four tubes were selected for pressure and leak testing (Nos. 6-9). Figure 3.5 shows one of the tubes (No. 8) after pressure testing. Some TS material remains around the tube after reducing the size of the tube to fit the apparatus for pressure testing. Fittings to carry out the pressure test are attached to the ends of the tube.

Tube Sheet Section

■ Plugged tube
■ Tubes never plugged
■ Tubes unplugged

Three letter codes are the result of examination after tubes were unplugged but before the section was removed from the steam generator. Results are for unplugged tubes and tubes that were never plugged.

4 37-43	3 37-44 VOL	2 37-45 NDD	1 37-46 MCI/MAI
5 38-43 SCI/VOL	12 38-44 MCI	11 38-45 MCI	10 38-46
6 39-43 MCI/MAI	7 39-44 MCI/MAI	8 39-45	9 39-46 MCI/MAI

MCI	multiple circumferential indications	MAI	multiple axial indications
SCI	single circumferential indication	VOL	volumetric indication
		NDD	non-detectable degradation

Figure 3.4   Map of a 12- tube retired steam generator tube sheet section examined in Argonne's NDE glove box using a motorized rotating pancake coil (MRPC). Tubes noted as 1, 6, and 9, were unplugged before the removed tube sheet section was delivered to Argonne. Blockages in tubes 8 (plug left in), and 10 (broken unplugging tool) were removed at Argonne when the section was reduced in size. Tube 4 remained plugged. Tubes 2, 3, 5, 7, 11, and 12 were never plugged, though before shipping to Argonne, results of MRPC data analysis suggested small circumferential indications in most of those tubes.

Figure 3.5   Photograph of Alloy 600, 19.1-mm (3/4-in.) diameter, test section #8 from retired steam generator after pressure testing. Some tube sheet material remains around the tube after reducing its size for pressure testing. Fittings to carry out the pressure test are attached to the ends of the tube. The top of the TS is on the right side of the photograph at the end of the tube.

Table 7.   Change of +Point volts from 1997 (before removal from SGD)
to 2002 (examined in ANL glove box) for selected TS tubes

Tube No.	2002 Maximum +Point Voltage @ 300 kHz	1997 Maximum +Point Voltage @ 300 kHz	Estimated Maximum Depth (%TW)
1	8.86	4.39	70
6	2.95	1.54	50
7	0.78	0.76	50
8	2.37	Plugged	87
9	24.85	2.36	90

Examples of change in +Point eddy-current voltage of ODSCC in the RTZ of retired SGD test sections are presented in Table 7. Table 7 compares, for five TS tubes, the +Point voltage at 300 kHz in 2002 to that measured in 1997. The 2002 measurements were made in the NDE glove box facility at Argonne with the 3 x 4 TS array intact. The 1997 measurements were made before the test sections were removed from the steam generator. Crack growth, if any, is not readily apparent from 3-D images of the crack voltage profiles. The maximum +Point voltages measured in the NDE glove box at Argonne are generally larger than measured in 1997 before the section was cut and delivered to Argonne. The deepest cracks showed the greatest change. Voltage changes are not expected to be the result of mechanical distortion of the crack during removal from the SG. The increase in voltage is attributed to changes in the electrical properties of the material between the crack faces (e.g., less conducting). Only tubes 6, 7, 8, and 9 were pressure tested. Tube 1 is shown because of its large change in voltage. BC voltages would not necessarily follow the same

18

trend as the +Point volts as the BC is a measure of degraded volume and the +Point voltage is a measure of localized conduction across a crack face.

Pressure testing was carried out using the Room-Temperature High-Pressure Test Facility that can produce pressures up to 51.7 MPa (7500 psi). Pressure is provided by a constant-rpm single-acting triplex constant-displacement pump driven by a 60-hp electric motor that provides a constant 48.4 L/min (12.8 gpm) flow of water at up to 51.7 MPa (7500 psi). Pump–generated pressure pulsation is <0.34 MPa (<50 psi). The pump has two overpressurization protection safety relief valves, one located on the pump and the other on the 139-L (40-gal) water accumulator suction tank. The lever-operated hydro-diverter control valve originally supplied with the pressurizer was modified to work in series with a screw unloader valve that allows more positive, finer control of pressurization. The pressurizer water pump system can operate with a continuous supply of water from the building water system.

The system can be used for testing field-pulled tubes. The module for testing radioactive tubes is also supplied pressurized water and controlled from the High-Pressure Facility. It is essentially a 380 L (100 gal) stainless steel holding tank that captures all the water that flows through the tube and flaw under test. Thus, any particulate contamination released from the tube will be captured. Upon completion of a test, the water in the tank is filtered to trap any particulate before the water is released. A breather/overflow vent prevents module pressure buildup during testing and is fitted with a filter to prevent any release of particulate contamination. A level sensor alarm in the containment module is used to indicate that the maximum water fill level has been reached and the test should be terminated.

One of the four tubes (#6) cut from the retired SG TS section was tested under pressure at Argonne to approximately 51.7 MPa (7500 psi). The tube has a circumferential OD stress corrosion crack in the roll transition zone (RTZ). The maximum depth was estimated to be 50% TW based upon phase analysis of +Point data. The crack started leaking at around 35.2 MPa (5100 psi) with a rate of 0.4-0.8 L/min (0.1-0.2 gal/min). Increasing pressure to about 51.7 MPa (7500 psi) did not lead to a significant increase in leak rate (less than 5% increase). Figure 3.6 compares the cross sections from +Point c-scans before and after pressure testing and the pre-test crack profile, both as a plot of signal amplitude and point-by-point depth by phase analysis. The point-by-point analysis suggests the presence of axial ligaments at circumferential location 140-180 degrees. The depth at that location is estimated to be about 20% TW. The maximum depth is estimated to be at circumferential location 80 degrees. Based on the small depth this crack should not have leaked. Nevertheless, the crack has grown around the circumference significantly (223° to 281°). Additional eddy current data was obtained after pressure testing. A few peaks became more prominent, and the voltage for the crack increased from 2.46 to 2.97 V, suggesting very little growth in overall crack opening. Sectioning revealed the CODSCC to be 0.5 mm below TTS at the EC indication. Where the amplitude increased during 2002 pressure testing, and where the presence of ligaments is suggested (140-180° in Figure 3.6), the +Point depth by phase grew to about 90% TW with little change elsewhere. A cross section through the point of maximum voltage revealed a crack only about 80% TW (Figure 3.7). The leak is presumed to have occurred at the location of the ligaments. The presence of ligaments led to a large underestimate of the crack depth at location 140-180 degrees. The ligaments are presumed to produce conducting paths for the eddy currents resulting in a smaller voltage amplitude and an underestimate of depth. Because the EC voltage was not a good indicator of the flaw size, it did not indicate the tube leakage behavior accurately. The phase angle also gave a misleading underestimate of the crack

depth. The importance of identifying ligaments in an eddy current scan, as seen in this example, cannot be overemphasized.

The second of the four tubes (#8) cut from the retired steam generator tube sheet section at Argonne was tested under pressure (Figure 3.5 shows the tube after pressure testing). The tube was pressurized to about 50.3 MPa (7300 psi) without leaking. The crack indication is at the very top of the TS in the roll transition and was constrained somewhat by the TS material during pressure testing. The 300 kHz +Point c-scans before and after pressure testing are relatively smooth, as shown in Figure 3.8. The pressure test resulted in an increase in the 300 kHz +Point signal from 2.37 to 3.08 V with a very small increase in +Point estimated depth (from 87% TW to 91% TW). No significant increase in length was observed. No significant increase in length was observed. While the 3-D image suggests a circumferential crack, the +Pt phase angle of the circumferential component of the Lissajous figure (not shown) indicates an axial orientation. One possible explanation is that the cracked area consists of numerous, closely spaced, short (~3 mm or 0.12 in. long), very deep axial SCCs in the RTZ extending about 120° around the tube. The axial length was determined from the number of hits in the flaw signal in the axial direction. The difficulty with this explanation is related to the shape of the EC profile, which is more representative of a deep circumferential crack. A review of the pancake data did not help resolve this issue. The EC technique is not able to resolve closely spaced axial cracks. The result (no leak and little change in EC crack profile with pressure) is consistent with the possibility of many deep but small axial SCCs in the RTZ constrained to some extent by TS material. Metallography revealed closely spaced axially oriented deep IGA (Figure 3.9) in support of the +Point phase analysis.

The EC +Point profiles before and after pressure testing of the RTZ SCC #9 are shown in Figure 3.10. This circumferential SCC had 90% TW initial +Point depth estimate. This CODSCC was called SCI with a 0.70 V pancake signal in 1994, a 2.36 V +Point signal in 1997, and a 24.85 V +Point signal in 2002. Pressure testing was carried out to 52 MPa (7500 psi) with no leak. Metallographic sectioning of the CODSCC in tube #9 shows a throughwall crack just below the TTS (Figure 3.11). The crack opening is about 40 μm. Leakage is blocked, presumably by obstruction in the crack or in the deposits at the TS. The 10-fold increase in EC signal may be the result of a change over time in corrosion products conducting current across the crack faces (i.e. less conduction in 2002). This example shows the possibility of leak detection systems missing a throughwall crack and the importance of maintaining EC inspection history that can indicate crack growth through analysis of +Point phase and amplitude data.   Not that the EC circumferential extent was about 270 degrees with out any significant change due to pressure testing to 52 MPa (7500 psi). The large extent of the crack could be a factor in the change of deposits across the crack face as the opening of such a long crack could be significant.
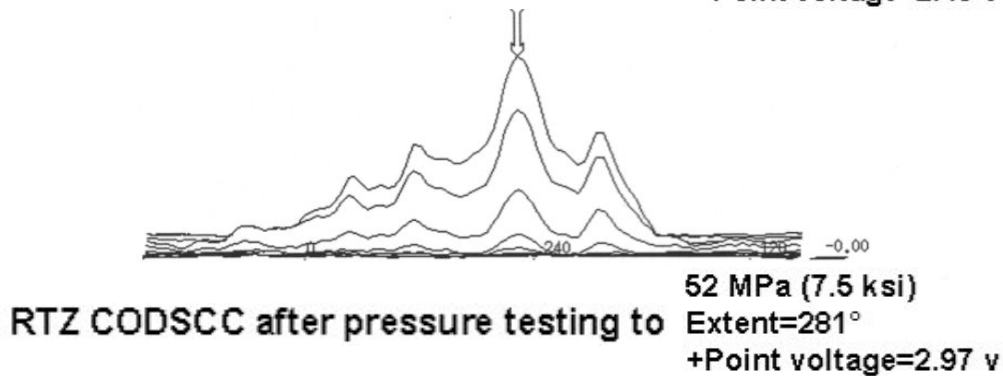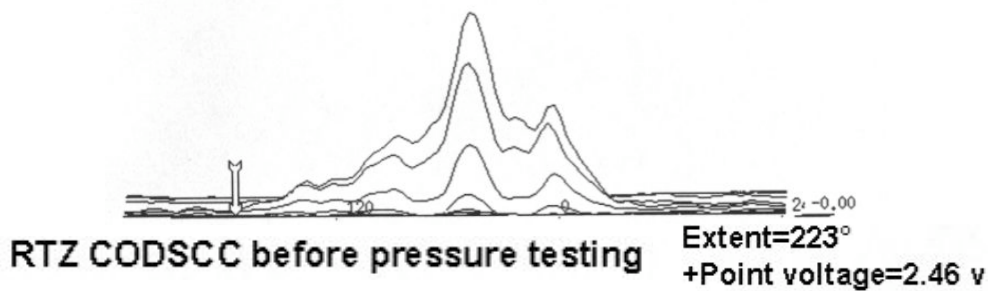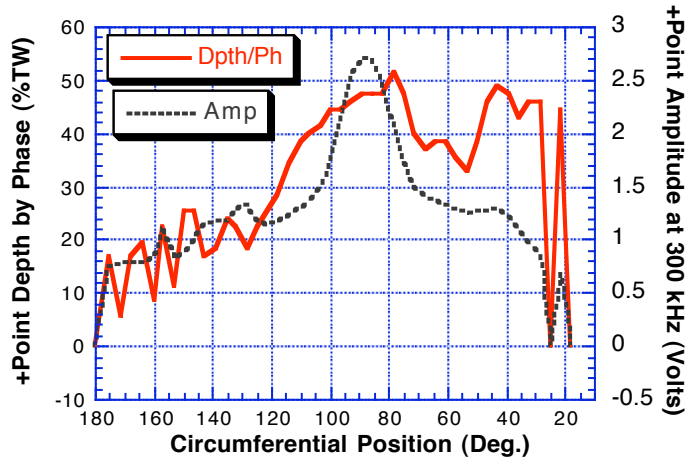
Figure 3.6   EC +Point profiles of CODSCC in RTZ with 50% TW depth (tube #6). The 1994 call was SCI with 0.73 V from a pancake coil. The 1997 +Point maximum signal was 1.54 V. The 2002 +Point maximum signal was 2.46 V. EC cross sections of this CODSCC were taken from standard +Point c-scans at 300 kHz. Pressure testing to 51.7 MPa (7.5 ksi) resulted in an increase in the extent of the crack (223° to 281°) and an increase in +Point voltage (2.46 to 2.97 V). A leak appeared at 35.2 MPa (5.1 ksi).
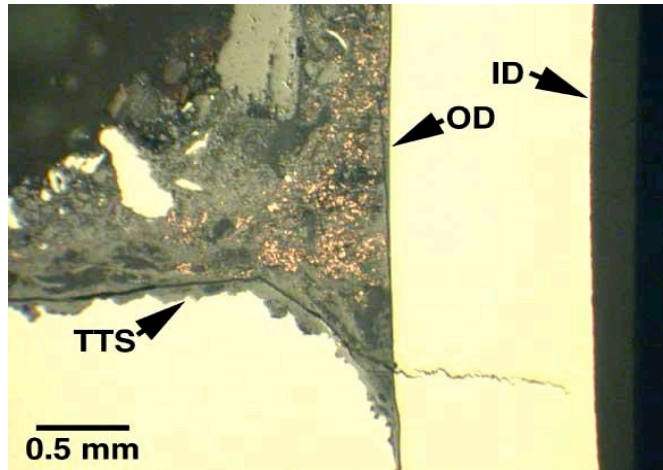
Figure 3.7   Micrograph of CODSCC in RTZ of tube #6 just below the top of the tube sheet. The cross section is through the point of maximum +Point voltage. The crack, which leaked, is only about 80% TW at this point (not 100% TW).

Figure 3.8   Image of +Point c-scans of tube sheet test section #8 at 300 kHz, before (top) and after (bottom) pressure testing to 50.3 MPa (7300 psi). The pressure test resulted in an increase in the 300 kHz +Point signal from 2.37 to 3.08 V with a very small increase in +Point estimated depth (87% to 91%TW). No significant increase in length was observed.

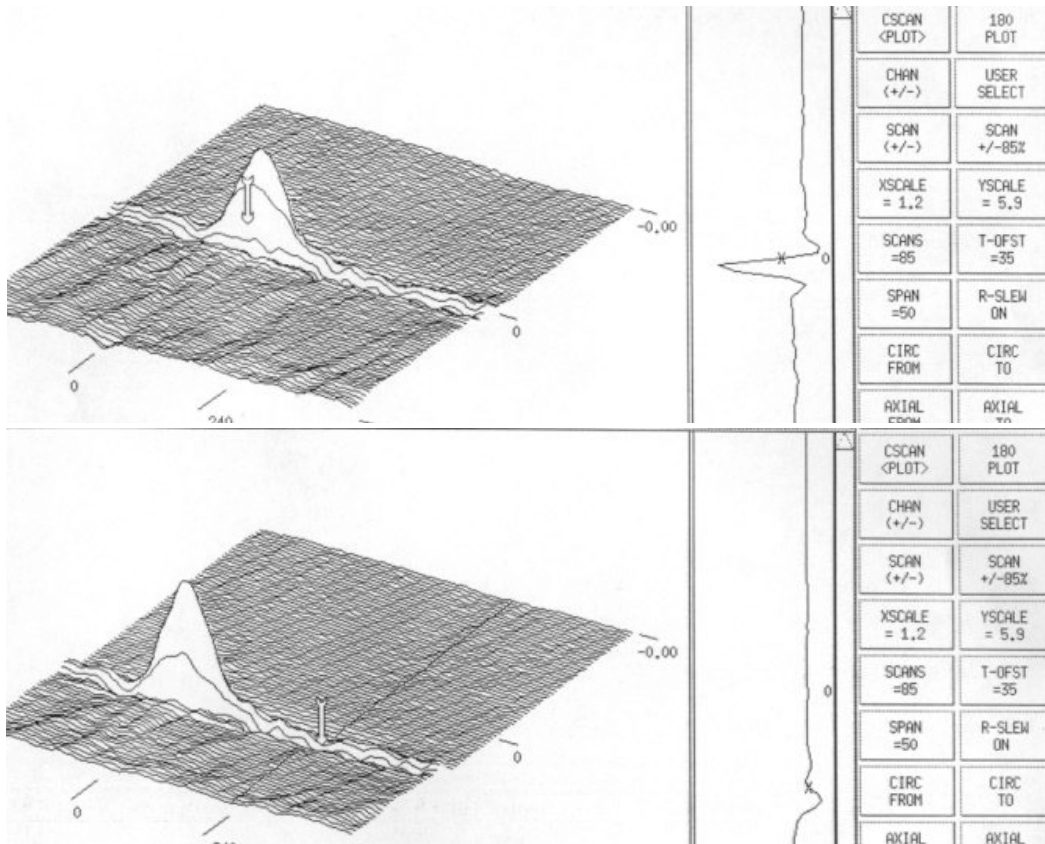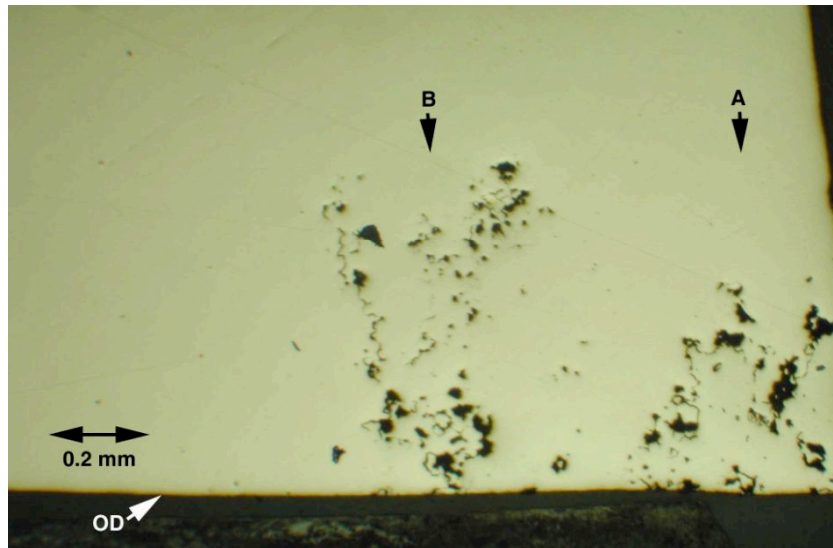Figure 3.9   Micrograph of cross-section perpendicular to the tube axis 0.5 mm below the TTS of #8. Axially oriented intergranular attack (IGA) is observed at the OD to depths of 65% TW. Flaw complexity adds to confusion in resolving flaw morphology from the EC signal.

Figure 3.10   C-scan EC +Point profiles of CODSCC (90%TW initial depth, estimated) in RTZ of tube # 9 before (top) and after (bottom) pressure testing to 52 MPa (7500 psi) with no leak.

Figure 3.11   Metallographic sectioning micrographs of CODSCC in tube #9 after pressure testing to 52 MPa (7500 psi). Throughwall crack just below the top of the tube sheet.

The EC results for tube #7, which was never plugged but leaked at 50 MPa (7300 psi) , are shown in Figure 3.12. This CODSCC had an initial +Point depth of 50% TW an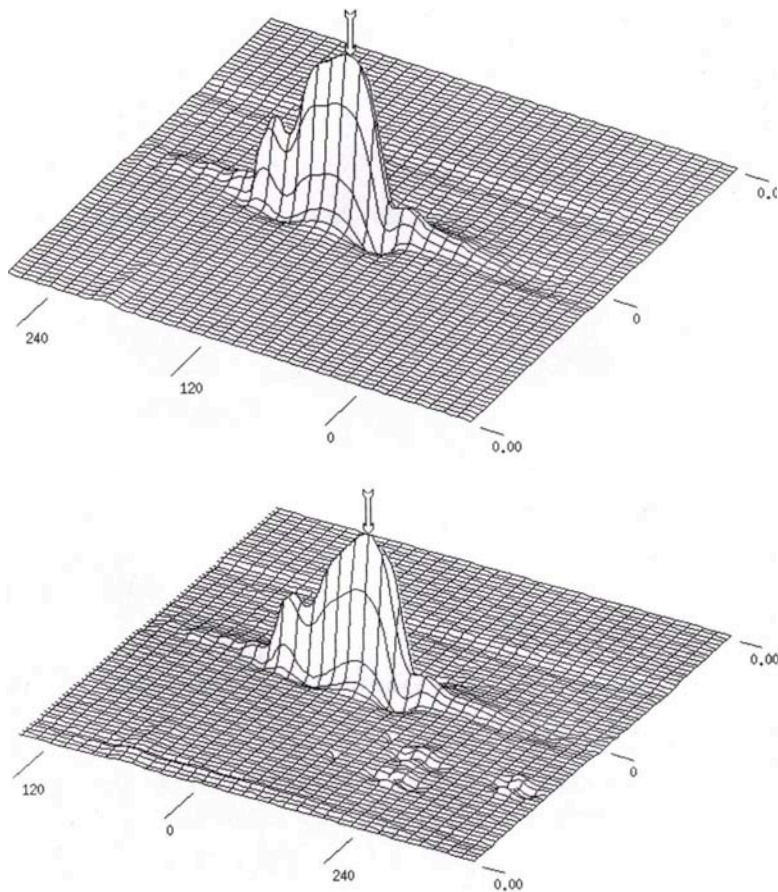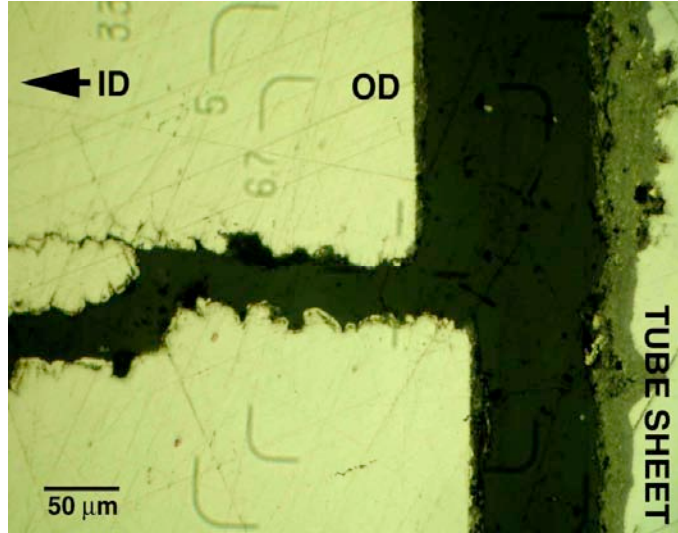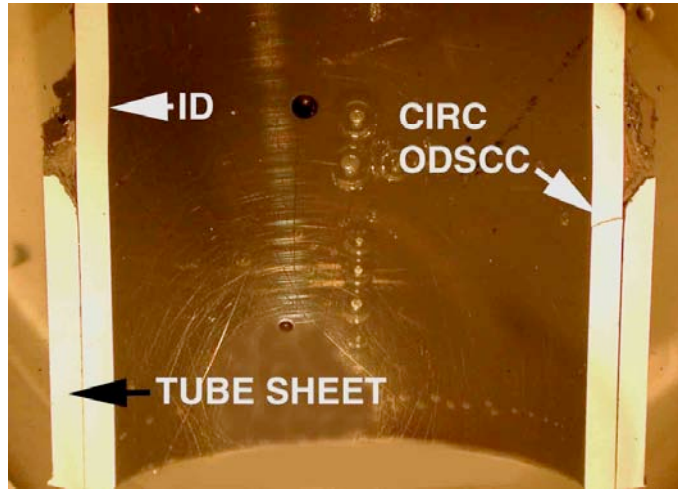d a low voltage, yet it was one of the few cracks that leaked under pressure. Three distinct peaks, separated by ligaments, are indicated with growth in amplitude of two peaks, consistent with the tube eventually leaking under pressure. Despite the growth of two peaks, the largest stayed about the same, leaving the maximum voltage with little change.
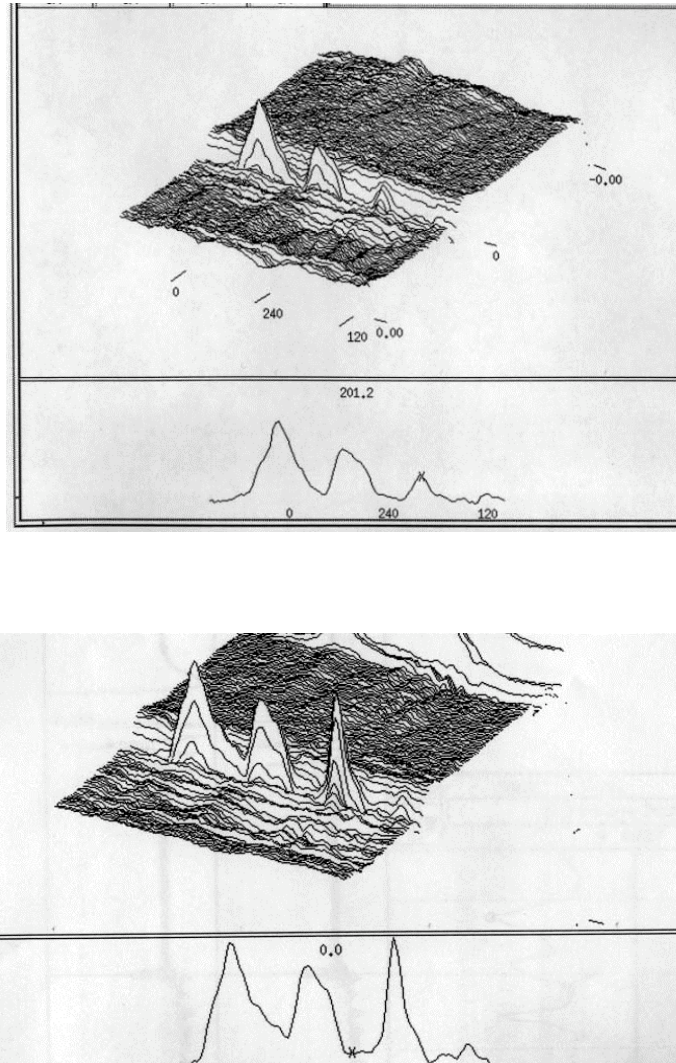
Figure 3.12   EC results (+Point C-scan) for tube #7, which was never plugged but leaked at 50 MPa (7300 psi). This CODSCC had a +Point depth of 50% TW. Three distinct cracks are indicated with growth in amplitude of the peaks (before, top; after, bottom), consistent with the tube eventually leaking under pressure. This tube was never plugged and had a +Point signal of 0.78 V in 1997 and 0.76 V in 2002.

Other TS tubes that were examined with eddy currents but not pressure tested and which had SCC indications are tubes 1, 10, 11, and 12. Other TS tubes listed in Table 10 were in a different section cut from the steam generator and were not prepared for evaluation. Figures 3.13

and 3.14 compare +Point C-scans taken in 2004 to those taken in 1997 for tubes 1 and 12. A comparison of 2004 data to 1997 data for tube #1 is indicates that while the amplitude of the +Point signal changed over time, the phase and extent did not. This finding suggests that the change in amplitude was not the result of change in the crack length or depth but a change in corrosion products on the crack faces. The 2004 image of CODSCC in the RTZ of tube #10 was generated using a +Point probe at 300 kHz (Figure 3.15). The three-letter code for the flaw before the TS section was removed in 1997 was MAI/MCI. The tube was plugged in 1994 with an MCI call and a pancake signal of 0.68 V. The 2004 +Point depth estimate from phase analysis is 65%TW. The EC signals in tube 11 had too low a signal-to-noise ratio for a meaningful evaluation to be carried out.

(a)

(b)

Figure 3.13   +Point signal of retired SG tube sheet #1 in (a) 2004 and (b) 1997. The 2004 image of the CODSCC in the RTZ was generated using +Point probe at 300 kHz. The three-letter code for the flaw before the TS section was removed in 1997 was MAI/MCI (plugged in 1993). The +Point at 300 kHz was 7.9 V in 2004 (80% TW by phase analysis) and 4.4 V in 1997 (80% TW by phase analysis).

26

(a)

(b)
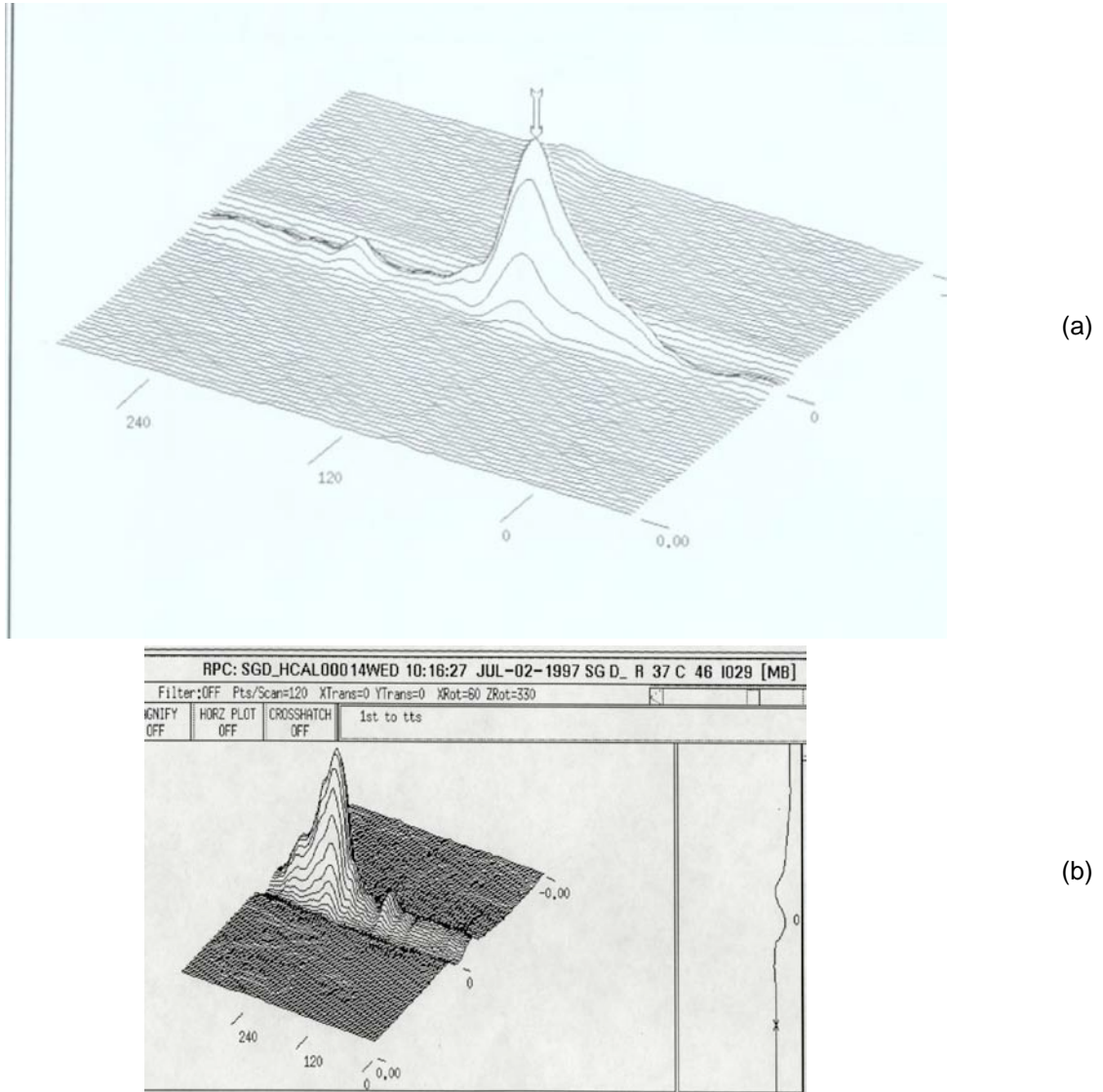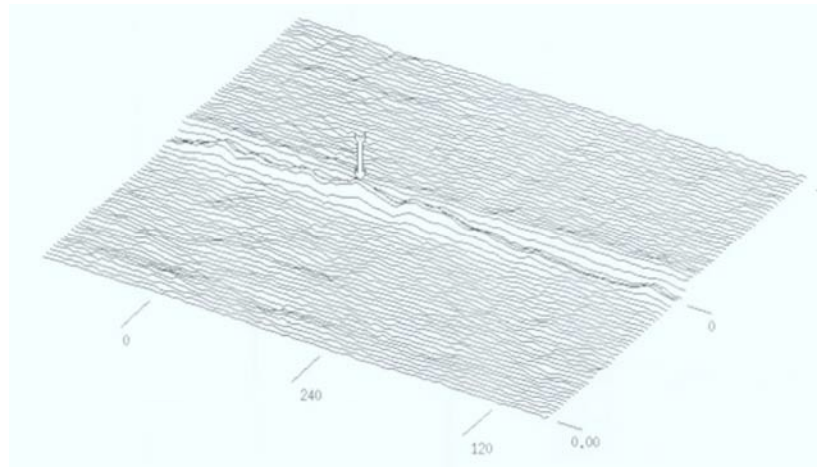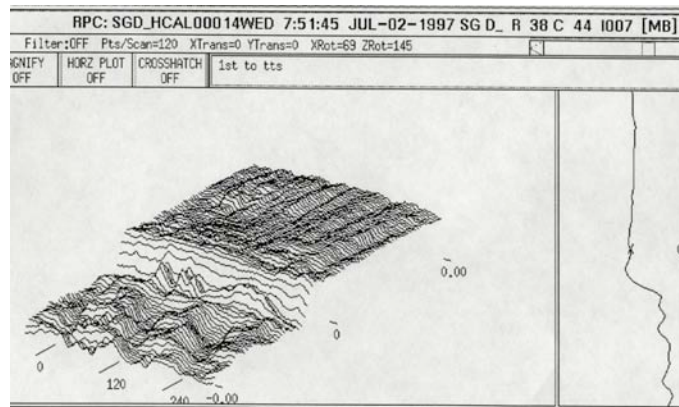
Figure 3.14   +Point signal of retired SG tube sheet #12 in (a) 2004 and (b) 1997. The 2004 image of CODSCC in the RTZ was generated using +Point probe at 300 kHz. The three-letter code for the flaw before the TS section was removed in 1997 was MCI. This tube was never plugged. The +Point at 300 kHz was 0.34 V in 2004 (poor signal-to-noise ratio) and 0.24 V in 1997.

(a)

(b)
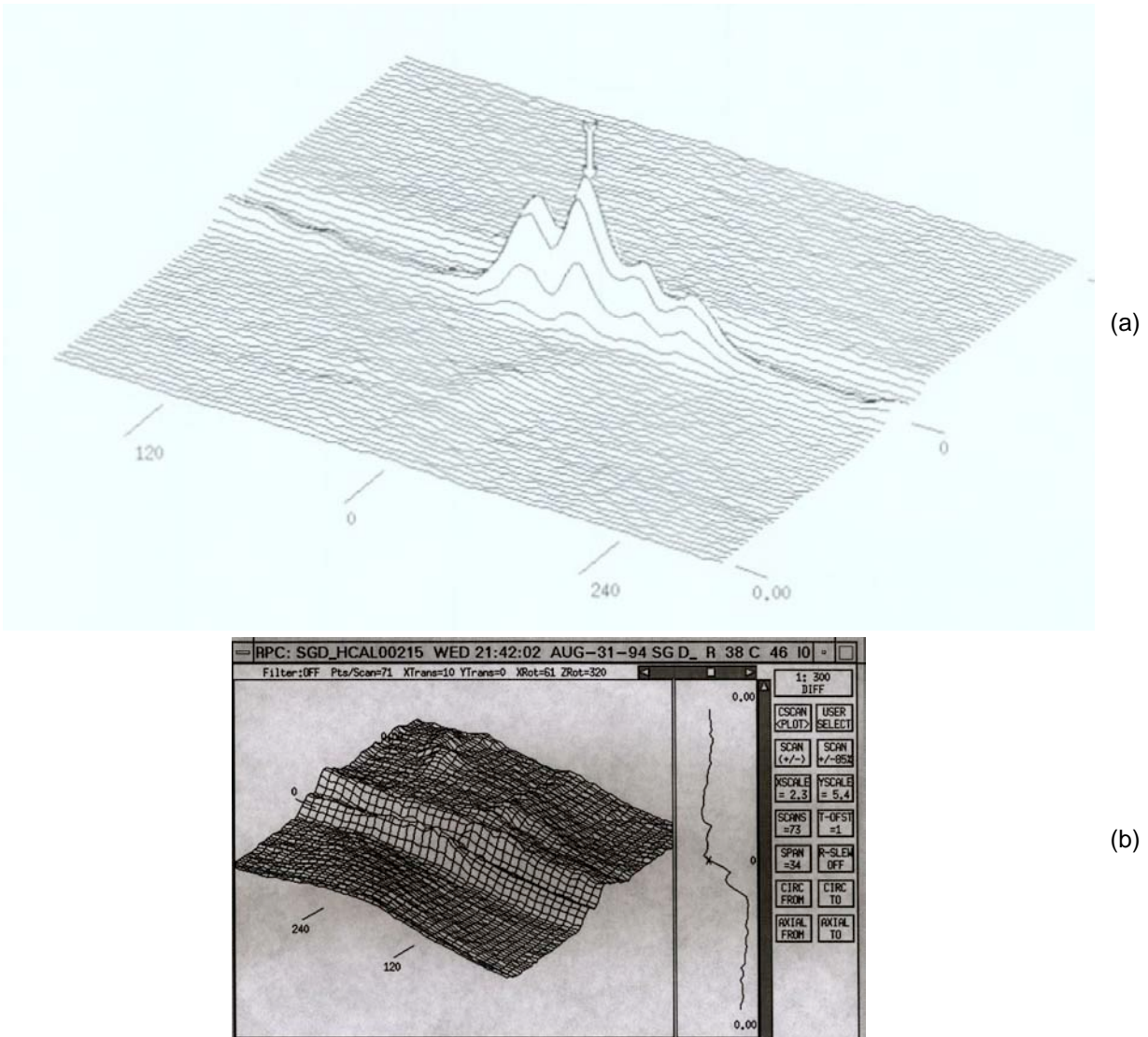
Figure 3.15   Comparison of (a) +Point C-scan of 2004 with (b) pancake coil C-scan of 1994 when retired
SG tube sheet #10 was plugged.

3.3   Compositional Analysis and Comparison of Destructive Evaluation with Eddy Current Profiles

The objective of the destructive evaluation of the retired SG tubing was to compare NDE and DE results and to characterize the defects and associated deposits.

Destructive examinations conducted at ANL include cross-sectional optical metallography of successive layers of polished surfaces, fractographic examination of a fractured surface that contained a crack, and scanning electron microscopy (SEM) and energy dispersive spectroscopy (EDS) for identification and distribution of elemental species. The EC NDE profiles were generated using the multiparameter algorithm validated on 22.2-mm (7/8-in.) diameter tubing [3]. While this algorithm was not developed nor validated for 19-mm (¾-in.) diameter tubes, a modification allowed profiles of the smaller diameter tubes to be generated. Only tubes from SGD with SCCs from TSP and TS regions were destructively analyzed. A TS section with 3/4-in. (16.8-mm) OD

28

tubing consisting of a 4 x 3 array is shown in Figure 3.16. A TS section consisting of a 4 x 2 array (not evaluated yet) is shown in Figure 3.17. Sections of the TSP from steam generator B (SGB) are shown in Figs. 3.18 and 3.19, though none of the SCCs in SGB have been evaluated.

Examination results for the TSP sections from SGD are shown in Figs. 3.20-3.25. Table 8 compares NDE and fractographic results from these specimens. There is less agreement between the depth profiles measured by EC and fractography for the 3/4-in. (16.8-mm) diameter tubing than for the 7/8-in. (22.2-mm) diameter tubing for which the algorithm was developed [3]. The complex character (multiple axial cracks and ligaments) was the cause of the undersizing of the EC profiles in some cases. Multiple OD axial cracks were observed within the TSP area. These small cracks initiated at different locations and evolved into a larger ligamented crack.

Sectional optical metallography, SEM, and EDS analyses were performed on specimens cut from the TS region after NDE and pressure/leak tests. The results given in Figs. 3.26 to 3.35 and Tables 8 and 9 indicate that the agreement between EC/NDE and DE measurements varies. Compositional analyses indicate a variety of species exists in the deposit. Detected elements include Fe, Ni, Cr, Al, Si, Mg, Cu, Ti, Mn, Ca, K, and S (Figs. 3.36 and 3.37). Note that the EDS signal for S/Pb is low and since the S and Pb peaks overlap the result for Pb is ambiguous. Iron is the most abundant element. Metallic copper is indicated by a metallic luster and a typical copper metal color under optical metallography. Copper was present in the metallic phase, indicating the potential was at the value where metallic copper and copper oxides exist. Copper deposits were mostly near the bottom area of the deposit above the TS. Copper deposits can distort the EC signal and lead to incorrect depth estimates.

HOLE DIA.	--- 0.767"/0.762"
HOLE PITCH	--- 1.0625"
TUBESHEET THICKNESS	--- 21.03"
PRIMARY SIDE CLAD THICKNESS	--- 0.15"
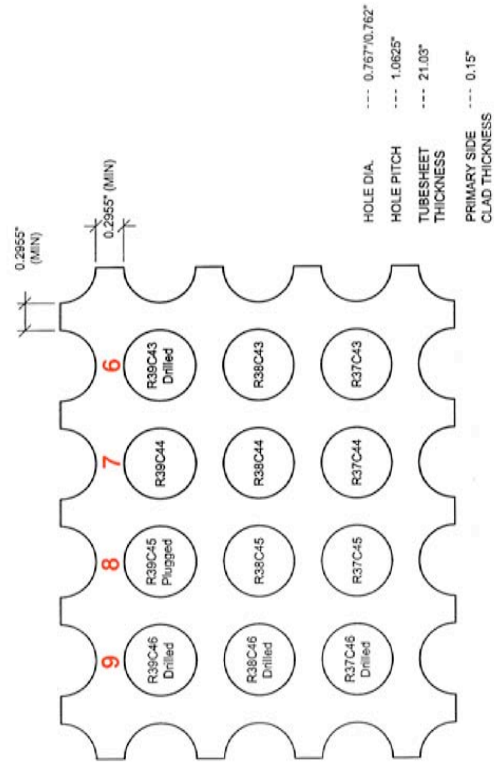
Figure 3.16   Tube sheet section TS1 removed from steam generator D (SGD) (4x3 array of 19-mm (3/4-in.) tubes).

HOLE DIA. = 0.767"/0.762"

HOLE PITCH = 1.0625"

TUBESHEET THICKNESS = 21.03"

PRIMARY SIDE CLAD THICKNESS = 0.15"

0.2955" (MIN)

0.2955" (MIN)

| R37C30 Drilled | R37C31 | R37C32 (Puller) | R37C33 Plugged |
| R36C30 | R36C31 | R36C32 | R36C33 Drilled |
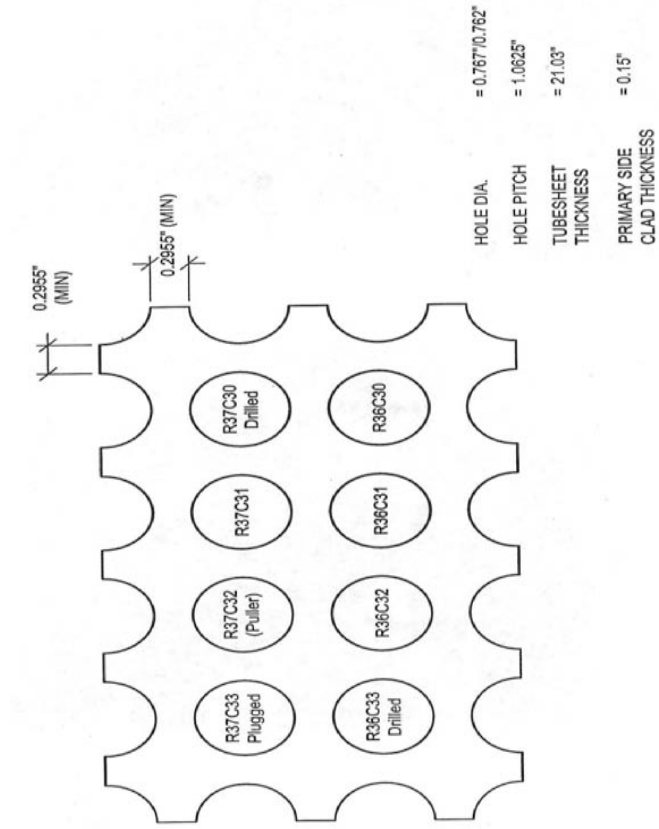
Figure 3.17   Tube sheet section TS2 removed from SGD (4x2 array of 19-mm (3/4-in.) diameter tubes).
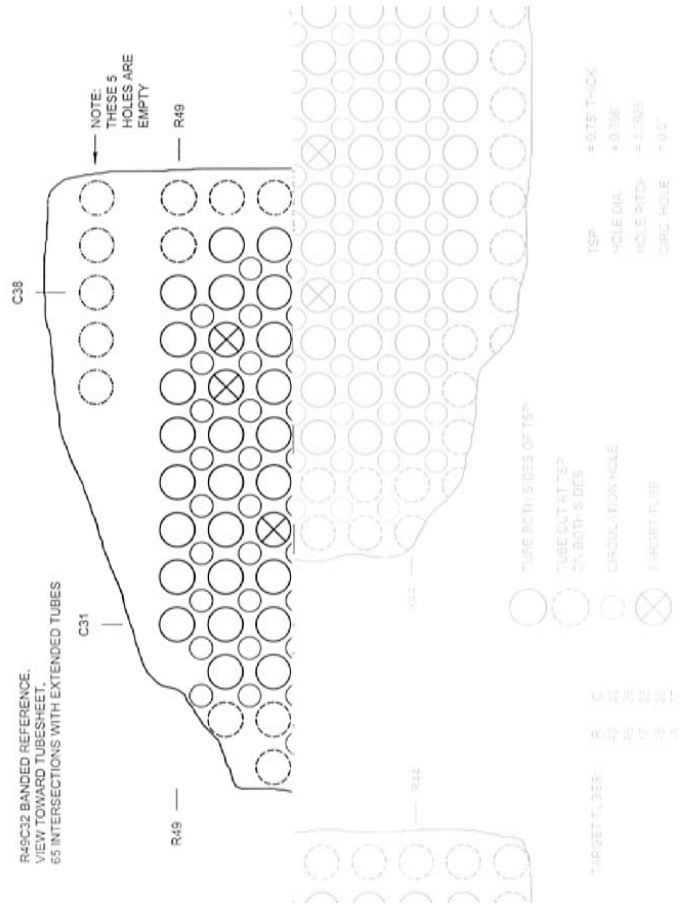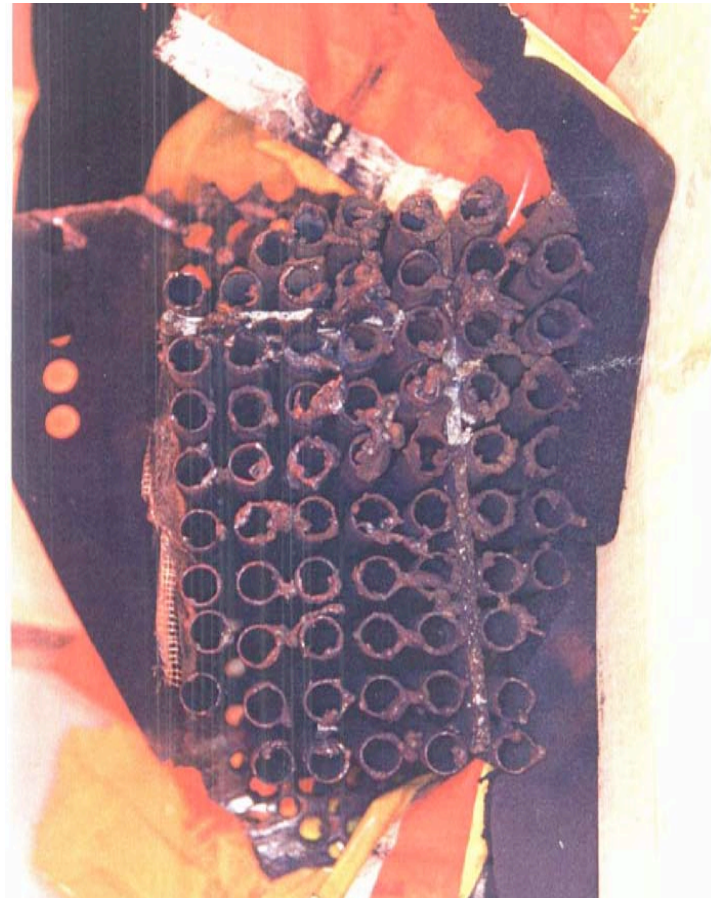
Figure 3.18   Tube support plate section TSP1 removed from steam generator B (SGB).

32

R35C14 BANDED REFERENCE.
VIEW FROM TUBESHEET

TSP   = 0.75" THICK
HOLE DIA. = 0.766"
HOLE PITCH = 1.0625"
CIRC. HOLE = 0.5"

(1) TUBE ONE SIDE OF TSP
○ TUBE BOTH SIDES OF TSP
◌ TUBE CUT AT TSP ON BOTH SIDES
○ CIRCULATION HOLE
⊗ TARGET TUBE
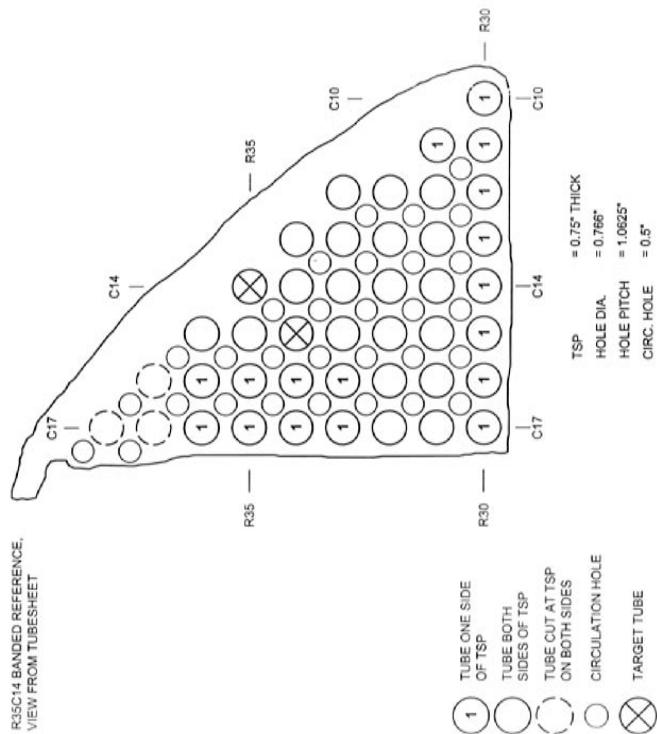
Figure 3.19   Tube support plate section TSP2 removed from SGB.
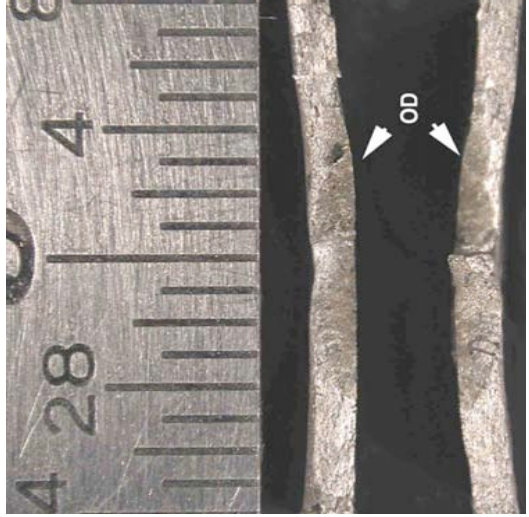
Figure 3.20 Comparison of fractography profile and NDE for axial ODSCC in 19-mm (3/4-in.) diameter tube specimen 4-43-2 (SGD). Area with the darker contrast represents the crack face. The complex character and ligament are the cause of the slight undersizing (NDE, blue dotted curve; fractography, red smooth curve) of the eddy current profiles. The arrow in graph indicates a 0.8-mm offset.
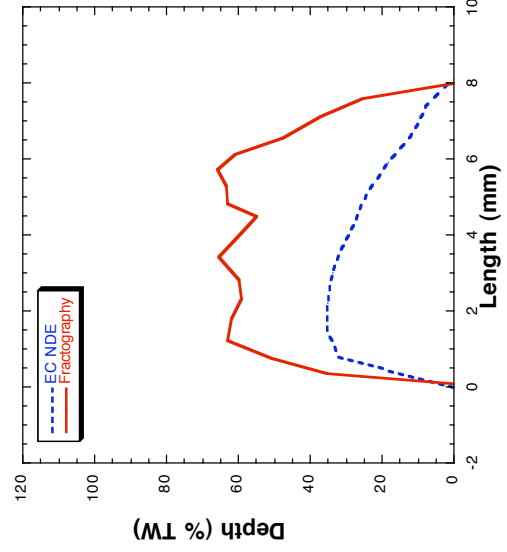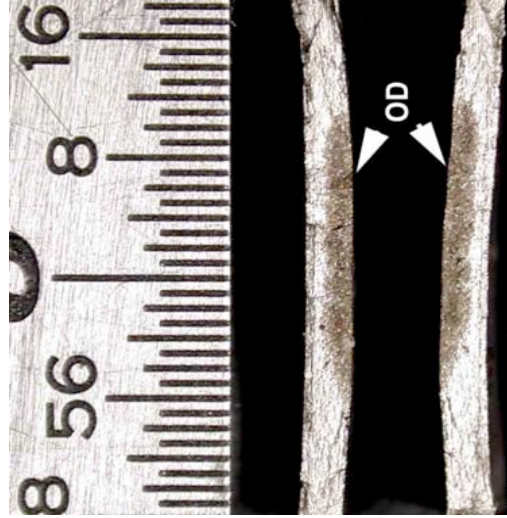
Figure 3.21 Comparison of fractography profile and NDE for axial ODSCC in 19-mm (3/4-in.) diameter tube specimen 5-51-2. The complex character is the cause of the undersizing (NDE, blue dotted curve; fractography, red smooth curve) of the eddy current profiles.

34

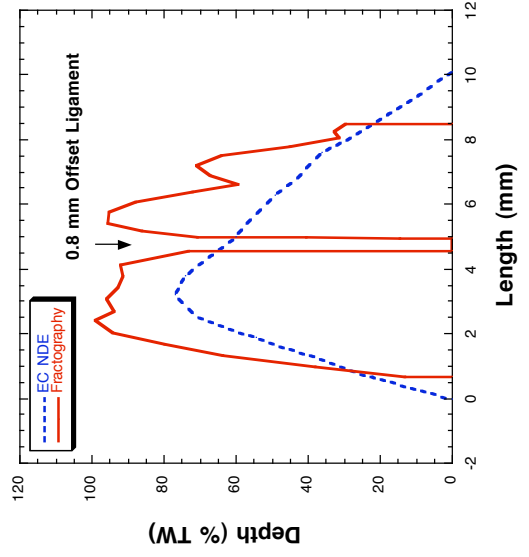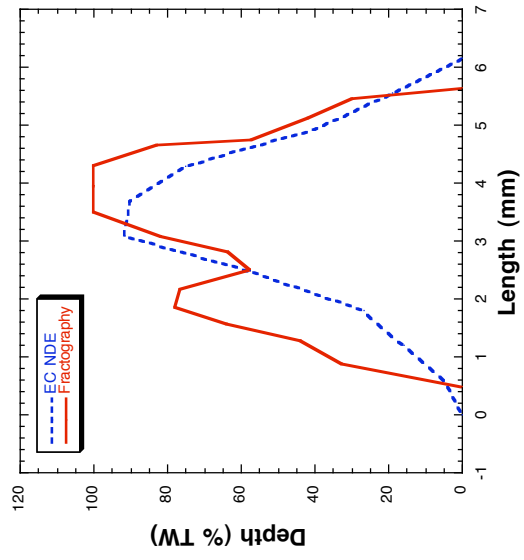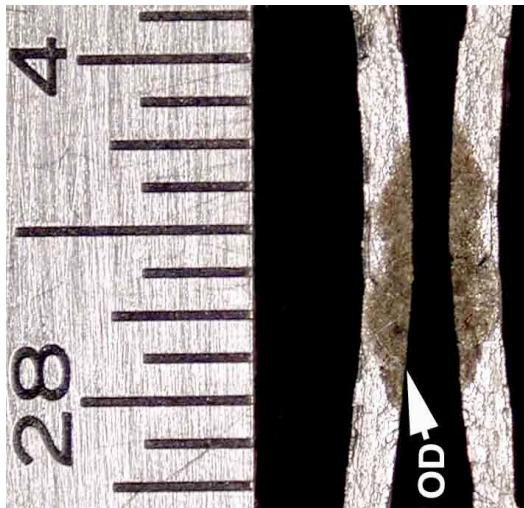Figure 3.22 Comparison of fractography profile and NDE for axial ODSCC in 19-mm (3/4-in.) diameter tube specimen 7-24-3. The fractography shows that two cracks have merged together. The NDE (blue dotted curve) and fractography (red smooth curve) are in good agreement.
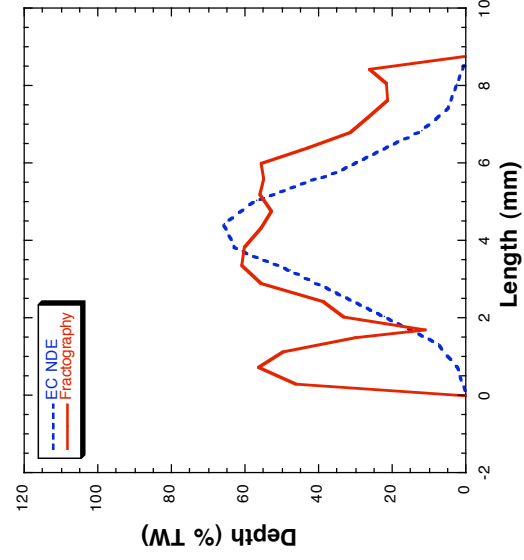
Figure 3.23 Comparison of fractography profile (red smooth curve) and NDE (blue dotted curve) for axial ODSCC in 19-mm (3/4-in.) diameter tube specimen 14-55-3.
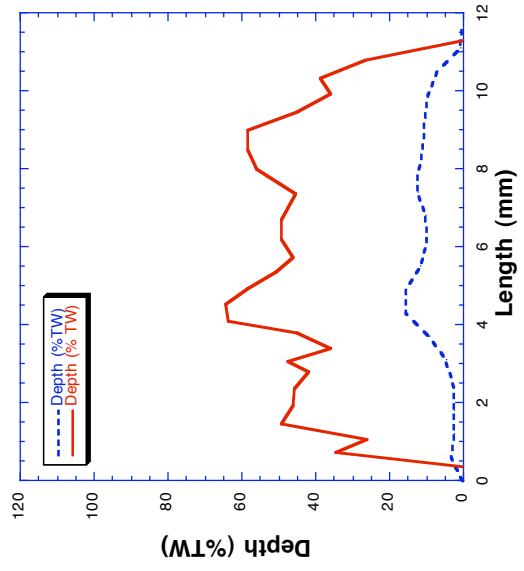
Figure 3.24 Comparison of fractography profile (red smooth curve) and NDE (blue dotted curve) for axial ODSCC in 19-mm (3/4-in.) diameter tube specimen 14-55-5. Multiple small cracks merged into one large axial crack.
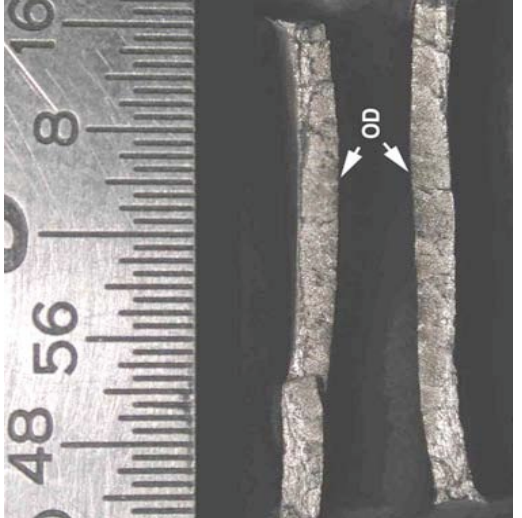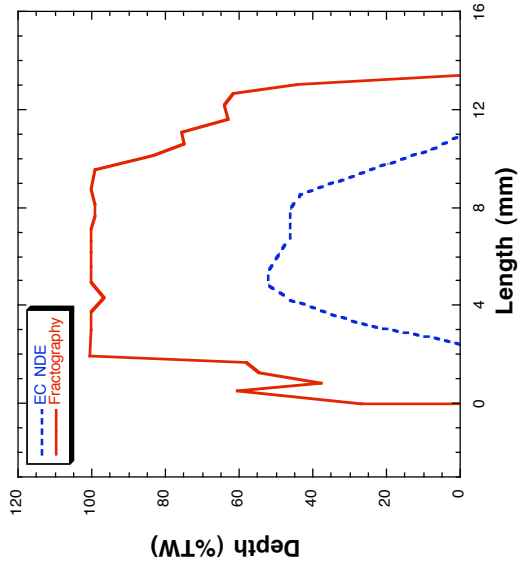
Figure 3.25 Comparison of fractography profile (red smooth curve) and NDE (blue dotted curve) for axial ODSCC in 19-mm (3/4-in.) diameter tube specimen 39-57-2.

Table 8.   Summary of cracks on pulled tube samples shown in Figs. 3.20 to 3.25. The agreement between NDE and fractography with respect to length is good.

Specimen ID	Crack Type (All in TSP Region)	Max Depth (%)		Length (mm)	
		EC	Fractograph	EC	Fractograph
4-43-2	Axial OD	77	100	10	8
5-51-2	Axial OD	35	66	8	8
7-24-3	Axial OD	92	100	6	5
14-55-3	Axial OD	66	61	9	9
14-55-5	Axial OD	15	64	12	11
39-57-2	Axial OD	52	100	9	13
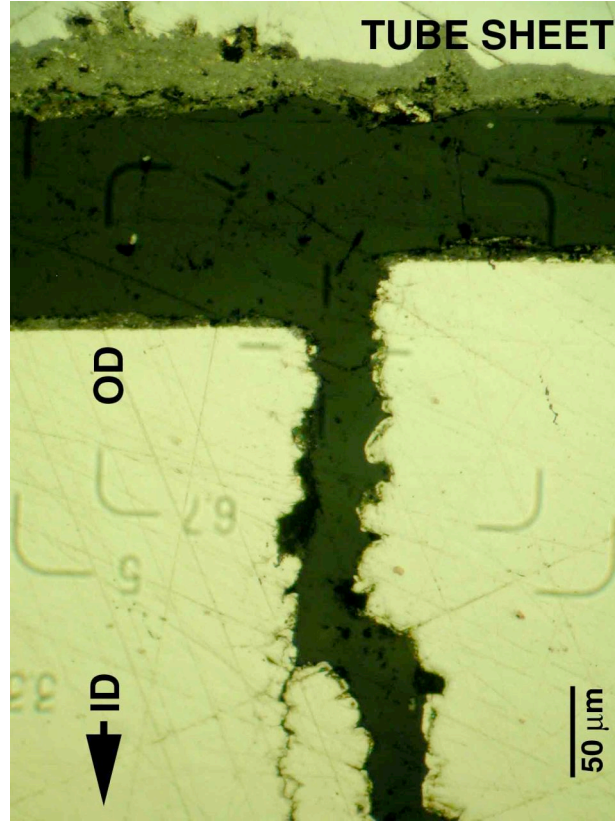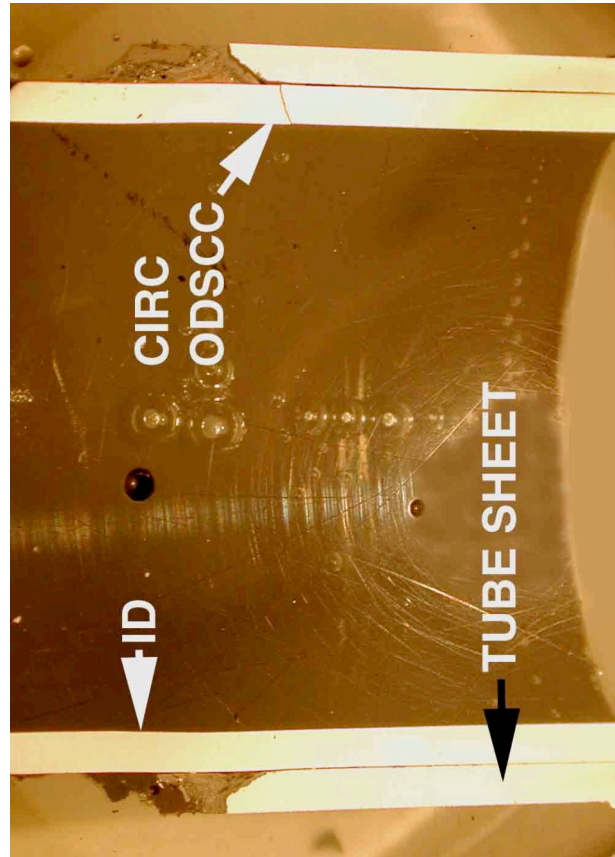
(a)

(b)

Figure 3.26   (a) Through-wall circumferential ODSCC in R39 C46 (ANL No. 9) Alloy 600 tube just below TTS. (b) Through-wall circumferential ODSCC in R39 C46 (ANL No. 9) Alloy 600 tube near TTS. Crack opening is about 0.04 mm (1.6 mils). The crack is a couple of mm below the roll transition.

37
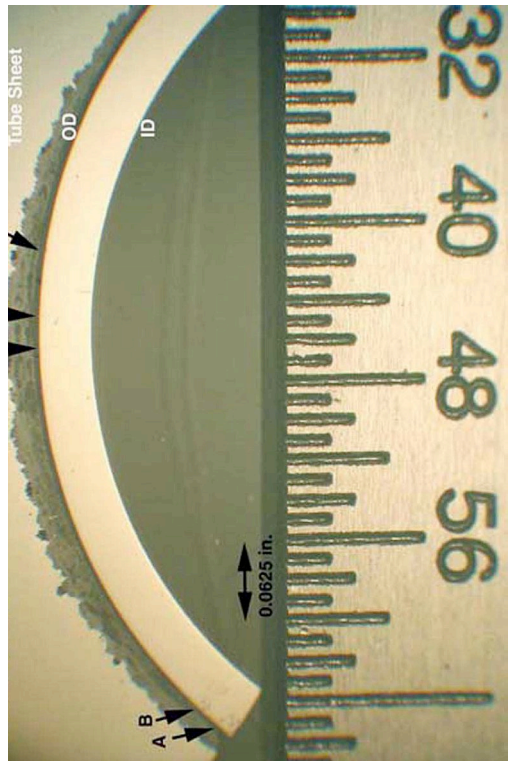
Figure 3.27 (a) IGA/IGSCC on OD at location indicated by arrows at cross-section perpendicular to tube axis in R39 C45 (ANL No. 8) at .5 mm (0.02 in.) below TTS. (b) IGA/IGSCC on OD to 30% TW (A) and 65% TW (B) at cross-section perpendicular to tube axis in R39 C45 (ANL No. 8) at 0.5 mm (0.02 in.) below TTS.
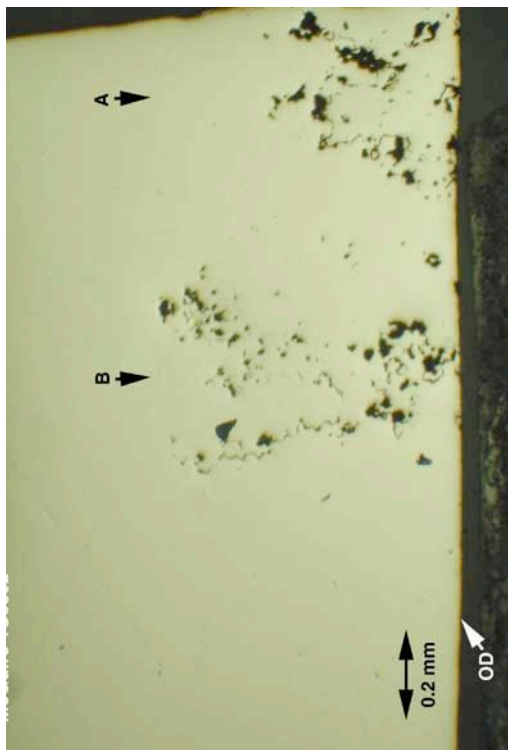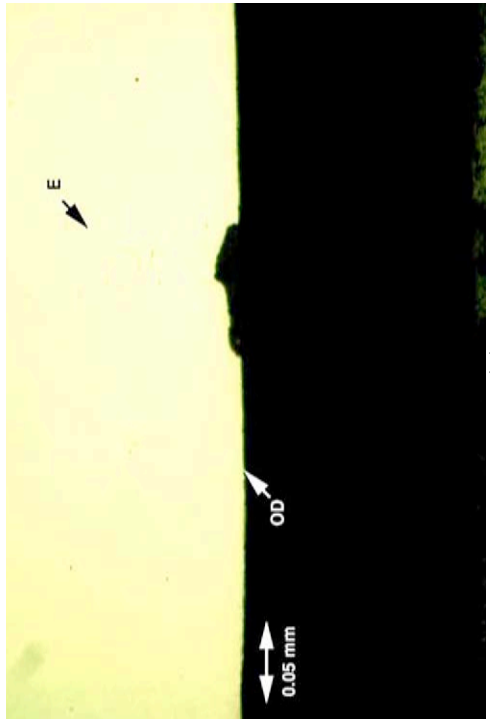
Figure 3.28 (a) IGA/IGSCC on OD at cross section perpendicular to tube axis in R39 C45 (ANL No. 8) at 0.5 mm (0.02 in.) below TTS. (b) Higher magnification view of the IGA/IGSCC on OD shown in (a).

38
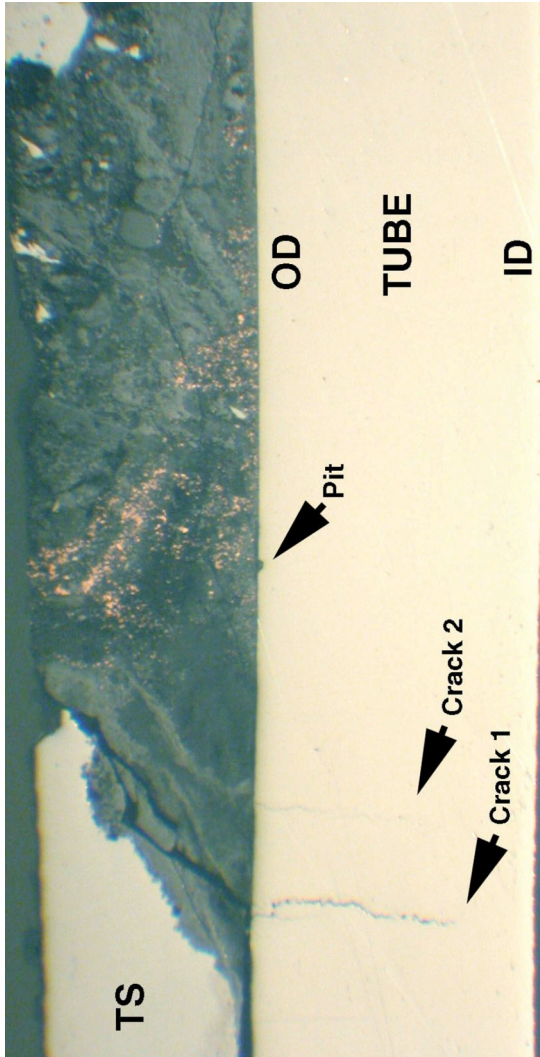
Figure 3.29
Cross-sectional optical metallograph of SG
R39 C44 (ANL No. 7) specimen showing
Alloy 600 tube, tube sheet, and various
phases in deposit. There are multiple
phases in the deposit, including metallic
copper.
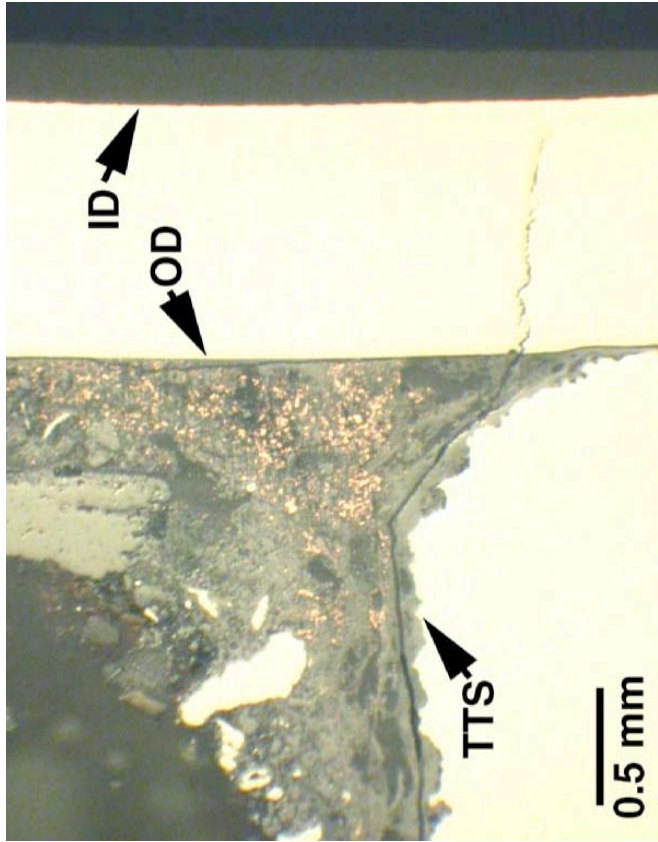
Figure 3.30
Cross-sectional optical metallograph of SG
R39 C43 (ANL No. 6) specimen showing
ODSCC in Alloy 600 tube. Copper is clearly
visible in the deposit.
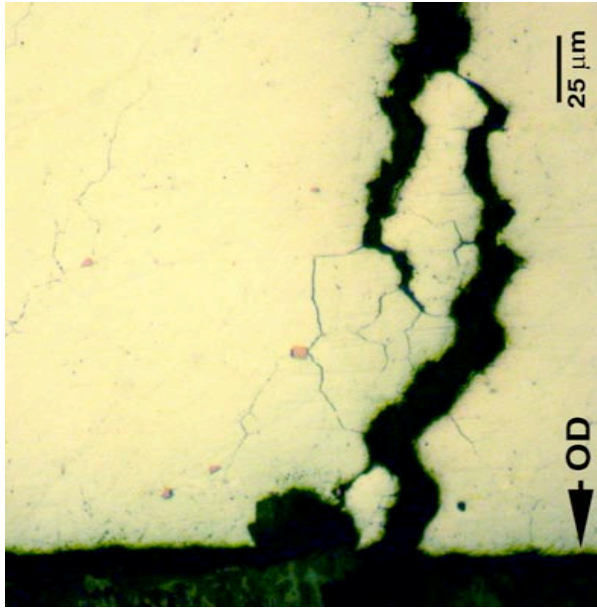
Figure 3.31
Cross-sectional optical metallograph of SG R39 C43 (ANL No. 6) specimen showing ODSCC in Alloy 600 tube. Note secondary cracks and branching.
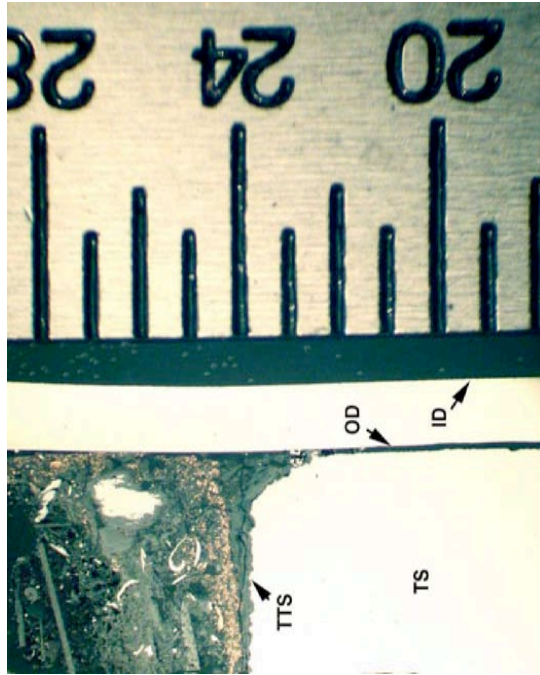
(a)
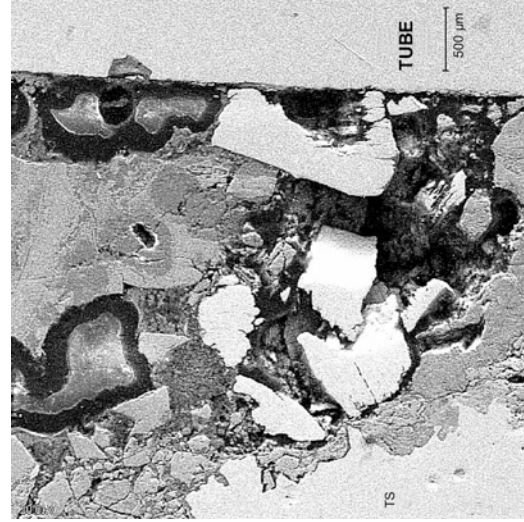
(b)

Figure 3.32 (a) Optical metallograph of cross section parallel to tube axis near maximum EC signals of R39 C45 (ANL-8). (b) Micrograph of bottom of the crevice between the top the tubesheet and the tube.

SEM image of cross section parallel to tube axis near maximum EC signals in deposit. (cf. Fig. 3.32a)
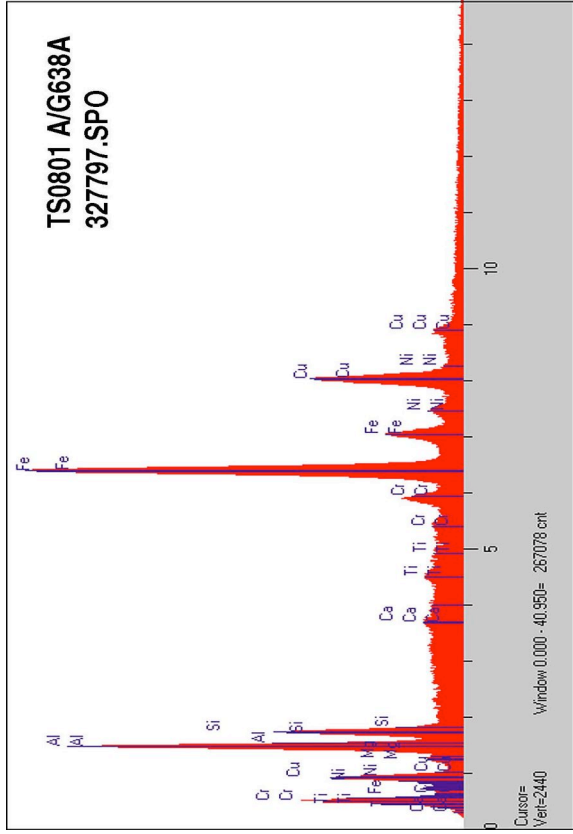
EDS analysis of deposit at 20 keV. Fe, Ni, Cr, Al, Si, Ca, Mn, Cu, Mg, Ti are detected.

Figure 3.33   Analysis of deposits of R39 C45 (ANL-8).

41
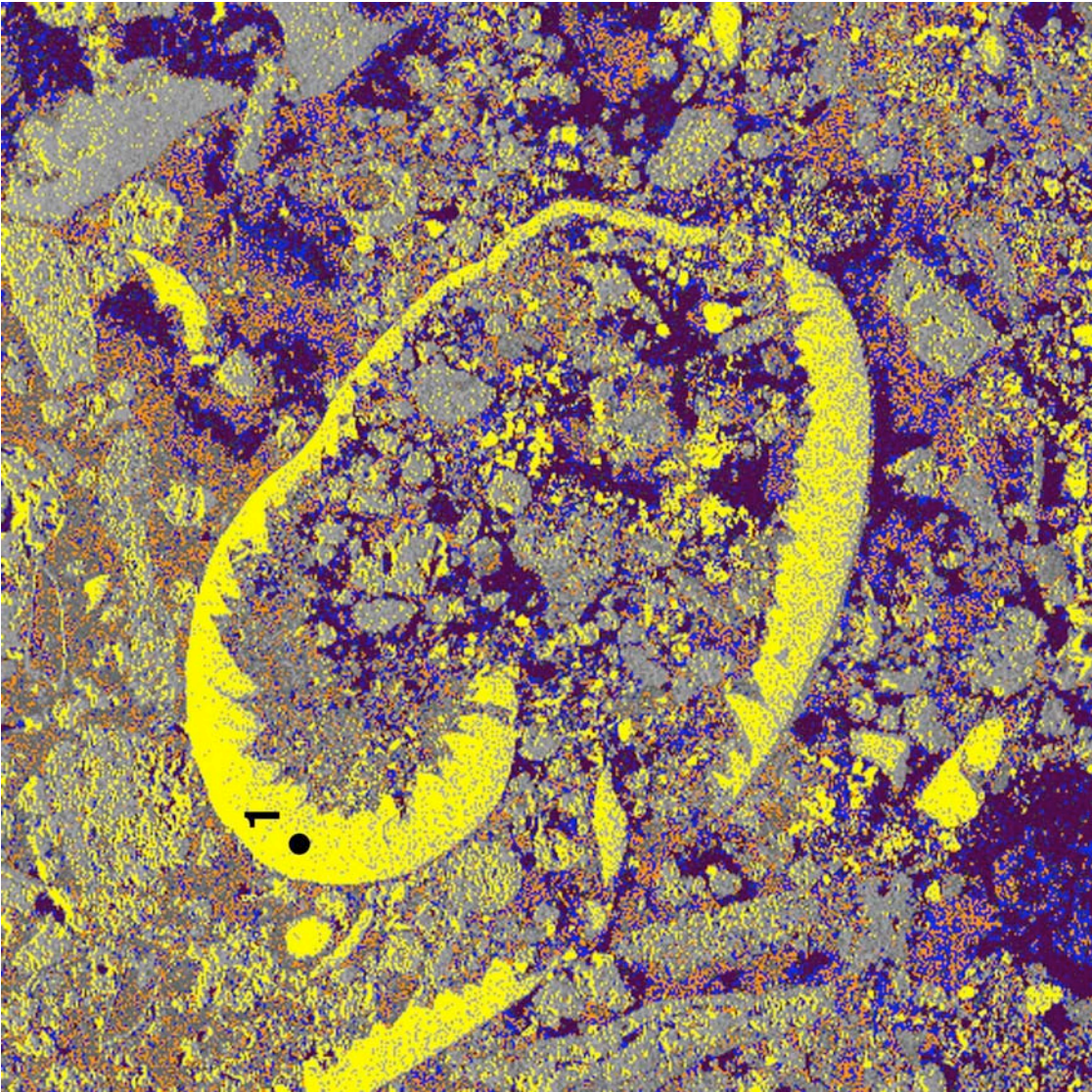
Figure 3.34
SEM image of cross section parallel to tube axis near maximum EC signals in deposit. Sample R39 C45 (ANL 8) at 100X. EDS analysis showed Fe 69.3, Cr 20.0, and Ni 10.7 (in wt. %).
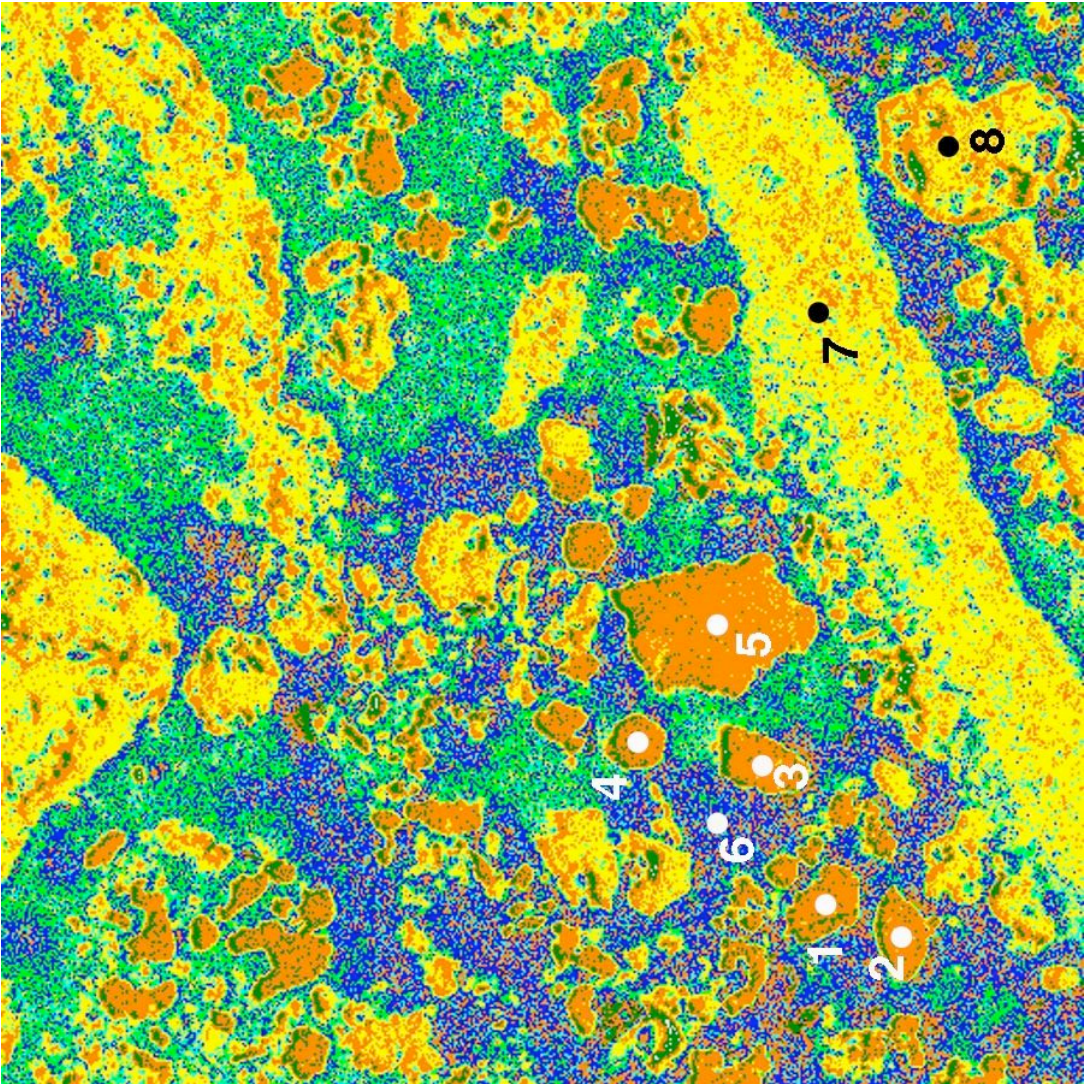
Figure 3.35
SEM image of cross section parallel to tube axis near maximum EC signals in deposit. Sample R39 C45 (ANL 8) at 600X. Spot EDS analysis at locations 1 through 8.

Table 9.   SEM/EDS analysis of various phases in sample R39 C45 (ANL 8) deposit.* Results are in weight percent. Metallic copper is indicated by metallic luster and typical metal copper color under optical metallography.

Spot	Fe	Cr	Ni	Cu	S/Pb? #	O	Al	Si	Co	Mn	Mg	K	Ca
1	2.0	–	0.4	95.0	2.6	–	–	–	–	–	–	–	–
2	2.9	–	0.7	96.4	–	–	–	–	–	–	–	–	–
3	–	–	0.9	87.9	2.6	5.5	1.7	0.6	–	0.8	–	–	–
4	15.9	–	1.4	31.7	–	33.1	11.4	4.0	–	1.7	0.7	0.2	–
5	–	26.0	–	–	3.3	–	0.2	9.6	68.0	1.6	–	–	–
6	3.4	–	–	37.6	–	26.2	32.8	–	–	–	–	–	–
7	73.8	–	–	–	–	18.5	2.5	2.6	–	2.2	0.4	–	–
8	69.4	–	3.9	1.8	–	17.3	2.2	1.3	–	2.9	0.5	0.1	0.5

– Not detected.
* Preliminary results without standards subject to re–analysis
# The EDS signal for S/Pb is low and since the S and Pb peaks overlap the result is ambiguous.

44
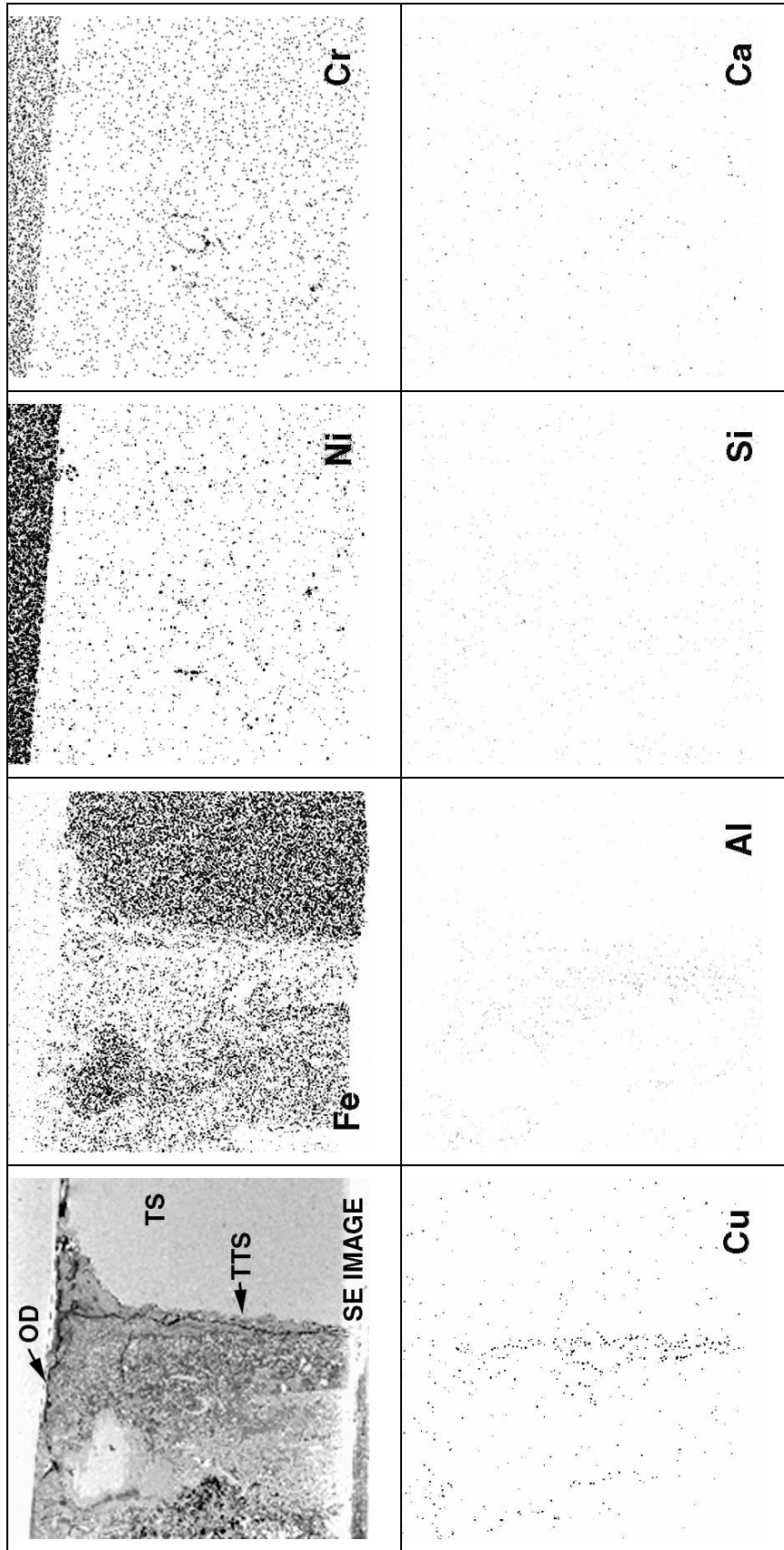
Figure 3.36   SEM image and EDS analysis showing distribution of Fe, Ni, Cr, Al, Si, Ca, Mn, and deposits of the specimen R39 C45 TS801 (ANL–8).
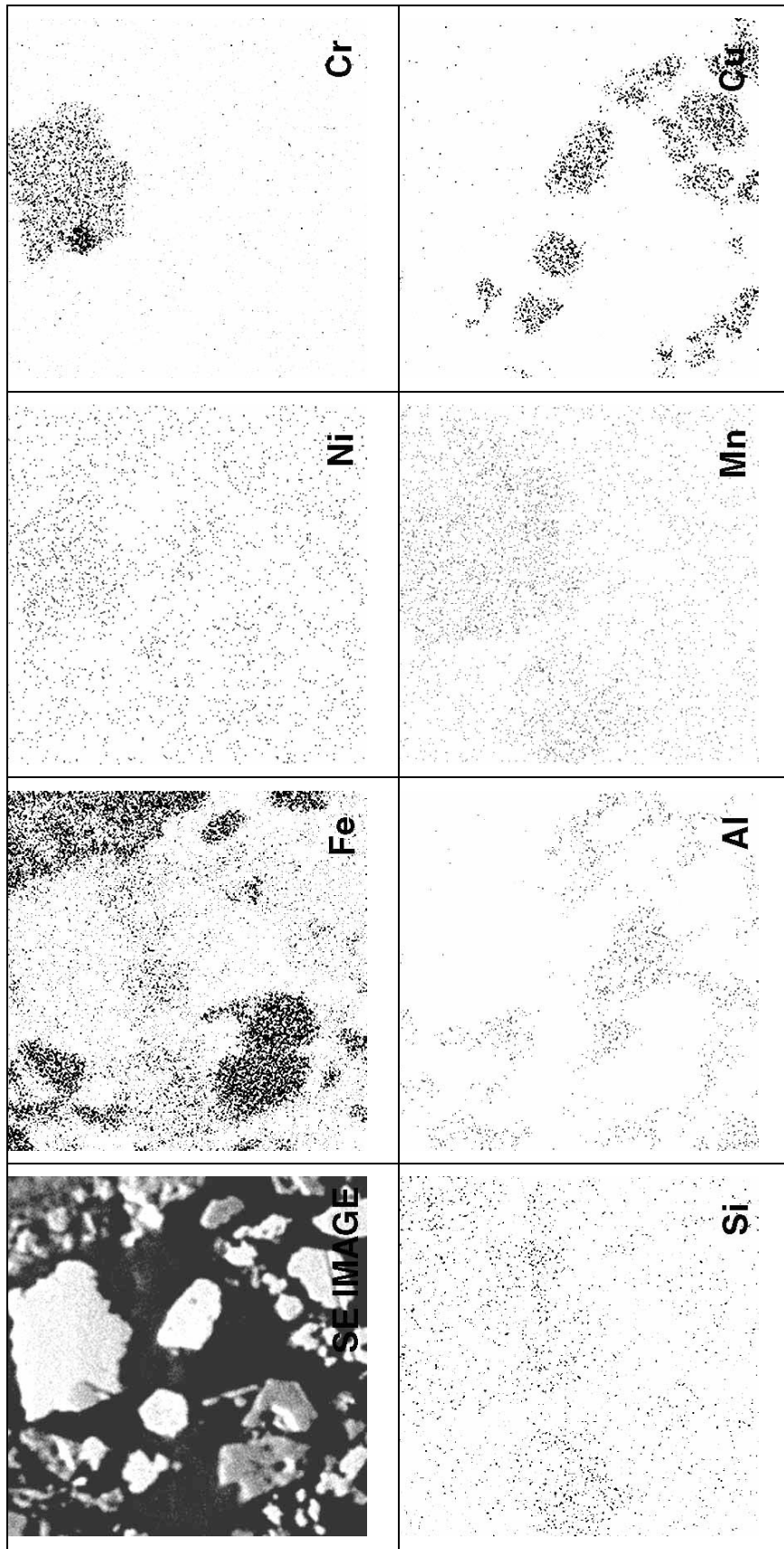
Figure 3.37   SEM image and EDS showing elemental distribution of Fe, Ni, Cr, Al, Si, Mg, Mn, and Cu at a local area in the deposit of the specimen R39 C45 TS801

4   Effect of Surface Oxide Films on Eddy Current Signals from SCC

In order to help understand the changes in the EC signal that were observed from the specimens removed from the retired SG, the effect of corrosion products (thin oxide films) formed on crack faces on the EC signal from ANL grown SCC were evaluated. Alloy 600 tubes with laboratory-grown axial ODSCC were exposed to water chemistry conditions (300°C and 3-8 ppb dissolved oxygen) for about two months at Argonne. The cracks were examined with both mag-bias (BCs) and a +Point coil before and after corrosion products (surface oxides) were formed. The voltages for the BCs increased significantly with the creation of the thin oxide film while the phase angle did not. The general shape of the Lissajous figures remained unchanged.

In contrast, the results for the +Point coil were inconclusive. In two cases, no change in +Point voltage was observed, while in a third, the voltage dropped significantly after the oxide film was formed.

While voltages of the bobbin coil increased significantly, the phase angle did not. The creation of corrosion products in the crack could lead to a reduction in the number of electrically conducting paths from contacting crack faces. In that case, the EC signal would be expected to increase, as observed, while the depth remains essentially the same. This result is consistent with observations for the field-induced specimens discussed earlier in the report.

This page is intentionally left blank.

5   Amplitude-Based Sizing using a +Point Probe

Since fall of 2001, the nuclear industry has been benchmarking the performance of a correlation using +Point amplitude to estimate axial and circumferential ODSCC maximum depth in pulled tubes. Pulled tubes with ODSCCs show a minimum +Point amplitude of about 2 V for 100% TW degradation. Industry representatives indicate that pulled tube data show less scatter for amplitude-based sizing performance than phase-based sizing (see Appendix C for standard industry phase-based practice and procedures). However, this process does have some limitations, in particular, when there are many closely spaced axial flaws (in series or parallel). In that case, if the analysis window were opened to encompass all flaws, the amplitude response will be overestimated, thus overestimating the maximum depth of the limiting flaw which is conservative. Furthermore, phase-based sizing does not work well in the case of circumferential ODSCC at hard-roll intersections. The hard-roll transition poses some issues that make maximum depth sizing somewhat problematic for this mechanism. The hard-roll geometry itself can affect results due to the very quick change in profile.

To prevent 100% TW flaws from distorting the sizing correlation, the industry limits the number of 100%TW flaws in their correlations.. The intent is to develop a conservative sizing program for flaws that may be <100% TW.

In general, the maximum depth of a crack should not correlate well with the amplitude of a +Point signal. While the dependency of the EC signal amplitude on the flaw size is a fundamental principle of electromagnetic (EM) induction, this relationship is not a function of a single variable, particularly for various forms of cracking. This dependency is related, more or less, to the volume of the defect. Aside from internal/external sources of signal distortion, the EC probe response is a function of many variables, such as length, crack opening, orientation, and origin and complexity of cracks (single, multiple, and ligamented). Unless specific criteria are used to isolate the effect of a particular variable (e.g., depth) while keeping other variables relatively constant, amplitude-based correlations for sizing of complex forms of cracking could produce a large scatter in the data. Examination of both amplitude and phase information is expected to increase the confidence in the sizing results.

A good correlation between +Point signal amplitude and maximum depth can be established if all the cracks used to establish the regression curve and all cracks subsequently detected have the same morphology (crack opening with depth) and have the same extent of deposits and ligaments. Phase angle is less dependent on factors other than depth and, in principle, should provide a better correlation with depth than signal amplitude. Cagle and Fuller [2] describe how +Point amplitude and phase can be used to estimate SCC depths, though the authors suggest that the best way to size cracks has not yet been established. Various calibration curves can be used to improve sizing. Currently, qualified techniques described in Examination Technique Specification Sheets (ETSSs) specify that the +Point signal from a 100% TW axial EDM notch should be set to a phase angle of 30 degrees and an amplitude of 20 peak-to-peak volts. The normal phase angle calibration curve is established with an axial EDM notch standard. Alternatively, the amplitude and phase angle approach can be evaluated using linear and non-linear curves, as well as notch and crack-based curves. Effective regression analysis plots based on burst pressure, effective flaw length, flaw depth and area, EC maximum depth, DE depth, and average maximum depth need to be developed to implement an amplitude and phase analysis.

Figures 5.1-5.5 pertain to the correlation between voltage and flaw depth. The first three are reproductions of the figures from Appendix G of EPRI report TR-107197-P2 [1]. These were selected because the database used in that study contains a statistically significant number of measurements, particularly for deeper flaws that are most important from the structural integrity standpoint. Note that the data pertain to two types of flaws only (primary water SCC and ODSCC at explosive and hard-roll expansion transitions) and are not representative of all flaw types and SG locations. Figure 5.1 shows +Point data from ID indications in hard-roll expansions. In this case, the data points for deep flaws (near 100% TW) vary between ≈0.25 V and >3 V, which essentially covers the range of calls from very shallow to very deep field indications. As expected, the correlations degrade for the OD indications shown in the next two figures. This is because the larger amplitude response from ID-initiated signals is better correlated with the flaw size. The EPRI report [1] contains more detailed analyses, including correlations developed from average depth and percent degraded area. Based on the results of that study, reasonable correlations could only be established for the percent degraded area from NDE depth estimates and for explosive expansions that produce very smooth and uniform transitions (i.e., minimal EC noise). Figure 5.4 shows the correlation of amplitude with flaw depth based on a subset of laboratory-grown SCCs that were destructively analyzed by fractography and sectioning at ANL. Data were acquired following industry practices with respect to standards and analysis procedures per appropriate ETSSs. Similar trends in the scatter of the data can be observed for this database of Argonne's laboratory-degraded tubes.

Although removal of high-amplitude 100% TW flaws from the analysis would improve the correlation in Figure 5.4, the correlation would still be inadequate for practical applications. Inclusion of high and low amplitude signals is intended to show the wide range of variability in the amplitude of deep cracks. Note that with the exception of a single ID point (0.8 V and ≈50% TW), all data points represent ODSCC-type degradations. While flaws of different origin should not be combined, the removal of the single ID point in this case will not have a notable effect on the observed scatter. Also, in developing their correlation, industry experts limit the number of samples with 100% TW degradation. The majority of their samples have <100% TW degradation. With deep flaws posing the greatest challenge to tube integrity, a conservative correlation model is expected to include a large number of more consequential degradations. Developing a correlation model based largely on low-amplitude part-TW flaws may not accurately represent the scatter of data at the extreme ends.

The maximum +Point voltage from the retired steam generator for axial ODSCC, acquired following industry practice, varies from 0.2 to 0.6 V for 60-65% TW and 0.7 -2.9 V for 100% TW. These data fall within the scatter of industry ODSCC data presented in Figure 5.3.

Figure 5.5 shows the maximum depth of axial IDSCC as reported for NDE (by phase analysis) vs. +Point maximum voltage. The data were extracted from an August 2005 TVA report on an inspection assessment at Sequoyah. The amplitude for longitudinal ID (LID) is 0.2 – 0.8 V for depths of 20-85% TW with a poor correlation between maximum +Point amplitude and estimated maximum depth. This result is similar to the ANL laboratory data (primarily ODSCC) presented in Figure 5.4, where the +Point amplitude varies from 0.08 to 1.2 V for DE depths of 20-80 % TW. In both cases, there is very little correlation of maximum depth with +Point maximum voltage.
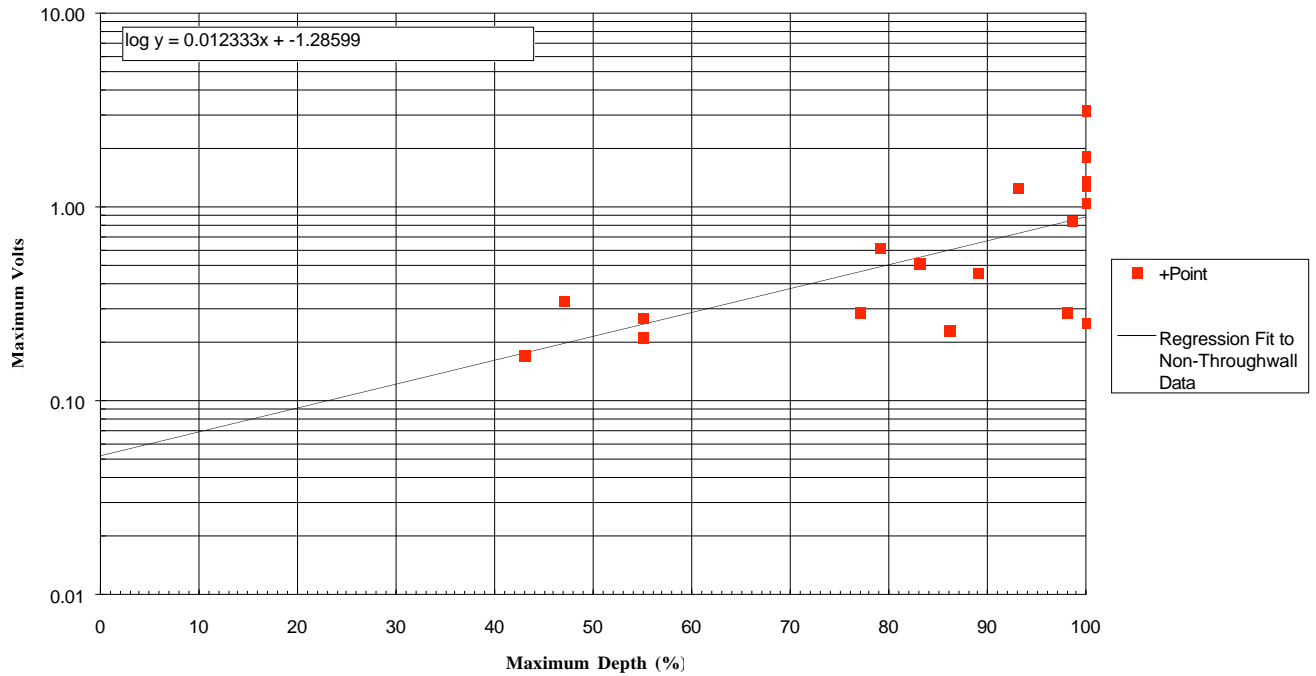
Figure 5.1   Maximum voltage vs. depth from +Point measurements in hard-roll expansions.
Reproduced from Figure G-14b contained in Appendix G of EPRI Report TR-107 197-P2 [1].
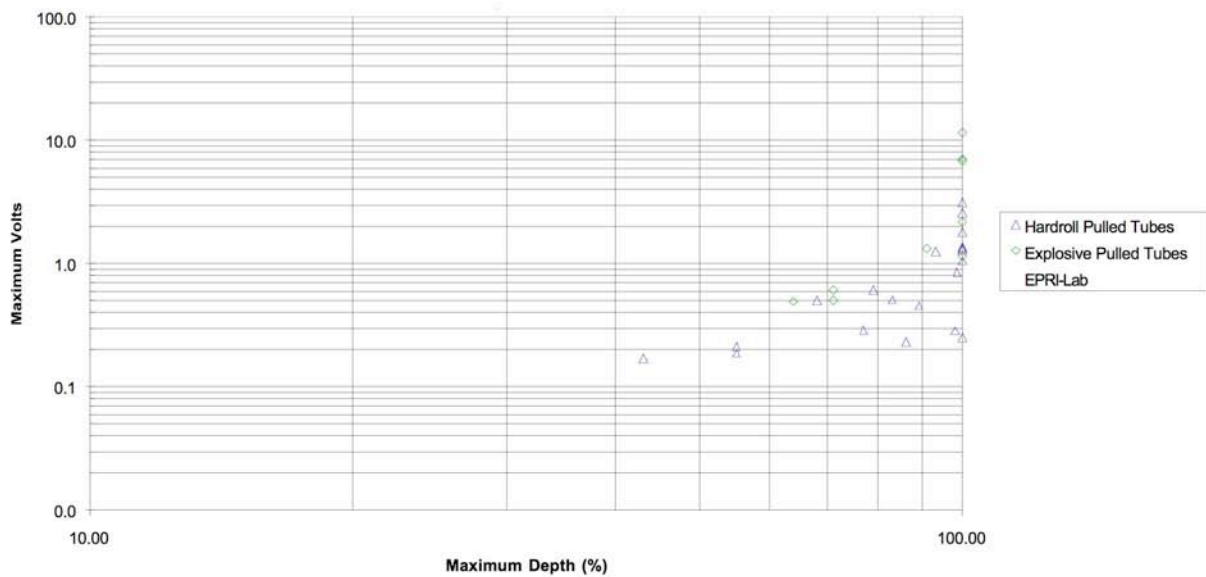
Figure 5.2   Maximum voltage vs. depth for OD indications in hard-roll pulled tubes and explosive pulled
tubes. Reproduced from Figure G-15a contained in Appendix G of EPRI Report TR-107
197-P2 [1].

51
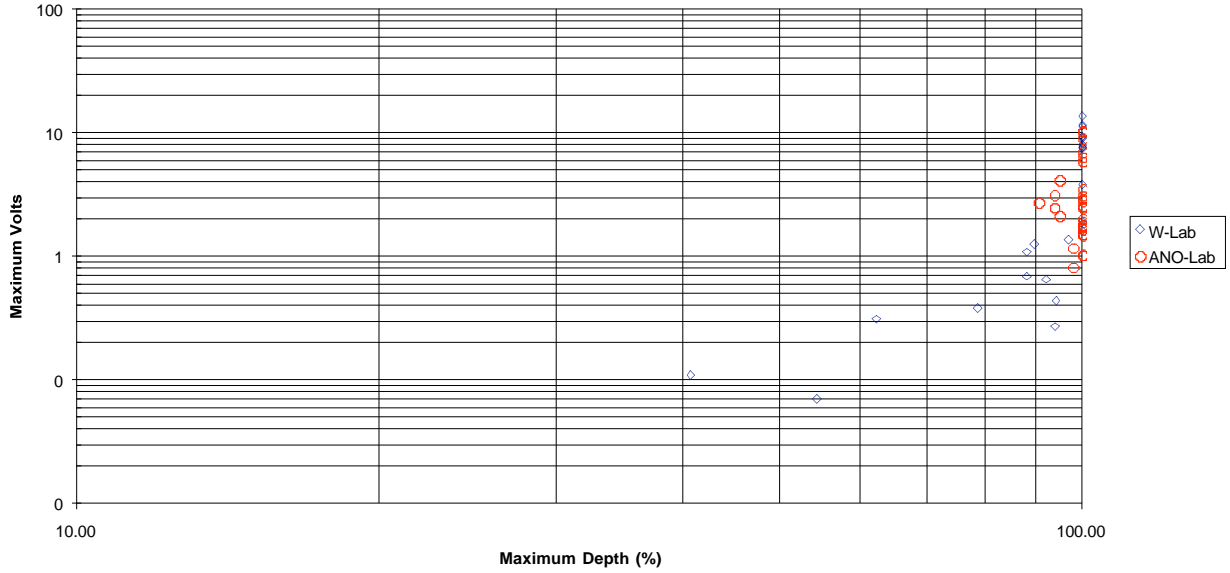
Figure 5.3   Maximum voltage vs. depth for OD indications in W-Lab and ANO-Lab tubes. Reproduced from Figure G-15b contained in Appendix G of EPRI Report TR-107 197-P2 [1].
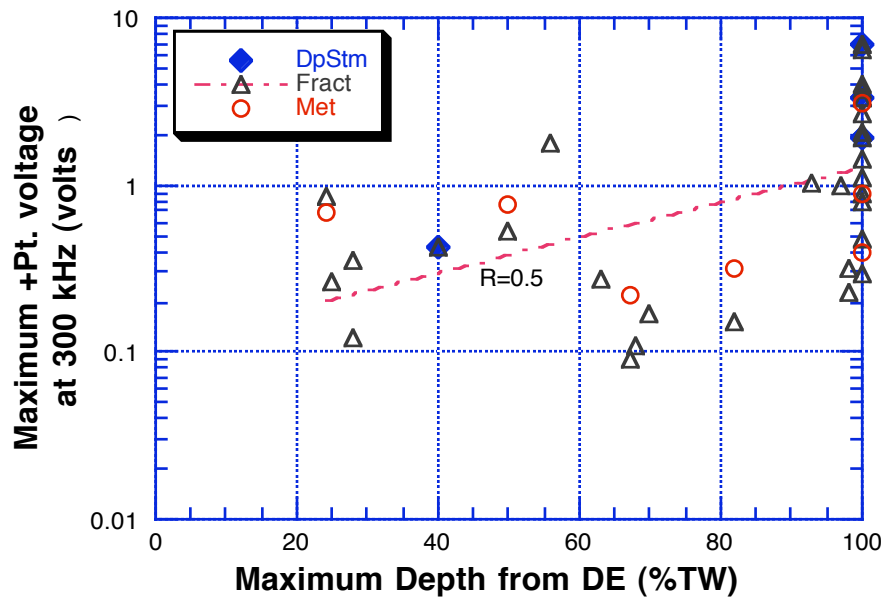
Figure 5.4   Maximum depth vs. +Point maximum voltage at 300 kHz for axial SCC in ANL mockup facility. DE was carried out by fractography and metallurgical sectioning. Some SCCs were prepared in a doped steam. The SCC include both ID and OD.
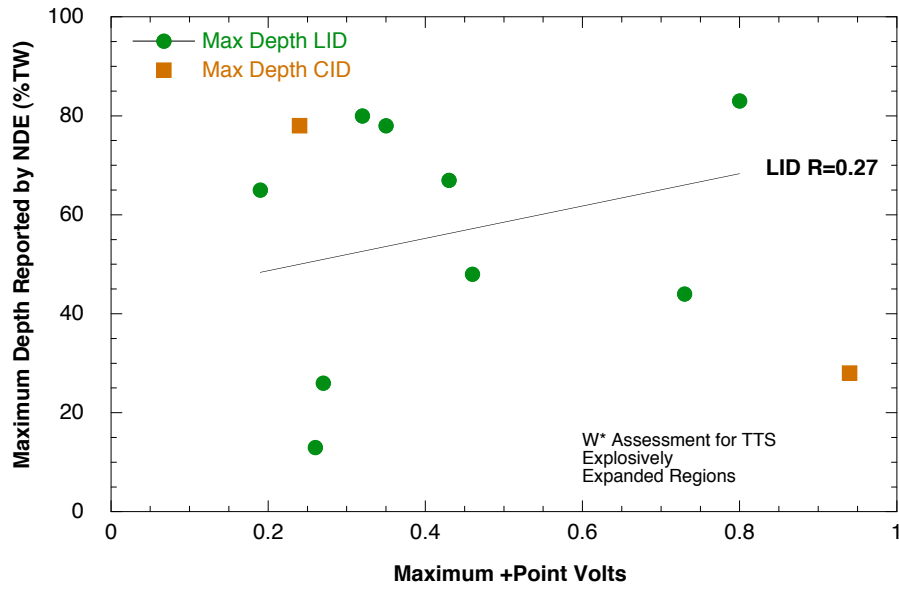
Figure 5.5   Maximum depth of axial IDSCC (dots) as reported by NDE (phase analysis) vs. +Point maximum voltage. The data were extracted from a TVA August 2005 report on a W* inspection assessment at Sequoyah.

This page is intentionally left blank.

6   Rupture and Leak Rate Predictions for Tubes from the Tube Support Plate

SG tube sections in the TSP and TS regions were retrieved from a retired SG early in the program during the NRC International Steam Generator Tube Integrity Program -2 (ISG–TIP–2). The tubes were stored at ANL until the radiation activity was reduced to a sufficiently low level so that they could be handled in the laboratory with less personnel exposure. Six SG tubes removed from the TSP region with axial flaw indications and four from the tube-sheet were subjected to pressure tests with room-temperature water in the ANL high-pressure test facility, which was modified to handle contaminated specimens.

6.1   Crack Depth Profiles Used in Analysis

Prior to pressure and leak rate testing, all of the specimens were inspected by EC/NDE, and the crack depth profiles were determined by the ANL multiparameter algorithm for the TSP specimens. This algorithm had been developed to analyze 22-mm ($7/8$–in.) tubing, and was not fully qualified for the 19 mm (3/4–in.) tubing from a retired SG, but it was still expected to be the most effective approach to obtain a crack profile by NDE. The crack depth profiles for pulled tubes with SCC at the TSP were also determined by post–test fractography. The depth profiles are shown in Figs. 6.1 to 6.3. Fractographic examination of specimen 4-43-2 revealed a 0.8-mm wide circumferential ligament in the middle of the crack that was not detected by EC/NDE. The crack in specimen 39–57–2 (Fig 6.4) was so tight that, although post–test fractography showed almost 100% penetration of the crack over an 8-mm (0.32-in.) length, the EC signal underestimated both the depth and the length significantly (Figure 6.3b). Crack depth profiles by both EC/NDE and fractography were used in the ligament rupture pressure and leak rate predictions.
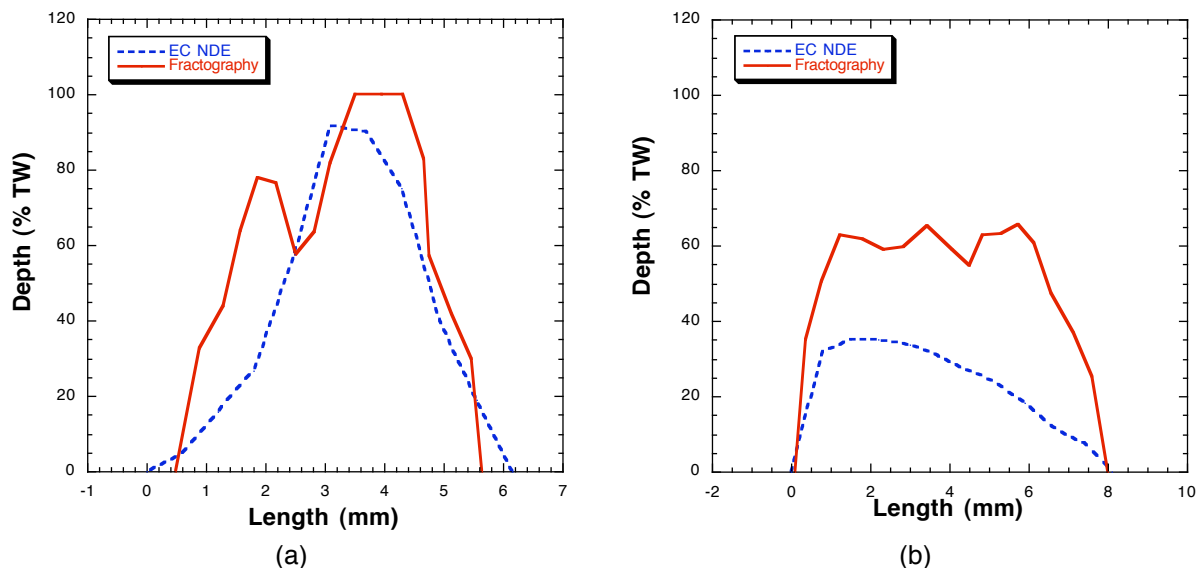
Figure 6.1   Crack depth profiles by EC/NDE (blue dotted) and fractography (red smooth) of tube (a) 7–24–3 and (b) 5–51–2.
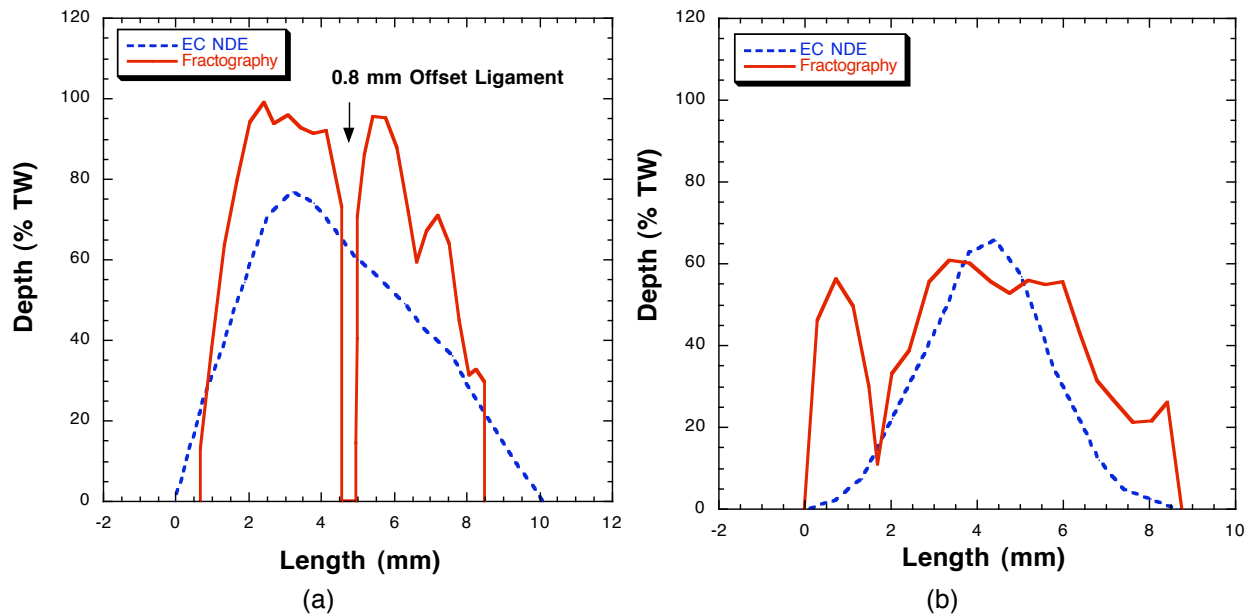
Figure 6.2   Crack depth profiles by EC/NDE (blue dotted) and fractography (red smooth) of tube (a) 4–43–2 and (b) 14–55–3.
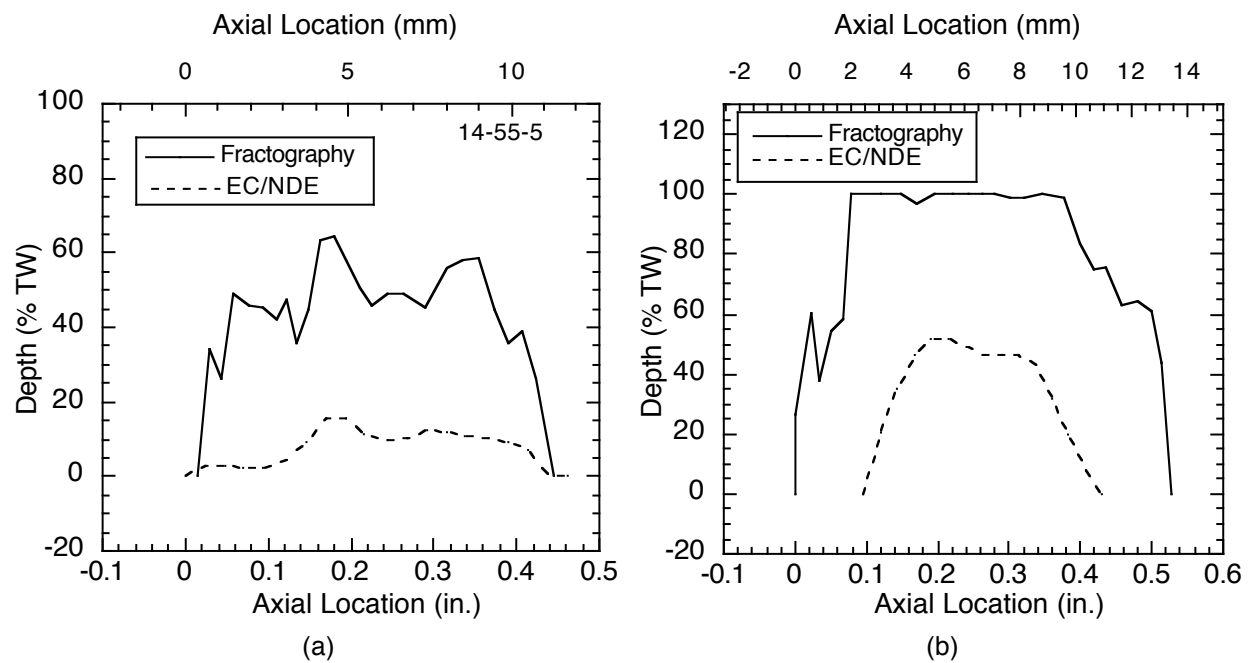
Figure 6.3   Crack depth profiles by EC/NDE and fractography of tube (a) 14–55–5 and (b) 39–57–2.

<center>(a)</center> <center>(b)</center>
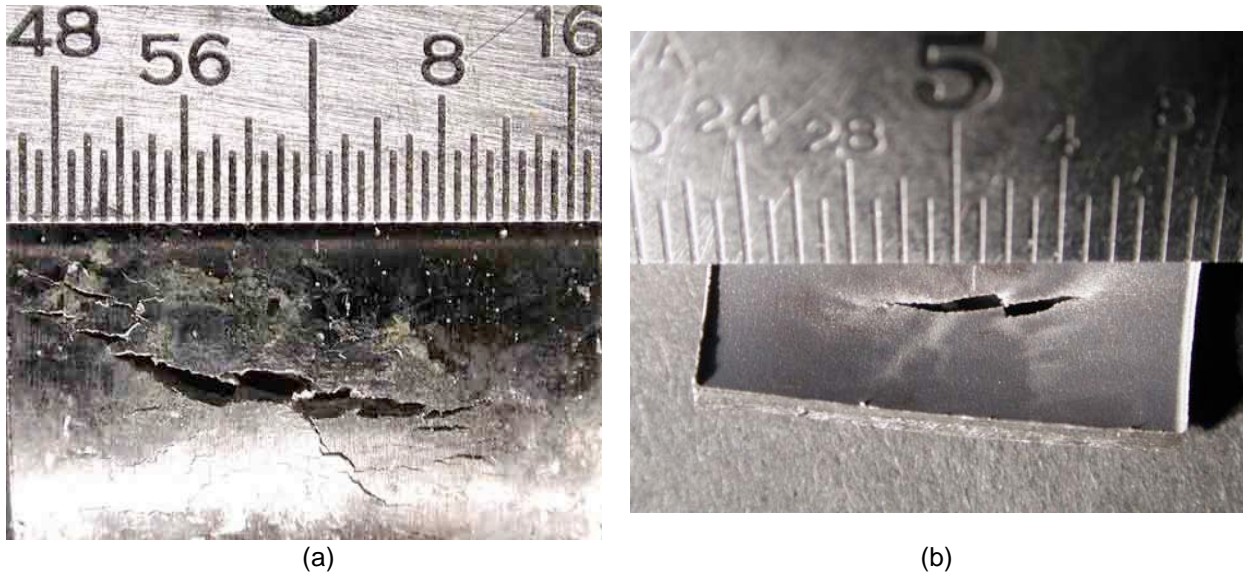
Figure 6.4   Picture of (a) OD and (b) ID surfaces of specimen 39–57–2 after the end of the test.

6.2 Material Properties

<center>(a)</center> <center>(b)</center>
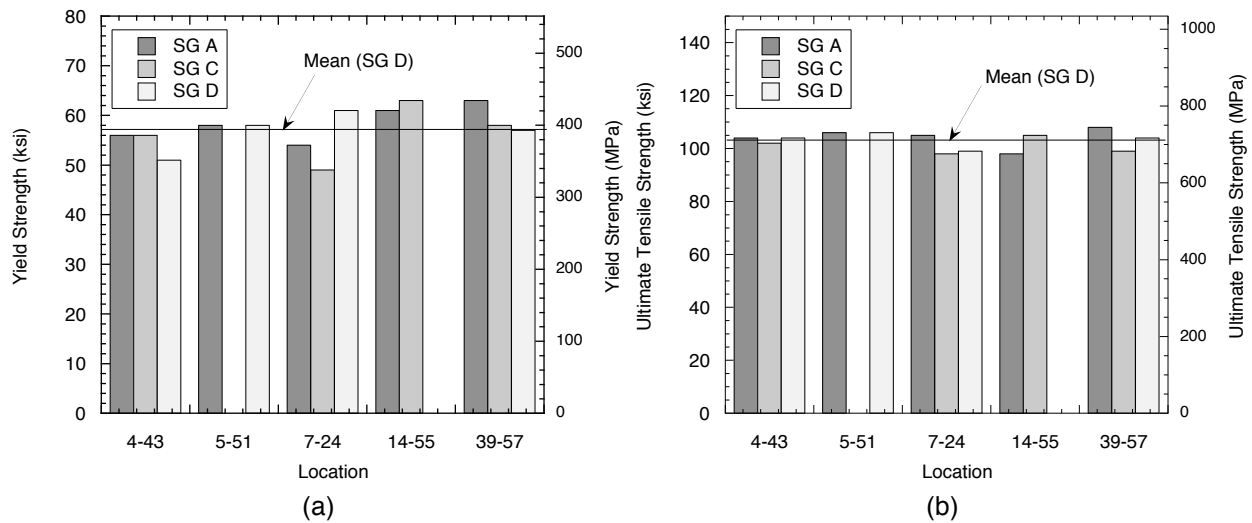
Figure 6.5   Reported (a) yield and (b) ultimate tensile strengths of tubes in retired SG tubes A, C, and D (data for B not available). Test specimens were obtained from SGD at the row–column locations shown.

Flow stress data of the retired SG tubes tested were obtained from the mill certificates[*] and are shown in Figure 6.5. Mean values of the yield and ultimate tensile strengths at locations from where the test specimens were obtained are also shown in the figures. As expected, the mean values of the flow stress of the 19–mm (0.75–in.) dia Alloy 600 tubes were at the high end, i.e., yield strength (S_y) = 400 MPa (58.1 ksi) and ultimate tensile strength (S_u) = 730 MPa (105.8 ksi).

---

[*] Private Communication, R. Keating, Westinghouse Electric Company, to S. Majumdar, Argonne National Laboratory, January 25, 2002.

6.3 Results

The pressure and leak rate tests were conducted at the ANL high–pressure test facility, which was modified to handle contaminated specimens. The pump in the facility can sustain a maximum leak rate of 87 L/min (12.6 gpm) at 51.7 MPa (7500 psi) indefinitely. The specimens were pressurized with room–temperature water, without bladder and foil, in a quasi–static manner. All but two of the axial ODSCC TSP specimens did not exhibit any leakage during the test. Results are summarized in Table 10 where predicted opening pressure were determined using profiles from the multiparameter algorithm.

Table 10.   Results from pressure and leak rate tests on tubes from the retired SG. All flaws were in the TSP region.

Tube ID	Pressure at First Leak, MPa (psi)	Leak Rate at Max. Pressure, L/min @ MPa (gpm @ psi)	Predicted Opening Pressure, MPa (psi)	Visual Flaw Characteristics
7–24–3	(no leak)	0.0 @ 51.6 (0.0 @ 7490)	62.0 (9000)	Bulge; hairline circ. crack 6.35–mm (0.25–in.) long; secondary cracks.
5–51–2	(no leak)	0.0 @ 51.0 (0.0 @ 7400)	66.2 (9600)	Bulge; hairline axial crack 6.35–mm (0.25–in.) long; secondary cracks.
4–43–2	49.0 (7100)	32.2 @ 49.0 (8.5 @ 7100)	54.5 (7900)	Bulge, two axial cracks with ligament between; total length 10 mm (3/8 in.).
14–55–3	(no leak)	0.0 @ 51.2 (0.0 @ 7425)	64.8 (9400)	No bulge; hairline axial crack 5–mm 3/16–in.) long; secondary cracks.
14–55–5	(no leak)	0.0 @ 50.9 (0.0 @ 7380)	72.4 (10,500)	No bulge; axial crack 6.35–mm (0.25–in.) long.
39–57–2	36.2 (5250)	28.0 @ 36.2 (7.4 @ 5250)	61.4 (8900)	Bulge; hairline axial crack 10 mm (3/8–in.) long; secondary cracks.

The radial ligament rupture pressure of each test was predicted by the equivalent rectangular crack method. A comparison between the predicted and observed radial ligament rupture pressures is shown in Figure 6.6. As was mentioned earlier, most of the predicted radial ligament rupture pressures using either EC/NDE or fractography profiles exceeded the maximum pressure capability of the test system. This finding is consistent with the observed test specimen behavior (i.e., no leakage).

Of the two tests in which radial ligament rupture (onset of leakage) did occur, the radial ligament rupture pressure for 4–43–2 was slightly overpredicted by analysis of the EC/NDE crack profile and slightly underpredicted by analysis of the crack profile measured by fractography. In Fig. 6.7 the observed leak rates for test 4–43 are compared with the leak rates predicted by the methodology described in Ref. [4]. The test was interrupted at 50 MPa (7.2 ksi) because it ran out

58

of pump capacity. The prediction based on the EC/NDE profile indicated unstable burst immediately after radial ligament rupture at 53.6 MPa (7.8 ksi). The prediction based on the fractography profile indicated radial ligament rupture at 42.4 MPa (6.2 ksi) followed by unstable burst at 46.9 MPa (6.8 ksi), assuming no additional ligament tearing after initial ligament rupture.

In reality, specimen 4-43-2 had two axial cracks separated by a circumferential ligament with an approximate length of 1 mm (0.04 in.), as shown in Figure 6.8. In all the tests conducted to date, the circumferential ligament never failed before the radial ligament. Therefore, for the following cases, an assumption is made that the radial ligament will always fail initially before a circumferential or axial ligament can fail, even if the pressure was above the circumferential or axial ligament rupture pressure.

If the radial ligament rupture pressure exceeds the pressure required to rupture the circumferential ligament (separating the two throughwall cracks that would result from the radial ligament rupture), then the two cracks would coalesce to form a single throughwall crack immediately after radial ligament rupture. If not, the final result after radial ligament rupture would be two through-wall cracks separated by a circumferential ligament and to rupture the circumferential ligament, the pressure has to be increased beyond the radial ligament rupture pressure. If the circumferential ligament rupture pressure is greater than the unstable burst pressure of the single through-wall crack thus formed, then the tube would undergo unstable burst immediately after the circumferential ligament ruptures; if not, the pressure has to be further increased to achieve unstable burst. Figure 6.9 shows that the predicted circumferential ligament rupture pressure for two 3-mm (0.125-in.) axial cracks separated by a circumferential ligament of 1-mm (0.04-in.) length is 55 MPa (8 ksi). Since this is greater than the experimentally measured radial ligament rupture pressure of 7.2 ksi (50 MPa), this analysis predicts that the circumferential ligament should survive the pressure test (as it did), because the system will depressurize when the radial ligament ruptures. Figures 6.8a–b show that the circumferential ligament did not rupture by the end of the test, in agreement with the prediction. The circumferential ligament is predicted to rupture at a pressure of 55 MPa (8 ksi). This rupture would then immediately led to unstable burst, because the predicted unstable burst pressure of the single 6-mm-long coalesced crack that is formed when the circumferential ligament fails is 50 MPa (7.2 ksi) (Figure 6.9). In this instance, the presence of the circumferential ligament prevented unstable burst from occurring during the test.
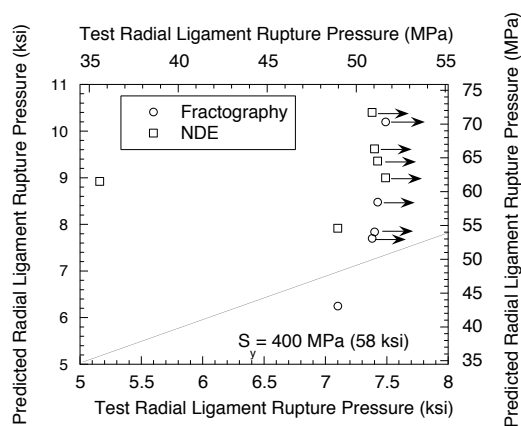
Figure 6.6
Observed vs. predicted radial ligament rupture pressures based on fractography and EC/NDE. Right arrows indicate no leakage during tests. The squares are for predictions based on NDE profiles before the test. The circles are for predicted rupture pressures based on fractography after the test.
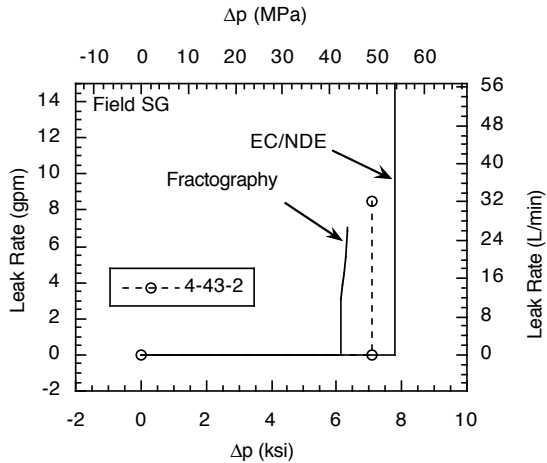
Figure 6.7
Observed variation of leak rate with pressure for Test 4–43–2 and the predicted leak rate variations based on crack profiles determined from EC/NDE (before testing) and fractography (after testing).
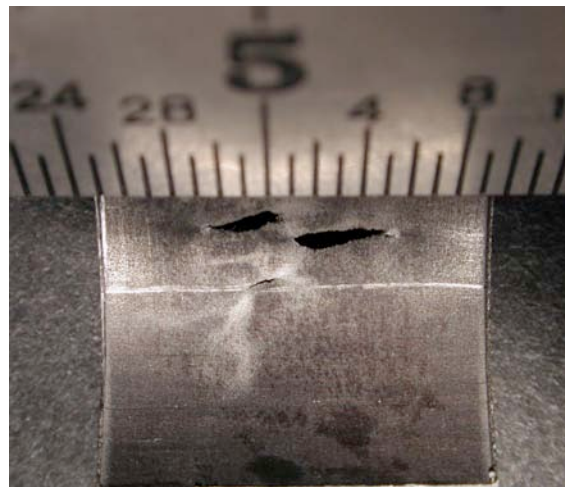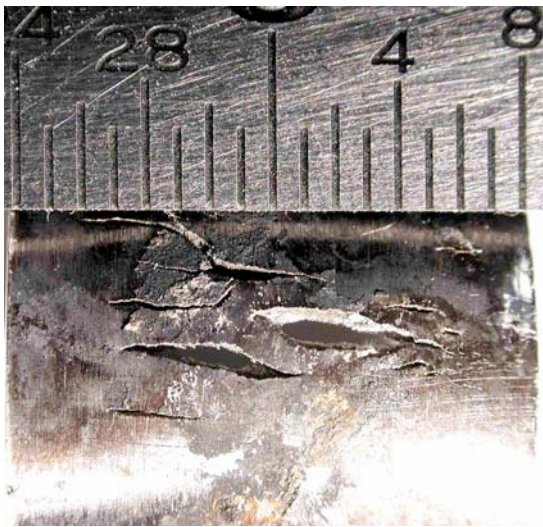
(a)

(b)

Figure 6.8   (a) OD and (b) ID surfaces of specimen 4–43–2 after the end of the test.
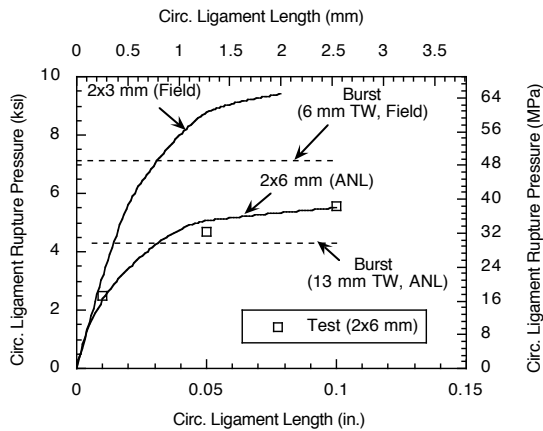
Figure 6.9
Predicted vs. observed circumferential ligament pressures for tests conducted at ANL on 2 x 6 mm axial throughwall cracks separated by a circumferential ligament of various lengths. Also shown are the predicted circumferential ligament rupture pressures for 2 x 3 mm cracks using the same predictive model but modified to account for the flow stress difference between the ANL tubes and the field tubes.

The second specimen that leaked during the test was 39–57–2. Fractography (Figure 6.3b) showed that this specimen had an 8–mm (0.32-in.)-long through-wall segment; however, EC/NDE analysis indicated the crack was much shorter and shallower. Therefore, the ligament rupture pressure based on fractography is essentially zero, whereas the ligament rupture pressure based on EC/NDE over predicts the observed value significantly. The leak rate vs. pressure plot from the test is reproduced in Figure 6.10, which also includes two predicted leak rate curves that correspond to fractographic data. The first predicted leak rate curve assumes an initial 8-mm (0.32-in.) 100% TW crack, and the second assumes an initial 8-mm (0.32-in.) 95% part–TW crack. Both overestimate the leak rate significantly. In contrast, the predicted leak rate based on NDE depth profile underestimates the leak rate and overestimates the ligament rupture pressure significantly. The crack openings on the OD and ID surfaces after the test are shown in Figs. 6.4a-b, respectively. It is evident that the crack is highly ligamented (at least four ligaments at the OD surface). These ligaments limit the crack opening area and consequently limit the leak rate. The steep rise in the measured leak rate is possibly due to simultaneous rupture of these ligaments. FEA–calculated axial ligament rupture pressures for four 100% TW cracks separated by three axial ligaments of various widths are shown in Figure 6.11. The observed ligament rupture pressure (36 MPa) and crack length (10 mm) for specimen 39–57–2 are consistent with a ligament width in the range of 0.8 – 1 mm (0.03 – 0.04 in.), which is a reasonable size for the ligaments.

In Figure 6.12 leak test results for the retired SG (19-mm (¾-in.) diameter) tubes with TSP SCC that were pressure–tested are compared with results for other field tubes [5] in terms of the probability of leakage as a function of relative bobbin coil amplitude. The tests at Argonne are indicated by arrows in the figure. Tubes that did not leak at 17.6 MPa (2560 psi) are plotted as a probability of leakage of 0.0; those that did leak are plotted as a probability of leakage of 1.0. None of the tubes tested at Argonne leaked at 17.7 MPa (2560 psi), and the figure shows the results of the Argonne tests are statistically consistent with the other field tube data. The data indicated as *a* and *b* in Figure 6.12 did leak but only at pressures of 36 MPa (5250) and 49 MPa (7100 psi).
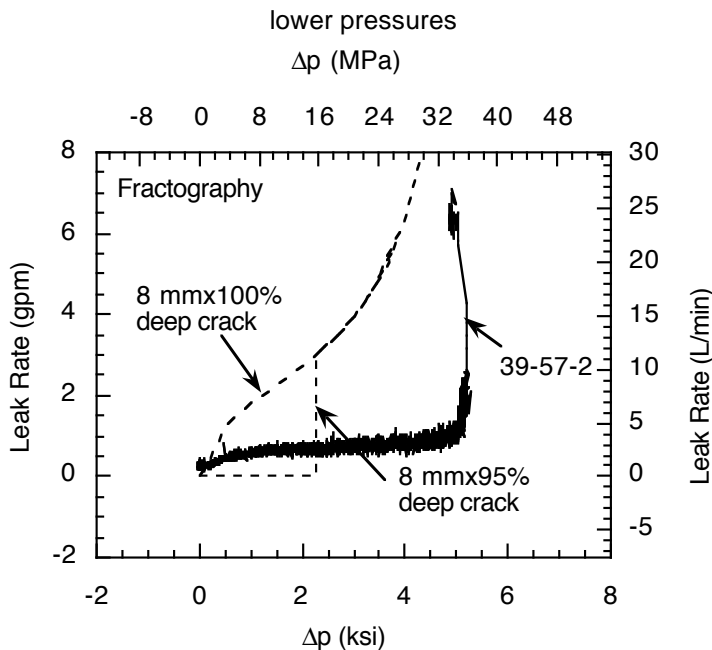
Figure 6.10
Observed and predicted leak rate vs. pressure plots for specimen C39–R57. The noisy signal suggests leakage at low pressure but no leakage at the was observed.
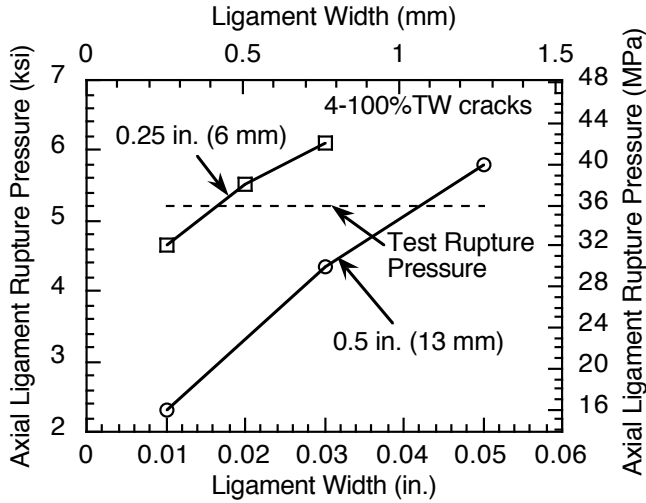
Figure 6.11
FEA (finite element analysis)–predicted axial ligament rupture pressures for 6- and 13-mm long 100% TW axial cracks separated by three axial ligaments with various ligament widths.
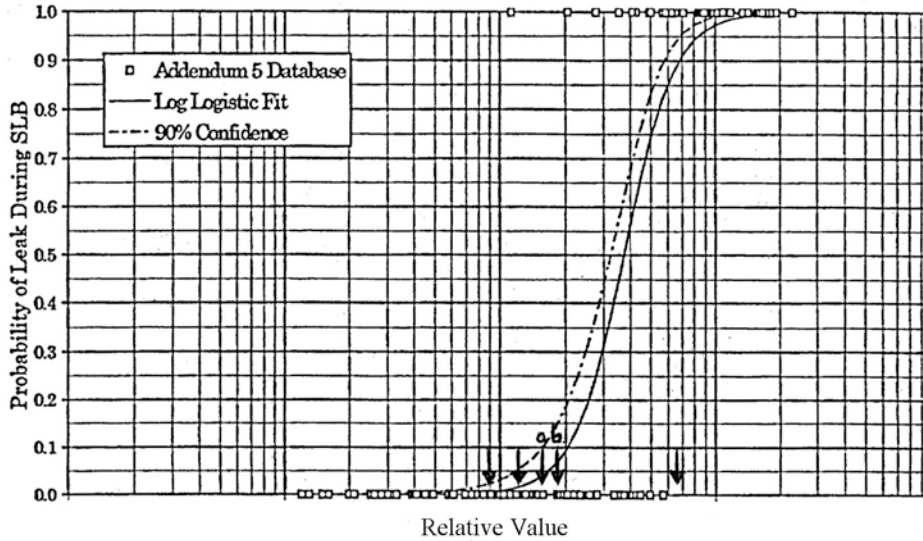
Figure 6.12 Relative bobbin coil amplitudes (before pulling) for the retired SG 19-mm (¾-in.) diameter tubes with TSP SCC that were pressure tested at room temperature at Argonne are shown as arrows. The Argonne tube data can be compared with other 19-mm (¾-in.) diameter field tubes that were pressure tested (Ref. 4). Tubes that did not leak at 17.6 MPa (2560 psi) are plotted as a probability of leakage of 0.0; those that did leak are plotted as a probability of leakage of 1.0. None of the retired steam generator tubes tested at Argonne leaked at pressures less than 17.7 MPa (2560 psi). Tubes a and b leaked at much higher pressures.

The BC amplitude versus the pressure when a leak was first observed was plotted for laboratory grown SCCs. Data from the retired SG were combined with data from the laboratory grown cracks. The ANL specimens were free of signal-distorting deposits. For this selected set of SCC the linear-fit correlation coefficient is 0.87. The BC volts for the two field SCCs that leaked fell slightly above the laboratory SCC data (Figure 6.13), but the results are within the uncertainties associated with the correlation.

62
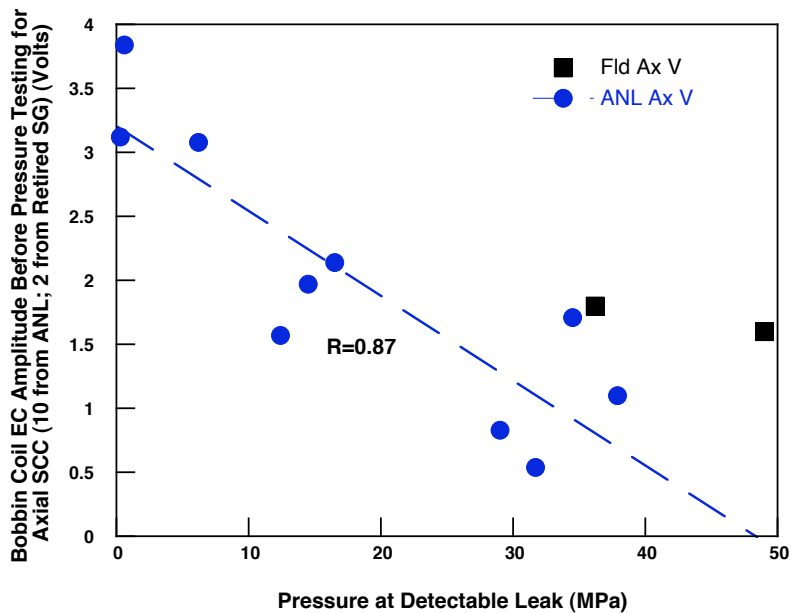
Figure 6.13   Graph of bobbin coil voltage before pressure testing for 10 axial ODSCCs grown at Argonne and 2 axial ODSCCs from the TSP of retired SGD versus the pressure at first observable leak. The linear fit correlation coefficient for the SCCs grown at Argonne under identical conditions is 0.87. In all cases samples were free of signal-distorting deposits.

This page is intentionally left blank.

7   Summary

The evaluation of field degraded tubing was performed to determine if burst pressure and leak rate predictions at Argonne using EC data from field-generated SCCs are consistent with industry findings, and to better understand field-induced SCC morphology using DE.

A summary of the effort carried out on the 20 tubes from the retired SGD is provided in Table 10. The table indicates if the tube was inspected with a BC and/or MRPC, if a profile was created using Argonne's multiparameter algorithm (MP), if the tube was pressure tested, if a leak was observed (and at what pressure), if a burst and leak pressure was predicted, if there is a fractograph for the crack, and if metallurgical sectioning was carried out. Three types of degradation are indicated. They are axial ODSCC, circumferential ODSCC, and IGA (intergranular attack).

Despite significant +Point indications from TSP axial outside-diameter stress corrosion cracking (ODSCC), only two of the TSP tubes leaked while pressurizing to 52 MPa (7.5 ksi). From a multiparameter algorithm, eddy current profiles predicted opening pressure (pressure at first leakage) ranging from 55 to 72 MPa (8.0 to 10.4 ksi). Only one of the leaking tubes had a predicted opening pressure in reasonable agreement with actual pressure. The tubes with the highest predicted opening pressure of 62 to 72 MPa (9.0 to 10.4 ksi) did not leak. A post–test examination of the specimen with a lower than expected leak rate showed the crack to have at least three ligaments, which could explain the low leak rate. Ligaments are very efficient in preventing unstable burst and reducing the crack opening area and the leak rate.

With respect to burst and leak predictions, most of the predicted radial ligament rupture pressures using either EC/NDE or fractography profiles exceeded the maximum pressure capability of the test system. This finding is consistent with the observed test specimen behavior (i.e., no leakage). For the two axial ODSCC tubes that leaked, the pressure was overestimated using NDE data. One pressure was underestimated using the post-test fractography profile. Ligaments in one complicated the prediction as ligaments influence unstable burst pressure. The circumferential ligament in one tube that leaked did not rupture by the end of the test, in agreement with the prediction. The presence of the circumferential ligament prevented unstable burst from occurring during the test. The importance of identifying ligaments cannot be overemphasized.

With respect to prediction of leak rates, those based on fractography overestimated the test leak rates and those based on NDE underestimated the test leak rates significantly. Fractographic data clearly showed that the crack was highly ligamented. The ligaments limit the crack opening area and consequently limit the leak rate. The steep rise in the measured leak rate observed during testing was possibly due to simultaneous rupture of the ligaments. FEA–calculated pressures of axial ligament rupture for four 100% TW cracks separated by three axial ligaments of various widths were consistent with the observed rupture pressure and crack length for one of the axial ODSCCs.

The data obtained at ANL were consistent with the industry probability of leakage database. None of the tubes tested at Argonne leaked at pressures under 2560 psi (16.7 MPa). The BC amplitude versus the pressure when a leak was first observed was plotted for SCCs. Data from the retired SG were combined with laboratory data produced at Argonne. The Argonne specimens were free of signal-distorting deposits. For this selected set of SCCs, the linear fit correlation coefficient

is 0.87. The BC volts for the two field SCCs that leaked fell slightly above the laboratory SCC data (Figure 6.13).

Very little correlation with +Point amplitude and maximum depth of SCC was found. The best prediction of the SCC profile and crack depth arose from the use of Argonne's MP algorithm applied to pancake coil data. The best chance for a good correlation between +Point signal amplitude and maximum depth occurs when all the cracks used to establish the regression curve and all cracks subsequently detected have the same morphology (crack opening with depth) and have the same extent of deposits and ligaments. Phase angle is less dependent on factors other than depth and, in principle, should provide a better correlation with depth than signal amplitude.

Changes in EC signals over time for SCCs in storage were observed. These changes are attributed to changes in corrosion products across the crack faces. EC voltages of plugged tubes can change from not only corrosion products but from applied stresses during reactor operation and continued crack growth.

References

1. *Depth Based Structural Analysis Methods for SG Circumferential Indications: Appendix G,* EPRI Report TR–107197-P2, December 1997. EPRI Licensed Report

2. L. Cagle and E. Fuller, "Axial ODSCC Performance Demonstration POD Results and Sizing Update," in *Proceedings of the 24th EPRI Steam Generator NDE Workshop*, EPRI Report TR–1012928, July 2005.

3. S. Bakhtiari, J. Y. Park, D. S. Kupperman, S. Majumdar and W. J. Shack, *Final Report on Advanced NDE for Steam Generator Tubing for the Second International Steam Generator Tube Integrity Program,* NUREG/CR-6814, Argonne National Laboratory, July 2003

4. S. Majumdar, S. Bakhtiari, K. Kasza, and J. Y. Park, *Validation on Failure and Leak–Rate Correlations for Stress Corrosion Cracks in Steam Generator Tubes*, NUREG/CR–6774, Argonne National Laboratory, 2002.

5. *Steam Generator Tubing Outside Diameter Stress Corrosion Cracking at Tube Support Plates Database for Alternate Repair Limits: Update 2002*, EPRI Report TR–1007660, 2003. EPRI Licensed Report

This page is intentionally left blank.

Appendix A: Procedure for Moving and Cutting Tube Sheet Sample

1. Carry out ALARA (as low as reasonably achievable) review.

2. Arrange for waste management to set up tent to clean tube sheet section.

3. Bring wrapped tube sheet piece (about 50 pounds) currently in wooden crate out of pit (with Health Physics personnel present to monitor radiation exposure).

4. Place crate on cart and survey. (Health Physics personnel present during all movement of crate and tube sheet section.)

5. Roll tube sheet in crate to Building 212 hot shop and place in tent.

6. Provide electronic monitor for radiation dose.

7. Waste management personnel clean tube sheet piece using vacuum, brush, and damp cloth (no fluids).

8. Remove unwanted contaminated material.

9. Bring in new crate to be used to move tube sheet section to saw.

10. Bag tube sheet piece and place in new crate.

11. Spread plastic over floor under saw.

12. Move new crate with tube sheet section to saw.

13. Tape tubes extending from tube sheet before cutting to prevent disturbing corrosion products in crevices.

14. Provide remote switch to turn off saw from outside hot shop.

15. Cut tube sheet piece per instructions.

16. Use "elephant trunk" to carry away mist during cutting.

17 Use file to remove burrs from tube ends.

18. Put small piece from cutting into new crate and return to H137 pit.

19. Put large piece from cutting into old crate and remove for disposal.

20. Collect particles from cutting in chip tray. Cover with lead bricks until waste management removes tray.

This page is intentionally left blank.

Appendix B: Decontamination Procedure for the Tube Sheet

The reading from the steam generator tubing is 200 mR/h @ 1 cm, 25 mR/h @ 30 cm, and 5 mR/h @ 3 ft. ET will transport the steam generator tubes to Building 306 (Room A160) to be decontaminated. Once decontaminated, Waste Management Operations (WMO) will repackage the steam generator tubes and transport them back to the Building 212 hot shop, where they will be reduced in size. All personnel shall be issued an alarm dosimeter and a finger rings. The steam generator tubing will be first dry decontaminated by using a baby bottle type brush and pressurized air, then decontaminated by using a rag wetted with rubbing alcohol.

PRECAUTIONS:

1. WMO-Health Physics (HP) shall be consulted on the appropriate Personal Protective Equipment (PPE) to be worn prior to beginning any work and shall continuously monitor all phases of this job plan.

2. A copy of the Radiation Work Permit (RWP), Work Clearance Permit (WCP), and the ALARA Review shall be posted at the work site.

3. Use tools previously used in radiological controlled areas for this job plan.

4. The steam generator tube sheet section weight is about 50 lb. To ensure fingers/hands are not pinched when it is placed on the decontamination table, WMO shall wear leather gloves.

5. To ensure that the vacuum hose does not become radioactively contaminated, WMO shall wrap the hose in plastic tubing.

6. All personnel shall wear a TLD, SAIC radiation monitoring dosimeter, and finger ring for the duration of the project.

PREREQUISITES:

1. Verify the foremen have been shown the work area prior to starting this job plan.

2. Conduct a pre-job meeting with ET, HP, CS, and WMO Foreman.

3. Ensure that WMO HP Technicians are at the job site.

4. Ensure the sorting table in room A160 has been set up for decontamination purposes. Place plastic sheeting on the sorting table, and affix a drop cloth from the front of the hood.

5. Prepare the room air sampler/monitors in accordance with WMO HP instructions, if so directed.

6. Ensure decontamination items, including alcohol rags/vacuum with HEPA filter, and bushes are set up in Room A160.

7. Place and secure plastic sheeting on the floor surrounding the band saw to collect the filings

from the cutting.

8. Ensure WMO HP surveys the work area and that air-monitoring equipment has been set up.

9. Attend the ALARA with Health Physics-WMO personnel.

PROCEDURE:

1. Have WMO-HP smear wooden box containing tube prior to transferring to Building 306, Room A160.

2. Have PFS-WMO mechanics transfer the steam generator to Building 306, A160 for decontamination.

3. Verify the RWP and WCP have been prepared and posted in the work area.

4. Don PPE as required by the RWP

5. Enter the work area.

6. Carefully unwrap the plastic that surrounds the steam generator, and place the steam generator on the sorting table.

7. While using a small brush and vacuum, carefully brush and vacuum any loose debris from the steam generator.

8. Carefully turn the steam generator to its backside and repeat steps 6 and 7.

9. After the steam generator has been decontaminated, wrap it in plastic and transfer back into the wooden crate. Ensure that WMO-HP has surveyed the steam generator prior to transport back to Building 212.

10. Transfer the steam generator to the Building 212 hot shop to be size reduced.

11. Place plastic sheeting for the filings under the band saw, where size reducing will take place.

12. Transfer the decontaminated steam generator to a CS employee for setup and cutting.

13. Once the tube has been set in the band saw, the CS person will leave the hot shop area and remotely start the band saw from the outside of the room and cut the tube per CS instruction. NOTE: Ensure that an exhaust hose has been set up to exhaust and mist during the cutting

14. After the tube has been cut, CS will return to the band saw and use a file to remove burrs from the tube end.

15. After tube cutting and filing have been completed, the steam generator will be removed from the band saw and wrapped. The larger section of the steam generator will be wrapped in plastic sheeting and placed into a 5-gal PC 5 and transferred to Room H137 for storage.

16. The smaller section will be wrapped in plastic sheeting and placed in the new crate and returned to Room H137 for storage.

17. WMO will drain the old coolant from the band saw and place it into a disposal container. NOTE: CS will prepare the WMO 195-requisition form for disposal.

18. WMO shall decontaminate band saw.

19. WMO shall wipe down the exterior of the vacuum and plastic covering on the vacuum hose.

20. WMO shall wipe down all tools used in this job plan and have WMO survey them.

21. WMO shall inventory all waste materials generated during this job plan on a WMDS-0050.

22. Ensure WMO-HP surveys the work area for contamination.

This page is intentionally left blank.

Appendix C: Industry Standard Practice for +Point Sizing

These instructions apply to line-by-line sizing of all indications.

For sizing circumferential indications:

Voltage normalization is performed in the axial Lissajous window and is set on the 100% circumferential notch at 20 V. Adjust the span such that the 40% ID circumferential notch is 3 div. for 300 kHz. Monitor the 300 kHz raw and process channels on the strip chart and scroll the region of interest while viewing the Lissajous. Terrain plot the 300 kHz raw and process channels in the area of interest. A phase curve is established on process channel P2 using 100%, 60%, and 40% circumferential notches in the axial Lissajous window; in addition, set a zero percent value in the curve. All phase measurements are performed on the Lissajous response in the axial Lissajous window. Careful analysis should be performed watching for any change in the Lissajous signal. Record a zero percent call prior to the first call of the indication and after the last call unless the indication is 360 degrees. Record only those indications which provide a flaw-like Lissajous response at a maximum of 10 degree increments. Filters are acceptable for detection but are not applied for sizing. Dent responses may also form in the same plane as the flaw response.

For sizing axial flaws:

Voltage normalization is performed in the circ. Lissajous window and is set on the 100% axial notch at 20 V. Adjust the span such that the 40% OD axial notch is 3 div. at 300 kHz (channel 6). Set phase so that the 40% ID axial notch is 15 degrees at 300 kHz. A phase curve is established on the 300 kHz raw channel using 100, 60, and 40% ID axial notches. Terrain plot the 300 kHz raw channel in the area of interest. Axial indications will form in the positive direction. Dent responses may also form in the same plane as the flaw response. Careful analysis should be performed watching specifically for any change in the Lissajous signal. Phase and amplitude measurements are performed on the Lissajous response from the circumferential Lissajous window. Record only those indications that provide a flaw-like Lissajous response. Use the strip chart to step through one scan line at a time along the length of the indication. Record a call for each step along the length of the indication. Record a zero percent call prior to the first call of the indication and after the last call.

Filters are acceptable for detection but are not applied for sizing.

Adjustment Procedure

At the completion of the initial analysis process, adjustment for data points at the ends of the cracks is required. Data points within 0.2 in. of the indicated crack ends will be adjusted as follows:

a) Ignore all data points from the 1st reading to the point at which phase angles change from ID to OD. (Paragraph does not apply if the crack exhibits primarily OD phase angles over its length.)

b) Less than 1 volt data points, with ID phases indicating 85% TW and greater will be ignored from the first reading to that point provided within 0.2 in. from the first reading.

c) Less than 1 volt, ID phase data points exhibiting depth increases of greater than 10% TW over approximately a 0.05 in. span will be ignored.